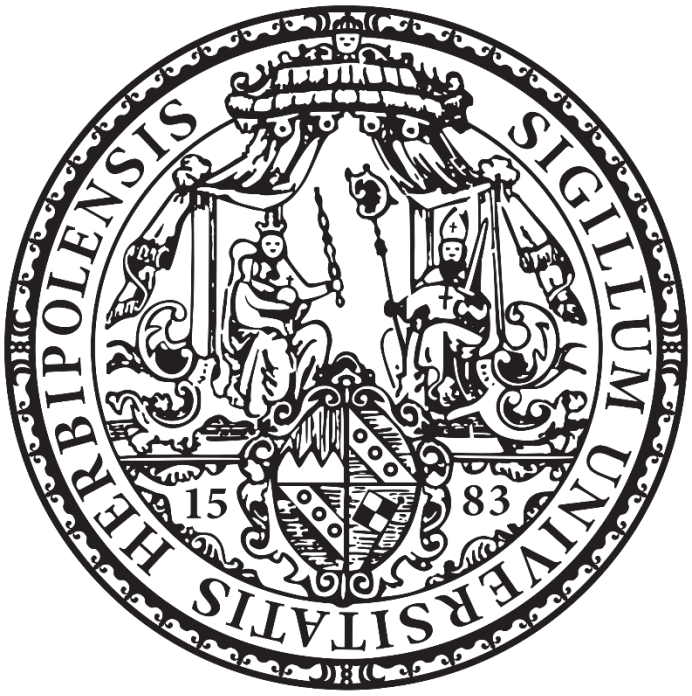

The transcription factor NFATc1 mediates cytotoxic T cell function *in vitro* and *in vivo*

Dissertation zur Erlangung
des naturwissenschaftlichen Doktorgrades
der Julius-Maximilians-Universität Würzburg

vorgelegt von
Tobias Pusch

geboren in Cottbus

Würzburg, 2015

Eingereicht am: 9. Oktober 2015

Mitglieder der Promotionskommission:

Vorsitzender: Professor Dr. Markus Engstler

Gutachter: Professor Dr. Edgar Serfling

Gutachter: Professor Dr. Thomas Rudel

Tag des Promotionskolloquiums:

Doktorurkunde ausgehändigt am: ……

Danksagung

Mein spezieller Dank gilt Herrn Professor Dr. Edgar Serfling für das Vertrauen und dafür, mir die Möglichkeit gegeben zu haben, in seiner Arbeitsgruppe zu promovieren, die wissenschaftlichen Diskussionen und seine vielfältigen Ideen, die mich immer wieder dazu antrieben, neue Sichtweisen zu erlangen. Sein wissenschaftlicher Forscherdrang war immer wieder eine Bereicherung für mich.

Für die Bereitschaft, das Zweitgutachten zu erstellen, bedanke ich mich recht herzlich bei Herrn Professor Dr. Rudel.

Herrn Dr. Andris Avots möchte ich zutiefst für die Übernahme der Betreuung gegen Ende meiner Promotionstätigkeit, das angenehme Arbeitsklima und die vielen anregenden Diskussionen danken, welche mir stets geholfen haben.

Bedanken möchte ich mich außerdem bei Frau Dr. Friederike Berberich-Siebelt und Dr. Martin Väth, deren Expertise mir auf dem Gebiet der $CD8^+$ T Zellen immer eine große Hilfe waren und die mir oft mit ihrer Fachkenntnis zur Seite standen.

Mein Dank gilt auch meinen Kollegen Dr. Hani Alrefai, Dr. Rhoda Busch, Dr. Lena Dietz, Dr. Stefan Klein-Hessling, Dr. Khalid Muhammad, Dr. Krisna Murti, Dr. Amiya Patra, Dr. Ronald Rudolf, Hendrik Fender und Duong Pham Anh Thuy, welche mir den Arbeitsalltag erleichterten und für eine angenehme Atmosphäre im Labor gesorgt haben. Sehr dankbar bin ich auch Doris Michel und Ilona Pietrowski, die mich im Laboralltag oft unterstützt haben.

Für die Möglichkeit, an der Universitätsklinik des Saarlands in Homburg/Saar am Institut für Biophysik wichtige wissenschaftliche Erkenntnisse zu gewinnen, möchte ich mich ganz herzlich bei Professor Dr. Markus Hoth, Dr. Eva Schwartz und Christian Backes bedanken. Besonders bedanken möchte ich mich hierbei bei Carsten Kummerow, der mich auch abseits des Labors immer sehr gut betreut hat und dessen wissenschaftliche Diskussionen sehr bereichernd waren.

Bei meinen Eltern möchte ich mich für die Ermöglichung des Studiums, die bedingungslose Unterstützung und ein stets offenes Ohr bedanken. Ihr wart immer für mich da.

Ebenso danke ich meinen Freunden für eine tolle gemeinsame Zeit, die ständige Unterstützung und die schönen gemeinsamen Erlebnisse.

Table of Content

Introduction

1.1 The immune system

For an efficient protection of organisms from pathogens, various defense mechanisms have evolved by almost all species from protists through plants to animals. The main task of the immune system is to distinguish self from foreign antigens (Ag) or malformed structures and to react against such harmful patterns. To do so, two important mechanisms have been developed during evolution in the mammalian system which are closely connected to each other with overlapping functions to ensure successful antigen clearance:

1.) The innate immune system: Mechanical and chemical barriers, like the skin or the mucosa, protect the organism from pathogen entry by physical barriers mediated by close cell-to-cell contact and secretion of e.g. lysozyme[1]. Another unspecific barrier is formed by the complement system whose parts detect and binds to bacterial surface patterns to opsonize and mediate destruction of pathogenic structures[2]. On the cellular level, innate immune cells like macrophages, granulocytes, mast cells, natural killer (NK) cells, monocytes and dendritic cells are able to recognize bacterial associated molecular patterns (PAMPs) by specific receptors that are designated as pattern recognition receptors (PRRs)[3]. The most famous PRR family is the Toll-like receptor (TLR) family[4] whose members are expressed on several types of immune cells. They recognize lipopolysaccharides (LPS), flagellins and other bacterial structures. Contrary to physical barriers, single cells are motile and able to move actively to sites of infection with the aim to support pathogen clearance. The clearance is maintained by toxic mediators, like nitric oxide (NO), reactive oxygen species (ROS) or cytokines, as interferon γ (IFN-γ). To increase blood flow in nearby vessels to attract other cells of the immune system, innate immune cells are able to secrete cytokines as interleukin 2 (IL-2), tumor necrosis factor α (TNF-α) and transforming growth factor-β (TGF-β). Those cytokines play a very important role in the innate immune system but occur also within the adaptive immune response. In general, the recognition mechanisms of the innate immune systeme are rather unspecific but serve as s first line of defense to quickly kill bacteria and virus infected cells which infected the organism.

To connect the unspecific immune responses to adaptive immunity, some cells serve as mediators between both mechanisms. Dendritic cells, for example, are able to take up, digest and present

pathogen-associated peptides on major histocompatibility molecules encoded in the complexes I and II (MHC-I, MHC-II) which represent the second pillar of the immune system:

2.) The adaptive immune system which acts in a different fashion. As mentioned above, it is highly specific recognizing a huge amount of diverse peptide sequences.

During infection, B cells are stimulated by APCs in lymphoid tissues, compete in the germinal center reaction for survival signals to become plasma cells. Immunoglobulin class switch leads to a massive production and secretion of antibodies binding to and labelling structures of potentially harmful origin. With one part of their protein structure - the F_c residue - antibodies opsonize attached structures, like bacteria, for getting attacked by other immune cells representing the humoral part of the adaptive immune system. The direct cell-to-cell mediated immunity is maintained by the T cells.

Naïve $CD4^+$ helper T cells (T_h) recognize peptides presented by MHC-II molecules on professional antigen presenting cells (APCs), as dendritic cells in lymphoid organs. The recognition is mediated mainly by the T cell receptor (TCR) and additional co-receptors forming a complex called the immunological synapse[5](IS). If a specific TCR recognizes its cognate peptide, the $CD4^+$ T cell becomes activated, proliferates, differentiates into a T_h subset and migrates to sites of infection. T cells can also provide help for B cells in the germinal centre (GC) reaction for the generation of high-affinity plasma cells. By reaching pathogen-associated areas, T_h cells support immune reactions against pathogens by secreting specific cytokines upon new antigen recognition on professional APCs. APCs are activated to gain effector functions, as to activate macrophages to destroy ingested pathogens, induce enhanced neutrophil killing or to stimulate eosinophils for eradication of helminth infections.

The role of $CD8^+$ T cells is rather different from the one of $CD4^+$ T cells. Contrary to T_h cells, $CD8^+$ T cells recognize peptides on MHC class I molecules, which are expressed on every nucleated cell of an organism. MHC-I molecules are loaded with intracellular peptides which are derived from the proteasome of each cell. Similar to T helper cells, naïve $CD8^+$ T cells have to become primarily activated by antigen presentation of dendritic cells in lymphoid organs to become activated and gain effector functions as cytotoxic T cells (CTLs). If a bacteria (like *Listeria monocytogenes*) gets ingested by a host cell, it is still able to stay alive due to its' intracellular surviving – and replication – strategy. To reach its target to gain in number, the proteins of the *Listeria* also have to be synthesized by the host cell protein synthesis machinery. For replication, the bacterial proteins are processed by the cellular proteasome and presented on the cell surface

enabling $CD8^+$ T cell to recognize and interact with the infected cell. By secretion of cytokines and activation of apoptosis-inducing killing mechanisms, intracellular infections can be cleared.

One other important point of adaptive immunity is memory. After an activation phase – in which pathogen specific cells arose from a few (1-10 in 10^6 immune cells) to 1 in 10 lymphoid cells by proliferation, differentiation and successful clearance of pathogens[6], large amounts of effector T- and B cells undergo apoptosis in the contraction phase. They do not survive for more than one month. To prevent the organism from a repeated infection with a similar pathogen, memory mechanisms have evolved. During the activation phase in the germinal centre, beside plasma cell differentiation, at a later time point also a small amount of long lived high antigen-affinity memory B cells are generated. Memory T cells can be generated at various time points during the differentiation. They can be subdivided into central memory T cells (T_{CM}), which reside in lymphatic organs, bear reduced cytokine expression but highly proliferative capacity whereas effector memory T cells (T_{EM}) home to peripheral tissues[7] and can produce large amounts of cytokines whereas their proliferative potential is reduced[8].

The memory T cell subsets can migrate into various organs and reside there until a re-infection of the same pathogen occurs. There, a much more rapid and efficient secondary immune response takes place.

1.2 Development and function of $CD8^+$ T cells

Derived from bone marrow stem cells, T cell licencing and lineage decision takes place in the thymus, the primary lymphoid organ for immature T cell populations. For the generation of the huge repertoire of TCR diversity, T lymphocyte precursor cells engraft the thymic organ. There, DNA-re-arrangement in the TCRα/β (for classical αβ T cells) or γ/δ gene loci is induced. γδ T cells are markedly lower in overall number compared to α/β T cells.

The α locus consists of three gene cassettes, the variable (V), the diversity (D) and joining (J) regions, whereas the β gene only bears V and J elements. This arrangement of gene cassettes is similar to the immunoglobulin (Ig) loci and leads to a broad TCR diversity. During thymocyte maturation to form the pre-T cell receptor, the recombination of the β locus takes place at first together with CD3ε and ζ chain signaling molecules. If this receptor is able to maintain extracellular signals to the cell, the α chain is re-arranged to generate the αβ TCR. If the affinity for self-antigens expressed on MHC complexes in the epithelium of the thymical cortex in is not too strong (negative selection) but the TCR is also functional to bind MHC molecules, survival signals lead to positive

selection[9]. At this stage, CD4 and CD8 co-receptors are expressed simultaneously and a lineage decision has to be made[10]. The tendency to bind MHC-II presented peptides leads to the loss of CD8 gene expression, and naïve $CD4^+$ T_h cells are generated. If MHC-I restricted peptide presentation gives a stronger TCR binding, CD4 gene expression is down-regulated, and naïve $CD8^+$ T cells arise to circulate in the lymphatic organs.

As mentioned above, $CD8^+$ T cells show a high cytotoxic potential. Although there are overlapping mechanisms between $CD8^+$ and $CD4^+$ T cells, some functions are significantly different: Classical primary activation of naïve $CD8^+$ T cells in lymphoid organs is mediated by activated dendritic cells that present ingested and partially digested peptide epitopes on MHC class I molecules. A small subpopulation of dendritic cells is needed to present microbial peptides[11] on their MHC class I peptides by cross presentation[12] as initial stimulation to highly specific naïve $CD8^+$ T cell clones in secondary lymphoid organs. The newly generated effector cytotoxic $CD8^+$ T cell clones rise in number, gain cytotoxic capacities and become able to enter the blood circulation to screen the body for sites of infection. Normal tissue cells which are infected with intracellular pathogens are processing and presenting self and non-self peptides on their cellular surface but usually lack co-stimulatory signals for clonal $CD8^+$ T cell expansion. Therefore, only professional APCs are able to drive $CD8^+$ T cell activation. The lack of co-stimulation on cells mediates CTL-derived cytotoxic activity towards the cognate cell for non-self peptide presentation.

In an inflammatory environment, where parts of the cellular innate immune system are activated by Toll-like receptors and $CD4^+$ T cell help, soluble inflammatory signals are released by parts of the innate immune system (mainly TNF by macrophages) and circulating cytotoxic effector T cells in the vascular system get attracted to the site of infection by surface modifications of the venules close to the infectious area. Once a CTL recognizes infected cells in a TCR-dependent manner, it provides effector function and induces apoptosis of target cells.

Two major killing mechanisms of cytotoxic T lymphocytes[13,14] (and NK cells) have been extensively studied. The secretion of cytotoxic granules toward target cells is the major pathway of rapid apoptosis induction of pathogen-infected or of tumor cells[15]. Upon successful screening for harmful peptides presented on MHC-I molecules, a CTL adheres to and forms a synapse with the target cell[16]. Cytotoxic granules in the $CD8^+$ T cell are formed and polarized towards the dense contact zone also called cytotoxic immunological synapse[17]. Trans-Golgi-network derived cytolytic enzymes of the granzyme family and perforins[18] are stored in those lytic granules. Upon dense target cell contact, these lytic granules get secreted by fusion with the cell membrane

resulting in degranulation and release of cytolytic particles into the synaptic cleft. These proteins are getting activated by the neutral pH at the extracellular environment[19]. To transiently protect the effector cell from getting attacked by its own activated cytotoxic proteins, lysosomal associated membrane proteins (LAMPs) are localized on the lysosomal membrane[18,20] and granzyme B inhibitors, notably proteinase inhibitor 9, are produced[21]. Upon cytotoxic granule fusion with the cell membrane at the immunological synapse, LAMP proteins are available on the CTL membrane and effectively protect the effector cell as well[22]. Lamp1 and 2 reside on the effector cell surface for several days and serve as strong markers for antigen-specific T cells which just degranulated[23]. Perforin itself acts as a carrier protein to facilitate granzyme entry to the target cell. E.g. granzyme B – as one of the most prominent granzyme family members - shows some tryptase activity to cleave its' substrate - caspase-3 - in the target cell leading to the activation of the caspase cascade which triggers the intrinsic apoptotic pathway[24]. Another important function of granzyme B is to act as an activator of the intrinsic induction of cell death by mediating cytochrome c release from and loss of mitochondrial membrane potential. Cytochrome c activates caspase-9 in an ATP dependent manner to cleave caspase-3 resulting again in downstream effector caspase activation for apoptosis induction[25].

The extrinsic pathway of apoptosis induction is receptor mediated and represents the second major killing mechanism. Upon activation, professional killer cells, like CTLs or NK cells, upregulate the expression of Fas ligand (Fasl), a pro-apoptotic member of the tumor necrosis factor (TNF) superfamily, on their cell surface[26]. The Fasl receptor – Fas – is constitutively expressed on most cellular surfaces, as well as on leukocytes. Therefore, the expression of Fasl to induce apoptosis in target cells has to be highly restricted to prevent misleading immune responses. As an example, in immune privileges sites of the body, as the eye, Fasl expressing cells actively suppress an invasion of inflammatory immune cells by Fas-Fasl interaction to induce apoptosis[27]. After cross-linking of several Fas domains on the target cell membrane, adaptor proteins (as FADD) and caspase-8 bind to the intracellular part of Fas to recruit an intracellular receptor complex – the death inducing signaling complex (DISC). This leads to the cleavage and activation of caspase-8 which triggers the cleavage of downstream effector caspases, notably caspase 3, leading to apoptosis induction in the target cell and finally to the eradication of malformed cells to prevent the organism from further damage.

1.2.1 T cell activation

Classical activation of T cells *in vivo* is mediated by peptide recognition. Sources of activation of either $CD4^+$ or $CD8^+$ T cells are derived from different origins. For $CD4^+$ helper T cells, MHC class II-restricted activation is mandatory. Upon activation by inflammatory signals, naïve professional APCs, like dendritic cells (DCs), get activated, take up proteins from their environment to process and cleave those molecules to short peptide fragments in specialized organelles – the lysosomes. MHC class II containing vesicles derived from the Golgi complex fuse with the lysosomes. The cleaved peptide sequences are loaded into the binding grove of MHC-II molecules. Due to chemokine receptor expression, these activated APCs than move into nearby lymph nodes. The final migration and homing into the T cell zone is mainly mediated by CCR-7. In the T cell zone, large amounts of circulating naïve $CD4^+$ T cells screen the APCs for MHC-antigen complexes. If a TCR shows a high affinity to the complex and other co-stimulatory molecules, like CD40, are expressed, the proliferation and $CD4^+$ T cell activation are maintained.
$CD8^+$ T cell activation by MHC I-peptide presentation is more diverse since all nucleated cells of the body are able to express MHC I molecules. The way of peptide-loading is based on cytosolic proteins rather than antigenic uptake from lysosomes. Endogenous cytoplasmatic proteins as well as proteins derived from intracellular parasites - like viruses and bacteria - get randomly ubiquitinylated and degraded by the proteasome. As a result, various peptides with a length between 6 and 30 amino acids are generated and transported into the ER where they get loaded onto MHC I molecules. After final processing in the Golgi complex, MHC complexes are externalized by membrane fusion of exocytotic vesicles to serve as recognition sites for matching TCR + CD8 molecules[28]. In an inflammatory environment, where parts of the innate immune system is already activated to attract further cellular compartments of the adaptive immunity, $CD8^+$ T cells are recruited from the blood vessels to scan the environment for pathogen-derived peptides. T cells reactive to self-peptides were already sorted out during thymical selection so that only exogenously reactive peptides on MHCI molecules are recognized. This recognition leads to the activation, proliferation and final gaining of effector $CD8^+$ T cell functions to kill the infected target cells.
Alternatively, T cells can also get activated by direct MHC-mismatch recognition where TCRs may directly recognize structures on foreign MHC molecules rather than peptides presented in the MHC class I or II binding grove. This natural reactivity is only maintained by a small proportion of the T cell compartment, but their role is mostly pronounced during organ transplantation to generate a

so called graft-versus-host-disease (GvHD) reaction. In a GvHD, allogeneically reactive T cells within the graft migrate into the host tissues to generate a massive inflammation since the immune system of the host is down-modulated with the original aim not to reject the graft tissue. A massive cytokine release from activated T cells may lead to severe complications after transplantation.

All $CD4^+$ and $CD8^+$ T cells share a typical activation modus. If naïve T cells are activated, a massive clonal expansion is followed by the gain of specific effector functions depending on costimulatory molecules. This T cell activation mainly depends on the TCR signaling cascade[6]:

The TCR heterodimer of α and β chains recognizes the peptide which is presented on a specialized binding region on the MHC molecule – the peptide binding grove, which is mounted with a random peptide in the endoplasmatic reticulum. If a presented peptide is recognized by a T cell as "foreign", i.e. that a T cell is able to bind with its TCR to the MHC-peptide complex with a moderate to high affinity, additional adhesion molecules serve as co-stimulators – such as CD8 binding at the MHC I region which is not directly involved in peptide presentation – moreover, a high contact time between target and effector cell are needed to induce full T cell activation cascade:

The cytoplasmic part of the TCR is associated with the ζ-chain and other CD3 complexes which contain immunoreceptor tyrosine-based activation motifs (ITAMs). These tyrosine residues are phosphorylated by the activated Lck upon clustering process during TCR re-arrangement on the cell surface. Lck is associated to the cytoplasmatic domain of CD4/CD8 co-receptor molecules and acts as a tyrosine kinase to phosphorylate ITAMs in close proximity. This activates further downstream kinases, as ZAP-70, which binds to completely phosphorylated ITAM motifs.

Another membrane adaptor molecule – LAT – is recruited to the immunological synapse, phosphorylated and binds phospholipase C (PLCγ). The enzymatic activity of PLCγ leads to cleavage of phospholipid phosphatidyl-Innositol-biphophate (PIP_2) in the plasma membrane into two products: diacylglycerol (DAG) and 1,4,5-triphosphate (IP_3) which act as inducers of two different pathways. Classical NFAT activation is triggered by the release of IP_3 into the cytosol and binding to receptors on the endoplasmatic reticulum (ER). This leads in turn to a release of Calcium stores from the ER stores resulting in elevated intracellular Ca^{2+} levels. This change in intracellular ion concentrations is sensed by STIM proteins on the ER membrane transducing the signal to ORAI proteins on the cell membrane. Finally, an activation of Calcium-release-activated Ca^{2+} (CRAC) channels on the cell membrane as a result of conformational changes induces a massive Ca^{2+} influx from the extracellular environment. In addition to many other important roles for Ca^{2+} in CTL functions[29], Ca^{2+} bind to calmodulin, a calcium-dependent regulatory protein

activating calcineurin. This serine/threonine phosphatase binds to NFAT proteins which usually reside phosphorylated and inactive in the cytoplasm[30]. Upon de-phosphorylation by calcineurin, NFAT are activated and translocate into the nucleus. In cooperation with other transcription factors such as AP-1 (Fos/Jun)[31], NFAT binds to specific promoter elements to induce the transcription on a variety of target genes. This approves the important role of NFAT family members in linking Ca^{2+} signaling to gene transcription and effector cell generation[32].

1.2.2 The role of $CD8^+$ T cells during *Listeria monocytogenes* infection

The primary function of $CD8^+$ T cells is to eradicate pathogens residing and replicating in host cells – in general, all intracellular infections are controlled by $CD8^+$ T cells[33]. Due to infections or tissue injury, pathogen-associated peptides are delivered to draining lymph nodes by dendritic cells either by cross presentation or direct infection to activate pathogen-specific $CD8^+$ T cells. Those T cell populations undergo many cell divisions and gain cytotoxic effector functions. Their migratory potential is modified during T cell maturation to recognize and infiltrate sites of infection/inflammation. Finally, the generation of memory cell populations from effector cells can be followed up by the investigation of surface receptor expression[34].

The recognition of malformed cells in infected sites is provided by MHC class I molecules on the host cell that continuously presents cleaved peptide fragments from its own protein repertoire. If a MHC class I delivered peptide is recognized as "foreign", the cognate cell is going to get killed by corresponding $CD8^+$ T cells by two major pathways: The Fas-Fas ligand interaction and/or granule mediated cytotoxicity.

By those mechanisms, $CD8^+$ T cells play a major role by defending the organisms from infections induced by viruses and intracellular parasites, such as *Listeria monocytogenes* (*Lm*).

Listeria monocytogenes is a gram-positive facultative anaerobe bacterium occurring ubiquitously in the environment. Upon administration, such as by contaminated food, individuals with a defective immune system or patients with immunosuppressive treatments are infected to suffer from a listeriosis. *Lm* particles are taken up by macrophages that are not lysed properly – they escape from intracellular degradation mechanisms actively by e.g. usage of the actin cytoskeleton[35] and other signaling pathways[36] in infected host cells. As a result, the bacteria are still viable and hidden from the immune system and, therefore, are able to spread within the organism[37] even without getting exposed to the extracellular environment[38].

The main target organs of *Listeria* are the liver and lymphatic organs, as the spleen and lymph nodes. But meningitis or encephalitis may also occur. The death rate among infected individuals is about 20-30 %[39] emphasizing the importance to investigate the role of cytotoxic T cells during intracellular infections. T cells – especially $CD8^+$ T cells – play a major role in the clearance of *Listeria* infections *in vivo*. These cells proliferate massively during primary infection. After eradication of *Listeria*-infected cells, a high percentage undergoes apoptosis and about 5 – 10% of the polyclonal population remains as long-lived memory $CD8^+$ T cells to rapidly protect upon re-challenge with an anew *Listeria monocytogenes* pathogen[40]. Functionally, $CD8^+$ T cells play a certain role during primary immune responses and are mandatory for a protective immune reaction upon secondary infections with *Listeria*[41]. In general, the situation *in vivo* is rather complex involving both innate and adaptive components of the immune system for an efficient immune response[42].

1.3 NFAT family of transcription factors

The first member of the Nuclear Factor of Activated T cells transcription factors was first described by Shaw et al. in 1988 by identifying a molecule which binds on the enhancer element of the IL-2 promoter[43] in a stimulated human Jurkart T cell line.

Somewhat later, more family members were found to be important in various organs regulating gene expression profiles, like in cardiocytes, NFATc1 is essential for calcium-mediated signal transduction and for overall heart cell function already during early embryogenesis[44].

One of the exclusive common features of NFATc factors is the Ca^{2+}/Calmodulin dependent calcineurin activation mechanism linking elevated intracellular Ca^{2+} levels to the process of gene transcription. The four family members NFATc1, NFATc2, NFATc3 and NFATc4 are sensitive to elevated intracellular calcium levels whereas the most distant family member – NFATc5 (also known as TonEBP) – which was first found and described in *Drosophila melanogaster* - can get activated upon hypertonic stress[45].

The importance of different NFAT family members in cellular signaling and gene transcription emerges by clinical investigations of several autoimmune diseases as well as in lung and colon cancer development[46], in which NFAT dysregulation plays an important role.

NFAT factors were described first as nuclear factors that bind to purine box-like sequence motifs within the *Il2* promoters of men and mouse[43,47]. These so-called NFAT motifs share the conserved sequence T/A GGAAA and occur in the promoters/enhancers of numerous genes that are activated

in lymphocytes upon immune receptor triggering. Soon after, these factors were recognized as indirect targets of CsA, the immunosuppressant that revolutionized transplantation medicine[48] by acting as reversible inhibitors for calcineurin in the TCR signaling cascade[49]. E.g., the *Il-2* expression in T cells was shown to be inhibited by CsA administration[50]. In 1993, the first *Nfat* gene, designated as NFATp (latter called NFAT1 or NFATc2) was cloned[51] followed by the gene cloning of other NFATc members, NFATc1, c3 and c4. Finally a fifth member, NFAT5, was identified which, however, shares only the DNA binding region with the other four NFAT members. Contrary to the four other members, NFAT5 is not regulated by Ca^{2+} and the calcineurin signaling cascade but by osmotic stress[45].

1.3.1 Structure

All NFAT proteins share one common structural element, the Rel-homology domain (RHD) which is highly conserved between all family members on the DNA and protein level[52] and serves as DNA-binding element to specific promoter regions. The amino acid sequence for DNA-binding is conserved throughout all family members and has the following amino acid sequence: RAHYETEG (with the underlined residues being in close contact to the DNA binding sequence[52]). The NFAT-binding core sequence consists of the sequence GGAAA and can be modified by base pair modifications to modulate the binding strength of nuclear NFAT proteins leading to a diverse transcriptional profile of target genes[32]. Additional modifications of NFAT transcriptional activity are mediated by other interaction partners of NFAT binding to different DNA motifs and therefore affecting NFAT binding efficiency[32].

The Ca^{2+} sensitive NFAT members NFATc1, c2, c3 and c4 share an additional motif called the NFAT-homology domain (NHD) which is only moderately conserved. It contains nuclear-localization-and nuclear-export signals (NLS, NES) and several serine-rich regions (SRR) that serve as phosphorylation sites. A calcineurin-docking site enables activated calcineurin to bind to NFAT and efficiently dephosphorylate the serine residues in the NHD. This leads to conformational changes and reveals the NLS to adaptor molecules resulting in the nuclear import of NFAT. This docking site is missing in NFATc5 and effects the inability to respond to Ca^{2+} signals and calcineurin activity.

The re-phosphorylation of serine-rich motifs in the nucleus leads to exposure of the NES on the protein surface. This enwraps the NLS structure and leads to the export of NFAT proteins to the cytoplasm, being again able to respond to Ca^{2+} signals and calcineurin-mediated activation.

1.3.2 NFATc1 and NFATc2 in T cell function

First experiments with *Nfatc1* and *Nfatc2* knockout T cells show a significant different phenotypes, although the DNA binding of both family members to the numerous promoters seems to be similar or identical.

Studies of chimeric *Nfatc1* - *Rag-1* deficient mice revealed the importance for the *Nfatc1* family member in T cell generation and proper effector cell function[53]. Yoshida et al. observed a decreased number of thymocytes and moderate proliferation defects in T cell compartments of Nfatc1$^{-/-}$ mice as well as an impaired cytokine production, most notably in IL-4[54] and IL-6, whereas *Il2* RNA and protein levels remained unaffected. These results led to the conclusion that NFATc1 is important for the generation of thymocytes and the differentiation from naïve CD4$^+$ T cells towards a T_h2 phenotype.

The generation of *Nfatc2* deficient mouse lines (*Nfatc2*$^{-/-}$ mice) showed that peripheral T cells need *Nfatc2* to modulate their proliferative capacities since T cells from *Nfatc2*$^{-/-}$ mice are hyperproliferative and show a slight splenomegalie[55]. NFATc2 is crucial for T_h1 mediated immune responses like defeating *Leishmania major* infections by regulation of the *Ifng* expression in CD4$^+$ T cells[56] whereas T_h2 responses are even elevated in knockout mice[57]. In 2002, Diehl et al. found NFATc2 to be a critical regulator for IL-6 mediated IL-4 cytokine expression in CD4$^+$ T cells to promote T_h2 differentiation[58].

Contrary to *Nfatc2*, *Nfatc1* is induced on the transcriptional level upon lymphocyte activation[59] which is regulated along with a downstream enhancer by the highly inducible P1 promoter in the *Nfatc1* locus. Another modulatory event in *Nfatc1* function is mediated by different splicing events and the use of two polyadenylation (polyA) sites leading to six diverse *Nfat* isoforms. Upon T cell activation, *Nfatc1* transcript composition changes from initial two distal polyadenylated isoforms to one smaller version with a more proximal polyA site – *Nfatc1 A* – which can be tracked on mRNA and in the latter translated form on protein level[60]. The most proximal isoform *Nfatc1 αA* is transcribed upon stimulation and NFAT activation - serving as an autoregulatory mechanism – and enhances lymphocyte activation[61].

A rather diverse role of NFATc1 and c2 transcription factors was found for the *Tnfa* gene which serves as an important mediator during infectious diseases[62] and cancer[63]. Kaminuma et al. discovered in human T cells that the *Tnfa* promoter is enhanced by NFATc2 whereas NFATc1 activity has no effect on *TNFα* transcription, although the binding capacity is maintained for both family members[64]. The c-terminal transactivation domain of NFATc2 seems to have a suppressive

effect on NFATc1 binding to the *Tnfa* regulatory element. This result confirms the findings on NFATc1$^{-/-}$ and NFATc2$^{-/-}$ T cell populations in the mouse model showing that *Nfatc1* inactivation has no effect on TNFα expression[53] whereas cytokine levels are impaired in the *Nfatc2* knockout mice[65].

Several NFAT-regulated genes have been identified so far. The promoter elements of those genes share all one key feature. A common NFAT signaling core-sequence A/TGGAAAA is available in the promoter region. For the most prominent NFAT-dependent gene – *Il2* - even multiple high- and low-affinity NFAT binding sites are occurring within the promoter region[50,66].

Soon after the finding that the *Il2* promoter contains several NFAT binding sites, more NFAT-dependent genes have been discovered to become induced after the nuclear translocation of NFATs which is mandatory for proper T cell activation, tolerance and differentiation[67,68]: By active binding to promoter elements of the *Ifng* and *Il4* genes in activated T cells, NFAT family members are able to enhance cell proliferation and support T cell differentiation towards the T_h1 phenotype (in the case of upregulated IFN-γ production by binding of NFATc2) or T_h2 polarization (by elevated IL-4 levels as a result of NFATc1 binding to the corresponding distal enhancer region)[69]. For this reason, NFAT family members are able to actively modulate T cell differentiation into diverse $CD4^+$ T helper (T_h) and $CD8^+$ cytotoxic T (T_c) cell subsets.

As mentioned above, the first gene in which NFAT was discovered to act as an enhancer of transcriptional activity is *Il2*. NFAT is a key factor for sufficient IL-2 production upon T cell stimulation[70]. Beside the capability of direct T cell activation without any TCR engagement[71], interleukin 2 serves as a co-stimulatory molecule during T cell activation to generate an optimal immune response. IL-2, which is released by activated T cells, acts in an autocrine manner by binding to activation-induced CD25 cell surface molecules (the high affinity α chain of the IL-2 receptor). This results in a positive feedback-loop to support further T cell proliferation and differentiation. The lack of IL-2 slightly impairs typical T cell mediated immune responses whereas overall T cell functionality is still maintained whereas latter differentiation pathways are affected[72]: For $CD8^+$ T cells, IL-2 is needed for proper memory cell generation[73] and additionally, it has been found that $CD4^+$ T cells need high concentrations of IL-2 to induce the expression of several transcription factors, like T-bet and Blimp-1, to preferentially generate $CD4^+$ effector T cells rather than memory cells[74]. In accordance to these findings, Liao et al. discovered a preferential generation of T_h1 cell compared to T_h17 cells or follicular T helper cells under the effect of IL-2[75].

By depletion of the main calcineurin isoform CnA β in T cells, with the result that NFAT family members c1, c2 and c3 cannot be de-phosphorylated anymore, Bueno et al. found in 2002 several effects on T cell function[76]. Due to the defective NFAT signaling cascade, beside an overall decreased T cell number as a result from impaired thymical maturation, a reduced TCR-induced activation and defective allogeneic tumor cell clearance was observed.

Interestingly, only overall NFAT protein levels – and not a specific family member - seem to have an impact on the generation of induced regulatory T cells (iTreg) from naïve $CD4^+$ T cells upon TGF-β co-stimulation, whereas suppressive capacities and cellular functions of natural regulatory T cells (nTreg) as well as of iTregs remains unaffected[77].

1.3.3 NFAT signaling in $CD8^+$ T cells

$CD8^+$ T cells maintain the integrity of the body by preventing intracellular pathogens and malformed cells from expansion. As described in 1.3.2, the expression of several key effector cytokines, such as IFNγ, TNFα and interleukin-2 depend on activated nuclear NFAT transcription factors. In a cohort of human patients suffering from bronchial adenocarcinoma, in 2009, Maxeiner et al. found a decreased level of *NFATc2* mRNA in lung tissues of those patients[78]. In an *Nfatc2*$^{-/-}$ mouse model for bronchoalveolar adenocarcinoma, these findings were verified by the finding that $CD8^+$ T cells lack the expression and latter production of TNFα and IL-2. In an adoptive transfer model, this group found a potential mechanism to inhibit lung cancer progression by the support of TGFβ1-mediated glucocorticoid induced regulatory T cells (GITR) inhibition by the transfer of $CD8^+$ T cell populations lacking *Nfatc2*. Agonistic anti-GITR monoclonal antibodies break self-tolerance by depletion of GITR cells and remove their suppressive capacity[79]. This removal of T cell tolerance leads to an elevated IFN-γ secretion which finally promotes $CD4^+$ T cell activation resulting in tumor growth inhibition connecting NFATc2 deficiency with impaired tumor cell clearance.

NFAT transcriptional activity in $CD8^+$ T cells was reported to be different from $CD4^+$ T cells since a signal motif for NFAT phosphorylation was triggered most exclusively in $CD4^+$ T cells whereas such phosphorylation events were missing in $CD8^+$ T cells. This should lead to the result that NFAT activity is impaired in $CD8^+$ T cells, shown as a general decreased IL-2 production[80].

Target cell killing by release of cytotoxic granules relies on TCR activation and clustering. Since there are several effector functions involved during rapid killing of malformed cells, the regulation of target cell killing appears at different levels. Key effector cytokines are directly under the control

of NFAT activation to enable gene transcription and - after translational processing and protein maturation in the ER – protein release into the extracellular space.

Lytic granule release followed by T cell activation is directly dependent on Ca^{2+} availability in the microenvironment close to the immunological synapse and can be provided immediately upon target cell contact[81]. In contrast, NFAT-mediated cytokine production requires multiple steps, namely TCR signaling, gene transcription, protein translation, ER maturation and final cytokine secretion. Therefore, in an CTL-exhaustive environment, NFAT activation can be inhibited whereas Ca^{2+} signaling is intact[82]. Apart from calcium-mediated effector functions of cytotoxic T cells, the Fas-Fas ligand mediated target cell killing pathway is clearly Ca^{2+} independent[83].

Specific blockage of the calcineurin-NFAT interaction by administration of the small peptide VIVID leads to a more punctual inhibition without influencing calcineurin phosphatase activity[84]. The peptide binds exclusively to the NFAT docking site on calcineurin showing a more specific abrogation of NFAT activation, compared to cyclosporine A. Administration of VIVID, bound to a cell permeable peptide for cellular uptake, to $CD4^+$ and $CD8^+$ T cells showed a decreased NFAT activity and IL-2 production upon stimulation. This suggests that also $CD8^+$ T cell-mediated diseases can be modulated by inhibition of calcineurin-NFAT interaction[85]. First experimental studies in a murine asthma model - which is mainly T_h2 mediated - showed less lung infiltrating inflammatory cells and milder clinical outcome. These results give the hint that NFAT is a critical regulator for inflammatory diseases in T cells[85].

In chronic viral infections, for example upon LCMV infections of mice, CTLs show a phenotype called exhaustion[86]. Those $CD8^+$ T cells are still able to degranulate and to kill target cells upon recognition since Ca^{2+} levels are not impaired so that direct effector functions can be provided. On the other hand, cytokine production (e.g. IL-2, IFN-γ[87] and TNF-α[88]) is markedly decreased because the nuclear translocation of NFAT is inhibited whereas other activation pathways, like NF-κB signaling, are still intact[89]. Calcineurin is also able to sense elevated Ca^{2+} levels in the cytosol through calmodulin but NFAT proteins are not dephosphorylated and specific target genes are not transcribed. This phenotype can also be found in patients suffering from HIV-1 infections[89] emphasizing NFAT as key regulator for proper cytotoxic T cell function.

Similar to the role of NFAT transcription factors in human and mouse $CD4^+$ T cells – especially with respect to cytokine expression profiles – in $CD8^+$ T cells, NFATs are involved in the expression of various cytokines as it was shown for $CD4^+$ and $CD8^+$ T cell populations in a murine GvHD model[90].

One other pillar in CTL-function – the lytic granule mediated target cell killing – has not yet been clearly investigated with regard to NFAT function. In T cells, NFAT activation can be blocked specifically by the addition of either FK506 or CsA[91]. First experiments dealing with the role of the immunosuppressive agent CsA[92] showed both CsA sensitive and CsA insensitive killing mechanisms of T cell populations towards various target cell lines. Another result shows that in a BLT esterase assay (as a readout for CTL mediated degranulation[93]), a clear reduction in human T cell degranulation upon target cell contact by addition of 100 nM CsA to the supernatant occurs[94]. This leads to the hypothesis that there are probably some alternative roles for the calcineurin-NFAT pathway that exist in addition to its classical role of the induction of gene transcription, acting more direct on the cytotoxic capacities of T cells[95].

1.4 Aim of the project

Because NFAT family members are key factors for T cell activation, proliferation and further effector functions, we investigated the role of the two main family members, NFATc1 and NFATc2, in purified $CD8^+$ T cells. While numerous experiments were already performed with $CD4^+$ T cells showing defective cytokine release and defective T helper cell development, no detailed studies existed for $CD8^+$ T cells. From these results, we want to examine the impact of NFAT abundance on the physiological functions of $CD8^+$ T cells *in vitro* and *in vivo* which play an important role in eradication of cells suffering from intracellular parasites, like various viruses or bacteria, as *Listeria monocytogenes*. We used the parasite *Listeria monocytogenes* as an infection model to study the role of T cells during intracellular infections.

Naïve $CD8^+$ T cells are developing to cytotoxic T cells upon antigen contact. This activates the T cell receptor signaling cascade, involving NFAT. Proliferation, affinity maturation and later generation of cytotoxic effector functions are maintained in the T cell zone of germinal centres *in vivo*. Mature cytotoxic T cells contain cytotoxic vesicles filled with preformed cytolytic proteins, as granzymes and perforin. Effector T cells show the ability to sense sites of infection by recognition of chemokine gradients spread by already activated innate immune cells. Upon activation by MHC-I T cell receptor (TCR) interactions, the lytic granules of the cytotoxic T cells fuse with the cell membrane in a calcium dependent manner. Due to this fusion event, the pH value in the lytic vesicles changes from acidic to neutral, and cytolyic proteins become activated to enter and induce apoptosis in the conjugated target cell by activation of the caspase-cascade. Lamp1 proteins are loaded on the cell surface to prevent the CTLs from self-damage.

Beside this primary function, cytokine release upon activation is also important to act as an attractant for other immune cells. Other cytokines, like TNF-α, may also directly act to induce target cell apoptosis. As there are multiple steps during cytotoxic T cell development, most of them starting with TCR activation leading to NFAT nuclear translocation and activation of specific gene profiles, NFAT family members – notably NFATc1 and NFATc2 - play an important role not only in cytokine production but also in other functions of CTL-mediated immune responses.

Materials and Methods

1.5 Materials

1.5.1 Mice

Mice were kept in the animal facility of the Center of Experimental Molecular Medicine (ZEMM) of the University of Würzburg. Offsprings were genotyped between week 4 and week 6 after birth (animal experiment license number: 55.2-2531.01-76/14).

For experiments, gender-matched littermates at the age from 6 till 12 wks were used. For some experiments, age-matched wild-type mice and knock-down mice from different breedings were used. If not mentioned otherwise, all mice were kept on C57/B6 genetic background.

BALB/c *wild type*	ZEMM/Würzburg
Cd4cre	Jackson Laboratory/Charles River
Nfatc1$^{fl/fl}$	A. Rao, Harvard University
Nfatc2$^{-/-}$	L. Glimcher, Harvard University
Nfatc1 ex3 eGFP	S. Klein-Hessling, University of Würzburg

1.5.2 Cell Lines

A20J	A. Beilhack, University of Würzburg
MOPC-315 FUG3 LW	A. Beilhack, University of Würzburg

1.5.3 Additives for cell culture

anti-murine IL-4 (polyclonal)	R&D Systems
human IL-2 (recombinant)	PeproTech
murine IFNγ (recombinant)	PeproTech
murine IL-12	PeproTech

1.5.4 Antibodies

Primary reagents for FACS analysis (anti-mouse)

Annexin V	FITC	BD Pharmingen
CD3ε (clone 145-2C11)	PE	BD Pharmingen
CD4 (clone GK5.1)	FITC	BD Pharmingen
CD8α (clone 53-6.7)	APC-Cy7	eBioscience
CD25 (clone PC61)	PE	BD Pharmingen
CD40l (clone MR1)	APC	BD Pharmingen
CD44 (clone IM7)	APC	BD Pharmingen
CD62l (clone MEL-14)	FITC	BD Pharmingen
CD69 (clone H1.2F3)	Biotin	BD Pharmingen
CD107a (clone 1D4B)	PE	eBioscience
FasL (clone MFL3)	PE	BD Pharmingen
Fc Block (αCD16/CD32)		eBioscience
Fixable Viability Dye	eFluor 450	eBioscience
Granzyme B (clone NGZB)	FITC	eBioscience
Granzyme B (clone NGZB)	PE	eBioscience
IFNγ (clone XMG1.2)	APC	eBioscience
IL-2 (clone JES6-5H4)	APC	Miltenyi Biotec
IL-17A (clone TC11-18H10)	PE	Miltenyi Biotec
MHC H-2 Kb OVA Tetramer, SIINFEKL	APC	MBL
Perforin (clone OMAK-D)	APC	eBioscience
Streptavidin	APC	eBioscience
Streptavidin	eFluor 450	eBioscience
TNFα (clone MP6-XT22)	PE	Miltenyi Biotec

Primary Antibodies for Western Blot analysis (anti-mouse)

Mouse-anti-NFATc1 (clone 7A6)	BD Pharmingen
Rabbit-anti-NFATc1α (polyclonal)	ImmunoGlobe
Rabbit-anti-NFATc2 (polyclonal)	CellSignalling
Mouse-anti-NFATc3 (clone F-1)	SantaCruz

HRP-coupled secondary antibodies for Western Blot analysis

Goat-anti-mouse HRP	Sigma-Aldrich
Goat-anti-rabbit HRP	Sigma-Aldrich

Primary antibodies (anti-mouse) and reagents for immunofluorescence

Granzyme B (clone NGZB) FITC	eBioscience
Fluoroshield with DAPI	Sigma-Aldrich

1.5.5 Antibiotics and Inhibitors

Ampicillin	Roth
Cyclosporin A (CsA)	Calbiochem
Golgi Plug (Brefeldin A)	BD Pharmingen
Golgi Stop (Monensin)	BD Pharmingen

1.5.6 Buffers

All solutions were prepared in freshly distilled H_2O.

PBS (1x)	NaCl (pH 7,4) 137 mM
	Na_2HPO_4 10 mM
	KCl 2,6 mM
	KH_2PO_4 1,8 mM
ELISA-stop buffer	H_3PO_4 1 M
ELISA-washing buffer	PBS (1x)
	Tween 20 0.05% (v/v)
FACS-buffer	PBS (1x)
	BSA 0.1% (w/v)
MACS-buffer	PBS (1x)
	BSA 0.1% (w/v)
	EDTA 2mM
Laemmli-buffer (1x)	Tris-HCl (pH 6.8) 125mM
	SDS 4% (w/v)
	Glycerin 20% (v/v)
	β-Mercaptoethanol 10%(v/v)

	Bromophenol blue 0.004% (w/v)
SDS-running buffer	Tris-HCl (pH 8.4) 25mM Glycin 192mM SDS 0.1% (w/v)
TAE (50x)	Tris-Acetate 2,5M Na_2EDTA (pH 8,0) 50mM
TBS (1x)	Tris-HCl (pH 7.5) 25mM Glycin 150 mM
TBS Tween (1x)	TBS (1x) Tween-20 0,05% (w/v)
Transfer buffer	Tris-HCl (pH 8.4) 48mM Glycin 40 mM SDS 14 mM Methanol 20% (v/v)

1.5.7 Chemicals

Acetic acid	Roth
Agarose	Roth
β-Mercaptoethanol	Roth, Gibco
Bradford Reagent	BioRad
Calcium Sensor Dye eFluor®514	eBioscience
Disodium hydrogen phosphate (Na_2HPO_4)	Roth
Dimethyl-Sulfoxide (DMSO)	Roth, Gibco
6 x DNA loading dye	Fermentas
Dithiothreitol (DTT)	Roth
EDTA	Roth
Ethanol (EtOH)	Roth
Ethidium Bromide (EtBr)	Roth
Fetal Bovine Serum (FBS, Qualified, US origin)	Gibco
Fluoroshield with DAPI	Sigma-Aldrich
Glycine	Roth

Glycerol	Roth
HEPES	Sigma-Aldrich
Hydrogen chloride (HCl)	Roth
Isopropanol	Roth
LB Medium	Roth
Listeria Selective Agar Base, Oxford	Sigma-Aldrich
Listeria Selective Supplement, Oxford	AppliChem
LysoTracker Green	Life Technologies
Magnesium chloride	Roth
Methanol	Roth
Midori Green	Nippon Genetics
MitoTracker Deep Red	Life Technologies
Monosodium phosphate (NaH_2PO_4)	Roth
2-(N-morpholino)ethanesulfonic acid (MES)	Roth
Non-fat dried milk powder	AppliChem
Ponceau S	Sigma-Aldrich
Power SYBR Green PCR Master Mix	Life Technologies
Propidium iodide (PI)	Sigma-Aldrich
Sodium chloride (NaCl)	Roth
Sodium dodecyl sulfate (SDS)	Roth
Sodium hydroxide (NaOH)	Roth
Tetramethylethylendiamin (TEMED)	Roth
Triton-X-100	AppliChem
Tris	Roth
Trypan Blue Solution	Sigma-Aldrich
Tween-20	Roth

1.5.8 Data acquisition and analysis

For acquisition, analysis and presentation of the data, diverse computers from Hewlett-Packard, Fujitsu-Siemens and Samsung were used. On these systems, Windows XP and Windows 7 were installed. Following programs were used:

Microsoft Word 2013	Thomson EndNote X7

Microsoft Excel 2013	Microsoft PowerPoint 2013
CorelDraw X4	GraphPad Prism 5.0
BD CellQuest 3.3	BD FACSDiva 5.0
Tree Star FlowJo 8.8.6	Image Lab 3.0
ImageJ 1.48v	Leica ImagePro Plus

1.5.9 Equipment

Cell culture plates (384 well), black walls	Greiner, Nunc
Cell culture plates (96 well)	Greiner, Nunc
Cell culture plates (48 well)	Greiner, Nunc
Cell culture plates (24 well)	Greiner, Nunc
Cell culture plates (12 well)	Greiner, Nunc
Cell culture plates (6 cm)	Greiner, Nunc
Cell separation columns (LS)	Miltenyi Biotech
Cell strainer (70µm)	BD Pharmingen
Cover slips	Paul Marienfeld GmbH
Cryoconservation tube (2ml)	Greiner
Cuvette (quartz glass)	Hellma
Cuvette (plastic)	Braun
Erlenmeyer Flasks (1000ml, 500ml, 250ml)	Schott
FACS tubes	BD Pharmingen
Falcon tubes (50ml, 15ml)	Greiner
Forceps	Hartenstein
Microcentrifuge tubes (2ml, 1.5ml)	Eppendorf
Object slides	Hartenstein
Parafilm	Pechiney Plastic Packaging
Pasteur pipettes	Hartenstein
PCR plates (96 well, white)	Thermo Fischer
Pipette tips (1000µl, 100µl, 10µl)	Sarstedt
Razor blades	Hartenstein
Scissor	Hartenstein
Serological pipette (25ml, 10ml, 5ml)	Greiner

Sterile filter (0,2µm)	Sartorius stedim
Syringe (10 ml, 5 ml, 2 ml)	Braun
Syringe needle (27 GA, 23 GA)	Hartenstein
Tuberculin syringe (26 GA, 3/8")	Braun
Protran BA 85 Nitrocellulose	GE Healthcare
Whatman 3mm filter paper	Hartenstein

1.5.10 Instruments

Autoclave	Systec
Biofuge 15R	Heraeus
Cell Observer AxioObserver	Zeiss
Centrifuge 5418	Eppendorf
Confocal microscope TCS SP5 II	Leica Microsystems
MultiRad CP160	faxitron x-ray
Cytospin 2	Shandon
Gel Doc^{TM} XR^{+}	BioRad
Electrophoresis chamber	CTI
Electrophoresis power supply	Micro-Bio-Tech
FACS Canto II	BD
Fridge (4-10°C)	Siemens
Freezer (-20°C, -70°C)	Liebherr
Fusion SL	Vilber Lourmat
Humidified tissue culture incubator	Heraeus
Ice machine	Genheimer
Light microscope CK2	Olympus
FLUOstar Omega	BMG labtech
pH-meter	WTW
Photometer	Pharmacia
Shaker C40	GLW
T100 Thermocycler	BioRad
Thermomixer compact	Eppendorf
Tpersonal PCR machine	Biometra

Varifuge 3.0R	Heraeus
Vertical electrophoresis unit	Hoefer
Voltage source, GPS 200/400	Pharmacia
Vortex mixer	RA
Waterbath	Hartenstein

1.5.11 Kits

CD8 (Ly2) microbeads, mouse	Miltenyi Biotech
CD4 (L3T4) microbeads, mouse	Miltenyi Biotech
CellTrace™ CFSE Cell proliferation kit	Molecular Probes
Dynal® mouse pan T cell purification kit	Invitrogen
Mouse Granzyme B ELISA Ready-Set-Go!®	eBioscience
First Strand cDNA Sythesis Kit	Fermentas
InnuPREP DOUBLEpure Kit	Analytic Jena
Intracellular Fixation and Permeabilization Buffer set	eBioscience
Long PCR Enzyme Mix	Fermentas
NucleoBond Xtra Maxi	Macherery-Nagel
PCR Mix 2x	Fermentas
RNeasy Mini Kit	Qiagen
SuperSignal West Pico ECL Substrate	Pierce

1.5.12 Oligonucleotides

Oligonucleotides were ordered from Sigma-Aldrich or Eurofins mwg/operon and dissolved in dH_2O to a final concentration of 100 pmol/µl.

Genotyping primers

Primer	Sequence
Cd4cre (for)	5′ CGAGTGATGAGGTTCGCAAG 3′
Cd4cre (rev)	5′ TGAGTGAACGAACCTGGTCG 3′
Nfatc1 M111	5′ AACATTTGGCCTGCTTGATAGAG 3′
Nfatc1 M112	5′ CAACAGAAGCCAGCTTTCACAG 3′
Nfatc2 Glin1	5′ CAAGCCTCAGTGACAAAGTATCCACTT 3′

Nfatc2 Glin2	5′ AGCGTTGGCTACCCGTGATATTGC 3′
Nfatc2 Glin3	5′ CGAGCTGCCCATGGTGGAGAGAC 3′

Real time PCR primers:

Primer	Sequence
β-actin forward	5′ GACGGCCAGGTCATCACTATTG 3′
β-actin reverse	5′ AGGAAGGCTGGAAAAGAGCC 3′
Nfatc1 forward	5′ GATCCGAAGCTCGTATGGAC 3′
Nfatc1 reverse	5′ AGTCTCTTTCCCCGACATCA 3′
Nfatc1 P1 forward	5′ CGGGAGCGGAGAAACTTTGC 3′
Nftac1 P1 reverse	5′ CAGGGTCGAGGTGACACTAG 3′
Nfatc1 P2 forward	5′ AGGACCCGGAGTTCGACTTC 3′
Nfatc1 P2 reverse	5′ CAGGGTCGAGGTGACACTAG 3′
Nfatc2 forward	5′ TCATAGGAGCCCGACTGATTG 3′
Nfatc2 reverse	5′ CCATTCCCATCTGCAGCAT 3′

1.5.13 Standards

Gene Ruler 1 kb DNA-Marker	Fermentas
Gene Ruler 100 bp DNA-Marker	Fermentas
Page Ruler prestained protein ladder	Fermentas

1.5.14 Stimulators

anti-CD3ε (clone 145-2C11)	BD Pharmingen
anti-CD28 (clone 37.51)	BD Pharmingen
Ionomycin	Sigma Aldrich
TPA	Merck
mouse T-cell activator beads CD3/CD28	Life Technologies

1.6 Methods

1.6.1 Cellular methods

1.6.1.1 T cell preparation

Mice were sacrificed by CO_2 inhalation. Abdominal cavity was opened by a median cut and the skin was fixed with syringe needles. Inguinal, axillary and mesenchymal lymph nodes were prepared and separated from residual fatty tissue. Then, the spleen was removed and all lymphatic organs were stored in BSS/BSA on ice. For single cell suspension, organs were smashed through a 70 µm cell strainer in BSS/BSA medium. To remove red blood cells from the suspension, red blood cell lysis was performed as described (1.6.1.2). After red blood cell lysis and cell counting, some cells (5%) were used directly for FACS analysis (1.6.4). The rest was used for $CD8^+$ T cell isolation.

For T cell isolation, the "CD8 (Ly2) microbeads, mouse" kit or the "CD4 (L3T4) microbeads, mouse" kit from Miltenyi Biotech were used according to the manufacturer's protocol. After enrichment, purity of $CD8^+$ T cells was measured by FACS analysis (1.6.4), and cells were re-suspended in X-Vivo 15 medium to a final concentration of 2 x 10^6/ml.

1.6.1.2 Red blood cell lysis

For the removal of red blood cells from cell suspensions, cells were centrifuged, the supernatant was aspirated and the cell pellet was re-suspended in 2 ml TAG buffer per spleen. Suspension was incubated for 5 min at 37°C and 5% CO_2 in a humidified incubator. The cells were again centrifuged, re-suspended in BSS/BSA and cell counting (1.6.1.5) was performed.

TAG Buffer:	NH_4Cl 150 mM
	Tris-HCl 20 mM, pH 7.2

1.6.1.3 T cell stimulation

T cells from spleen and lymph nodes were stimulated in 3 different ways to measure diverse response activities referring to different experimental settings:

1. αCD3/CD28 stimulation.

These antibodies bind specifically to the CD3ε component of the TCR complex, and additional CD28 co-receptor stimulation provides full activation of T cells. To achieve efficient stimulation, T cell receptor crosslinking was simulated by attachment of the immunoglobulins to the surface of the wells.

For optimal binding, 5 µg of CD3ε antibodies and 2 µg of CD28 antibodies were diluted in 1 ml of ice cold PBS. The following volumes were transferred into multi-well plates:

Plate	Volume of diluted stimulators per well (µl)
12-well	1000
24-well	500
48-well	200

Prepared plates were incubated for at least 30 minutes at 37°C in an incubator before washing 3 times with pure PBS to remove residual unbound antibodies. Finally, T cell suspensions were pipetted onto the coated wells.

2. BALB/c splenocyte stimulation of $CD8^+$ T cells:

To generate oligoclonal antigen-specific cytotoxic $CD8^+$ T cells (CTLs), freshly prepared naïve $CD8^+$ T cells were co-cultured with γ-irradiated BALB/c splenocytes that serve as target cells for 6 d. The $CD8^+$ T cells either directly recognize allogeneic antigens on the target cell surface or low amounts of residual dendritic cells are able to take up and present allogeneic peptides to the $CD8^+$ T cells. Irradiation leads to irreversible DNA double strand breaks in the target cells so that survival and proliferation of those cells is not maintained.

For this kind of stimulation, a spleen from a BALB/c mouse was prepared as described in (1.6.1.1) until red blood cells were removed by TAG Buffer lysis. Splenocytes were re-suspended in 2 ml BSS/BSA, transferred to a cryotube and irradiated in a MultiRad CP160 (faxitron x-ray) with a 30 Gy (5 min, 16kV) dose. After irradiation, cells were re-suspended at the desired concentration in X-Vivo 15 medium (1.6.1.4) for co-culture with B6 T cells.

3. TPA/Ionomycin stimulation:

12-*O*-tetradecanoylphorbol-13-acetate (TPA) is a phorbol diester. By binding to and activating protein kinase C[96], lymphoid cells become activated and start to proliferate[97]. Ionomycin calcium salt raises the intracellular Ca^{2+} level by releasing calcium from the endoplasmatic reticulum into the cytosol[98] resulting in activation of distal TCR-signaling. Together, both chemicals are potent activators of T cell signaling independent from antigen recognition or TCR binding of antibodies. This stimulation was mainly used to induce a secondary stimulation of already activated T cells for

stimulation of cytokine production to be detected for FACS analysis (1.6.4). TPA was added to T cell suspension at a concentration of 10 ng/ml, and ionomycin at a concentration of 5 nM for 6 h before analysis.

1.6.1.4 Cell culture

All cells were cultured under sterile conditions in a humidified incubator at 37°C and 5% CO_2. Cells were cultured in following media with indicated additives:

A20J cells:	
RPMI (prepared in the Institute of Virology and Immunobiology)	β-Mercaptoethanol (0,1%) FCS (10%)
T cells:	
X-Vivo 15 (Lonza)	β-Mercaptoethanol (0,1%) FCS (10%) L-Glutamine (1%) NEAA (1x) Penicillin/Streptomycin (1x) Sodium Pyruvate (1%)
MOPC cells (A.Beilhack, ZEMM, Würzburg):	
IMDM (Gibco)	β-Mercaptoethanol (0,1%) FCS (10%) L-Glutamine (1%) NEAA (1x) Penicillin/Streptomycin (1x) Sodium Pyruvate (1%)

1.6.1.4.1 Cryoconservation and thawing

Cell pellets containing 4 x 10^6 cells were re-suspended in 500 µl of cell culture medium in 2 ml cryotubes. 500 µl of 2x Freezing medium was added to the cell suspension and aliquots were placed in a freezer at -70°C. After 24 h, samples were transferred into a liquid nitrogen (N_2) container for long-term storage.

Freezing medium (2x):	36% DMEM
	44% FCS
	20% DMSO

For thawing, cryotubes were transferred in a waterbath at 37°C, until the solid phase disappeared. Cells were then transferred into a 15 ml tube, 5 ml of pre-warmed cognate culture medium was added and the suspension was centrifuged at 1400 RPM for 3 min. Supernatant was discarded, cells were again re-suspended in pre-warmed culture medium and finally seeded on cell culture plates.

1.6.1.5 Cell counting

Cell counting was performed using the Neubauer chamber: Cells were diluted with cell permeable dye Trypan Blue for dead cell staining to exclude membrane-disrupted dead cell from intact living cells. Non-blue cells were counted in four large fields. The mean value of these fields corresponds to the cell number in 1 µl of trypan blue-prediluted sample. Multiplication with 1 x 10^4 and the trypan blue dilution factor gives the cell number per ml of medium.

$$D = \frac{n}{S} \times d \times 10^4$$

D: cell density (cells/ml); n: absolute cell number in all fields; S: number of fields counted; d: dilution factor with trypan blue solution.

1.6.1.6 Centrifugation

If not mentioned otherwise, cells were sedimented in 15 ml/50 ml Greiner tubes for 3 min at 1400 RPM and 4°C in a Varifuge 3.0R. For cellular probes in 1.5 ml Eppendorf tubes, samples were loaded into a "Centrifuge 5418" (Eppendorf), and centrifugation was performed at 5 000 RPM for three minutes.

1.6.1.7 CFSE staining

Tracking of proliferation kinetics was performed with the cell permeable proliferation dye CFSE (Molecular Probes). This method was also used to differentiate two cell populations by labelling one of them prior to co-cultivation.

Non-fluorescent CFSE molecules passively diffuse into the cells where acetate groups are cleaved by cellular esterases. The cleaved CFSE form is membrane impermeable and stays within the cell. It emits light at wavelength of about 517 nm when excited at 492 nm. During cell division, CFSE

amount and signal intensity of each daughter cell decreases by 50% and can be traced by FACS analysis.

In general, 1 x 10^7 purified $CD8^+$ (or culture cells) were washed twice with 5 ml PBS and were re-suspended in 5 ml pre-warmed PBS solution. 2 µl of a 5 mM CFSE stock solution were then added to the cell suspension for 3 min. After incubation, samples were filled up with 3 ml pure FCS to stop labelling reaction. Cells were centrifuged, re-suspended in culture medium and used for further experiments.

1.6.1.8 Cytotoxicity assay

This assay was performed to determine the ability of generated allo-reactive CTLs to induce cell death in target cells.

A20J cells were labelled with CFSE (1.6.1.7). 1 x 10^4 cells in 100 µl X-vivo medium were pipetted into each well of a 96-well round bottom plate together with 100 µl of CTLs (1 x 10^6/ml). After 4 h of incubation at 37° C in the incubator, samples were transferred into Eppendorf tubes and FACS staining (1.6.4) for $CD8^+$ T cells was performed. Prior to FACS analysis, 2 µl of PI solution were added to the cell suspension to differentiate living A20J target cells ($CFSE^+$,PI^-) from dead cells ($CFSE^+$, PI^+).

1.6.1.9 Degranulation assay

One major physiological function of CTLs is the release of lytic granules upon target cell contact to induce target cell death. CD107a (Lamp1) is a membrane molecule which resides on the internal layer of lytic vesicles. Upon fusion with the cell membrane bilayer, the vesicles release their lytic stores, and CD107a remains on the cellular surface. These molecules can be detected by FACS analysis to differentiate cytotoxic ($CD8a^+$, $CD107a^+$) and non-lytical ($CD8a^+$, $CD107a^-$) CTLs.

A20J cells were labelled with CFSE (1.6.1.7), and 3 x 10^4 cells in 100µl X-vivo medium were pipetted into each well of a 96-well round bottom plate together with 100 µl of CTLs (1 x 10^6/ml). After one h of incubation at 37° in the incubator, 2 µl of CD107a-PE antibody were added to the well. After a total time of two h, cells were additionally stained with fluorescence-labelled $CD8^+$ antibodies for FACS analysis.

1.6.1.10 Luciferase assay

The mineral oil induced plasmacytoma (MOPC) cell line on the genetic background of $H2^b$ - similar to BALB/c cells - was used as a target cell line for the luciferase killing assays. These cells contain a luciferase transgene which is constitutively expressed. Therefore, upon cell membrane disruption and addition of luciferin, light emission can be detected in a luminometer. As this cell line originates from an allogeneic donor, allo-reactive B6 CTLs which naturally occur in the whole T cell pool recognize the MHC mismatch and are able to induce target cell death.

To detect the luciferase activity in target cells at several time points during co-culture with $CD8^+$ T cells, cells were re-suspended and aliquots were transferred into 1.5 ml Eppendorf tubes. After centrifugation at 10 000 RPM for one min, the cell pellet was washed once with PBS and finally re-suspended in 100 µl harvesting buffer to lyse cell membranes. After centrifugation at 10 000 RPM for one min, 50 µl of supernatant was transferred into a white, non-transparent 96-well plate. For determination of protein amount, 2 µl were taken for Bradford assay (1.6.8).

The injection needle of the LUMIstar Omega luminescence detector was primed with 1 ml of ready-to-use luciferin solution before luciferase-activity measurement could be performed. 50 µl of luciferin solution per well were automatically added to the samples and the measurement was performed.

Harvesting buffer:	DTT (1mM)
	Tris-HCl, pH 7.8 (50mM)
	2% Triton-X 100
	MES (50nM)
Luciferin solution:	K_2PO_4, pH 7.8 (5mM)
	10% luciferin

1.6.1.11 Calcium flux measurements of T cell populations

Calcium signaling is an important step in T cell function. Not only in the T cell receptor signaling cascade but a rise in Ca^{2+} is also mandatory for lytic granule release at the immunological synapse of $CD8^+$ T cells after target cell recognition. Thapsigargin is cell permeable and an irreversible intracellular Ca^{2+} inhibitor acting on Ca^{2+} sarco- and endoplasmic reticulum[99] ATPases (SERCAs) and, therefore, inhibits Ca^{2+} re-import from the cytoplasm into the ER. But still a continuous passive Ca^{2+} leakage through the ER membrane occurs. This lack of Ca^{2+} ions in the ER is sensed

by the stromal interaction molecules STIM on the ER membrane to activate ORAI-channels on the cell surface which induce an influx of extracellular Ca^{2+} ions. High calcium concentrations in the supernatant lead – in turn - to a massive Ca^{2+} uptake into the cell to fill intracellular stores again. This uptake/loss can be monitored by calcium sensitive dyes like Fura-2/AM which changes its' emission peak from 380 nm in calcium-free environment to 340 nm when calcium is available.

Cells were washed once in PBS and loaded with 2 µM Fura2-AM in Ringer's solution for 30 min at room temperature. After incubation, the cells were washed with Ringer's solution and stored for 10 min at room temperature and immediately used for the next steps. Glass coverslips were covered with poly-L-ornithine (0,1 mg/ml) and cells were settled on the surface of the coverslips in the flow chamber. The self-made sandwich flow chamber was used for the measurements and allowed a medium exchange within less than 1 s. The flow chamber with the attached cells was transferred on the stage of an Olympus IX 70 microscope equipped with a 20x (UApo/340, N.A. 0.75) objective. Alternating illumination at 340 and 380 nm was applied to the cells with a Polychrome IV Monochromator (TILL Photonics) by the usage of DCLP4 as dichroic mirror. The fluorescence at 440 nm was detected by a CCD camera system (TILL Imago) and analyzed by TILL Vision software. Ratios were recorded and calculated every 5 s.

For the experiments, Ca^{2+} free Ringer solution was generated by addition of 1 mM EGTA and Ringer solutions containing Thapsigargin with or without Ca^{2+} were applied by a syringe to the flow chamber.

Ringer's solution (ion concentrations)	155 mM NaCl
	4,5 mM KCl
	1 mM CaCl
	2 mM MgCl
	10 mM D-glucose
	5 mM HEPES (pH set to 7.4)

1.6.1.12 Tracking of cellular structures upon T cell activation

Upon formation of an immunological synapse, $CD8^{+}$ cytotoxic T cells polarize several cellular compartments towards the contact zone between target structure and their own cell membrane to provide a rapid delivery of effector functions. For example, cytotoxic granule release to mediate target cell death. This energy-dependent membrane fusion needs rapid energy delivery from

mitochondria and a continuous Calcium flux across the membrane to provide a strong activation signal. Therefore, those organelles need to be in dense contact with the generated IS.

For this assay, 1 x 10^5 cytotoxic $CD8^+$ T cells from MLR cultures were stained with cell permeable 100 nM Mitotracker Deep Red and 400 nM Lysotracker Green in X-Vivo medium containing 1% HEPES buffer for 30 min in an incubator. Labelled cells were centrifuged, re-suspended in 100 µl X-Vivo medium containing 400 nM Lysotracker Green and transferred into a black clear-bottom imaging 384 well plate. The plate was inserted into an incubation chamber connected with a microscope which provided 37 °C and 5 % CO_2. Cells were settled for 10 min so that most of them were attached on the cell culture plate bottom to ensure optimal focus over time. Pictures from bright field and corresponding Mitotracker Deep Red and Lysotracker Green channels were taken every 10 s with a 20x objective for 2,5 h and an exposure time of 300 ms. After adjustment of the focus, 2 x 10^4 mouse T activator beads (CD3/CD28) were added to the wells, and the measurement on the microscope (Cell Observer, Zeiss) using transmitted light and epifluorescence started.

Analysis was done by combination of single channels to a movie by ImageJ software (Version 1.48, Wayne Rasband, NIH, USA) and manual evaluation of bead-to cell contact events followed by movement of mitochondria/acidic lytic granules towards the contact zone. Active movement of cell compartments was assumed when the fluorescent structures remained at the contact site continuously for at least one minute.

1.6.2 Cytospin centrifugation of T cells

To visualize proteins at single cell level and their localization, cells were attached to a glass slide followed by antibody staining and confocal microscopy.

To attach T cells to a glass surface, 100 µl of cell suspension containing 1 x 10^5 cells were injected into a cone which was tied to a glass slide separated by a filter paper. A hole on the tip of the cone and in the filter paper led to a direct contact of the suspension to the glass surface. This assembly was inserted into a Cytospin 2 centrifuge (Shandon) and centrifuged for 3 min at 300 RPM. For latter recognition, cell spots were marked with scratches on the glass slide made by a diamond pen. Cytospin slides were dried for 30 min before immunofluorescence staining (1.6.5).

1.6.3 Enzyme linked immunosorbent Assay (ELISA)

In the context of $CD8^+$ T cell stimulation, culture supernatant was taken for granzyme B specific ELISA assay (eBioscience). The volume amounts of the manufacturers protocol were slightly

modified because costar® round 96-well half area plates (high binding, Corning) were used. The wells of the plate were first filled with 50 µl of capture antibody dilution (in 1 x coating buffer) against granzyme B, plate was covered with aluminum foil and incubated overnight at 4°C.
On the next day, wells were washed three times for one min with 100 µl washing buffer. To block unspecific binding sites, wells were incubated with 1 x ELISA diluent for one h. During this time, supernatant samples were diluted 1:20 with 1 x ELISA diluent to be within the detection range of the ELISA assay. Serial dilutions of standard granzyme B samples were performed to generate a standard curve and to calculate granzyme B levels in diluted supernatants. 50 µl of samples and standard dilutions were pipetted as duplicates into the wells and incubated overnight at 4°C.
After incubation, the wells were washed five times with 100µl of washing buffer. 50 µl of a biotin-tagged detection antibody was given to the wells to bind to the granzyme B proteins on the capture antibodies for one h. Wells were than washed again five times, and streptavidin-HRP (horseradish peroxidase) was pipetted into the wells. Again, five washing steps were performed. Streptavidin binds to biotin-tagged proteins so that HRP activity correlates with the amount of bound granzyme B. In a last step, a HRP-substrate solution was given to the wells for 15 min and the peroxidase reaction led to a color reaction to yellow, which was stopped by addition of 50 µl of stop solution turning into blue. Absorption was than measured on a FLUOstar Omega ELISA reader. The strength of absorption was proportional to initial granzyme B amount in culture supernatants. Dilutions of antibodies and standards was performed as described in the manufacturers protocol from mouse granzyme B ELISA Ready-Set-Go!® kit (eBioscience).

Washing Buffer:	1 l PBS
	0.05% Tween-20
Stop Solution:	1 M NaH_2PO_4

1.6.4 FACS analysis

The Fluorescence Activated Cell Sorting (FACS) analysis is a high throughput technique to visualize the expression of surface or intracellular molecules on single cell level, in addition to the investigation of more basal features, like cell size and granularity which can be detected via a system of lasers and detectors. Molecules expressed by cell populations can be visualized by addition of and co-incubation with fluorescence labelled immunoglobulins or other antibodies.

Staining of cell surface antigens

For optimal staining, 1 x 10^5 to 1 x 10^6 cells were transferred into 1.5ml Eppendorf tubes and washed twice with 1 ml FACS Buffer. For splenic cell suspension, F_c block (1:200) was added in the second washing step to prevent unspecific antibody binding mediated by F_c binding to granulocytes, macrophages, monocytes and NK cells. After centrifugation at 10.000 RPM for one min in a centrifuge (Centrifuge 5418, Eppendorf), the supernatant was discarded, the cells were re-suspended in 100 µl FACS buffer supplemented with 1:200 fold diluted antibodies and incubated for 30 min on ice. The cells were washed again twice with FACS buffer, re-suspended in 100 µl, transferred into FACS tubes and finally used for FACS analysis.

Staining of intracellular antigens

Prior to intracellular (IC) staining, cells were treated with TPA/ionomycin (1.6.1.3), or MOPC cells were added as an allogeneic stimulus for 4 h. To track cytokine production upon T cell activation, release from the endoplasmatic reticulum and transport to the Golgi complex had to be inhibited by adding brefeldin A (3 µg/ml) and monensin (2 µM) to the culture supernatant during stimulation. IC staining was performed either separately or directly after staining of surface antigens (see above). Cells were centrifuged, supernatant was discarded and samples were re-suspended in IC fixation buffer. After incubation for 15 min at room temperature, cells were washed twice with 1 x permeabilization buffer and incubated in 100 µl of 1 x permeabilization buffer together with 0.3 µl of antibody in the darkness at room temperature for another 20 min. Before FACS analysis, cells were washed again with 1 ml 1 x permeabilization buffer and 100 µl were transferred into FACS tubes for measurement.

AnnexinV/PI staining

For viability staining, annexinV/PI staining was performed on $CD8^+$ T cells. When cells become apoptotic, phosphatidylserines –which are usually located on the internal side of the membrane-bilayer – turn to the outer membrane and can be stained with labelled annexinV. Propidium iodide (PI) is a non-membrane permeable dye, intercalates with double-stranded DNA and, therefore, shows membrane-disrupted dead cells.

Similar to the IC staining protocol, cells can be surface-stained prior to the annexinV/PI protocol. Cells were washed once in annexinV binding buffer (ABB) and re-suspended in 100 µl of ABB. Then, 1 µl of annexinV FITC reagent was added, and the cell suspension was incubated for 15 min at room temperature. After incubation, additional 100 µl of ABB were added, and cells were

transferred into FACS tubes. Right before FACS measurement, 1 µl of PI was added and cells were vortexed.

AnnexinV binding buffer:	$CaCl_2$ (2.5 mM)
	HEPES (10 mM)
	NaCl (149 mM)

1.6.5 Immunofluorescence staining

Prepared cells on glass slides (1.6.2) were fixed in 3% formaldehyde in PBS for 20 min and washed 3 times for 5 min with PBS. To permeabilize the cell membranes, slides were treated afterwards with 0.2% Triton-X 100 in PBS on ice for 15 min before washing was repeated (3 x PBS for 5 min). Incubation with granzyme B - FITC was done by putting single drops of 50 µl PBS and 1:200 diluted antibodies on the marked spots of the glass slides. The slides were transferred into a wet chamber and incubated overnight in the dark at 4°C. On the next morning, slides were washed again 3 times for 5 min in PBS. Glasses were left for 10 min at room temperature for evaporation of residual droplets. A drop of paramount+DAPI was put on the cells, and samples were sealed with a cover slip. Protected from light, the prepared samples were stored at 4°C for up to one month. Finally, the samples were analyzed by confocal microscopy (Confocal microscope TCS SP5 II (Leica) with the ImagePro Plus software (Leica)).

1.6.6 T cell differentiation assay

Under different stimulatory regimes, naïve T cell populations are able to differentiate towards different T-helper (for $CD4^+$ T cells, T_h) or cytotoxic T cell subsets (for $CD8^+$ T cells, T_c). As those two major T cell populations need similar cytokine/stimulatory conditions to differentiate towards T_h1/T_c1 subsets, whole splenic T cell populations were purified and stimulated for T cell differentiation.

1.6.6.1 Negative isolation of pan T-cells

For the T cell differentiation assay, a slightly modified protocol for T cell purification from splenic cell suspensions with a Dynal® Pan-T cell negative Isolation kit (mouse) from Invitrogen. This kit allows the purification of the whole $CD3^+$ T cell population of $CD4^+$ and $CD8^+$ T cells in one step. By antibody (and latter magnetic bead) binding to several other cell types like e.g. B cells, dendritic cells and granulocytes, the T cell population remains unaffected by this method.

Prior to T cell enrichment with the Pan-T cell negative Isolation kit, an erythrocyte lysis with TAG buffer was performed (see above). Cells from splenic cell suspensions were counted. Per 1 x 10^7 splenic cells, 500 µl FACS buffer was added and cells were re-suspended. To block unspecific binding of antibodies, 100 µl of heat-inactivated FCS was applied additionally to 100 µl antibody mix per 1 x 10^7 cells. The suspension was incubated for 20 min at 4°C to achieve optimal antibody binding. Meanwhile, one ml of dynabeads (per 1 x 10^7 cells) was washed and re-suspended in the same amount of FACS buffer. After incubation in the refrigerator, cells were centrifuged, the supernatant was discarded and washed with 30 ml FACS buffer. Finally, the cell pellet was re-suspended in 5 ml FACS buffer, and one ml of washed dynabeads was added to the cells. Binding of beads to the attached antibodies was done by incubation for 15 min at room temperature under continuous rotation of the tube. After incubation, additional 15 ml FACS buffer were added. The tube was placed in a magnet for 2 min to enable separation of bead-labelled cells from unlabelled ones. The residual supernatant not being attached to the tube walls contained negatively purified T cells and was transferred to a fresh tube. After centrifugation, cells were re-suspended in 5 ml RPMI+10% FCS, and the cell number was determined before proceeding to the next step (1.6.6.2).

1.6.6.2 T_1 differentiation

Purified pan-T cell populations were re-suspended in RPMI+10% FCS in a concentration of 1 x 10^6 cells per ml. Before, a 24 well plate was coated with CD3/CD28 monoclonal antibodies for 1 h in PBS at 37°C and 5% CO_2. For the differentiation towards T_1 phenotypes, the culture plates were coated with 4 µg/ml αCD3 and 2 µg/ml αCD28. To remove residual antibodies, the plates were washed twice with 1 ml PBS each per well. 1 x 10^6 cells were transferred into the wells and the following cytokines/antibodies were added:

hIL-2	10 ng/ml
mIL-12	10 ng/ml
mIFNγ	50 ng/ml
anti-mIL-4	5 µg/ml

After differentiation for 3 d, T cells were analyzed for protein expression upon TPA/ionomycin re-stimulation for 6 h followed by IC FACS staining.

1.6.7 *Listeria monocytogenes* infection model

To investigate the role of the transcription factor NFATc1 in $CD8^+$ T cell populations during an immune response to a pathogen *in vivo*, a model infection system of a facultative intracellular bacteria – *Listeria monocytogenes* (*Lm*) – was chosen. The impact of *Lm* infections on *Nfatc1*$^{fl/fl}$ *Cd4cre* mice was compared to *wild type* mice to determine the effect of NFATc1 in T cells during a T_h1 immune response. As *Lm* is an intracellular pathogen, $CD8^+$ T cells represent the major effector cell population of the immune system to eradicate the infection[100], whereas the $CD4^+$ T cell population remains mainly unaffected, but is still needed for development of a protective immunity[101].

Due to safety instructions from the animal facility, an attenuated *Lm* strain was used for the *in vivo* infections. Therefore, animal-to-animal transmissions could be excluded. The *ΔActA* mutated *Lm* strain is defective in the expression of the ActA protein, normally mediating direct cell-to-cell transmission of replicated bacteria drastically increasing the virulence up to 1000 fold[102].

To verify the induction of an immune response and for monitoring animal health parameters, the weight of the infected mice was measured at each day of the experiment. Values at the start of the

experiment (day 0) were taken as 100%, and weight changes of each mouse at the following days were calculated respectively.

1.6.7.1 Infection of C57/B6 mice with *Lm-Ova ΔActA*

The *Lm-Ova ΔActA* strain is an attenuated *Listeria* strain lacking the *ActA* gene and expressing the ovalbumin protein. To enable active intracellular movement of the *Listeria* and efficient infection of nearby host cells, the availability of ActA interacting with the actin filaments of the infected host cell is mandatory. If this mechanism is missing, the pathogenicity is reduced dramatically.
Bacteria titer from frozen stock solutions were determined by plating out serial 10-fold dilutions on *Listeria*-selective agar plates. Cultures for two d at 37°C were set up. Single colony forming units (CFU) were counted, and the stock concentration of *Listeria* was calculated.
To induce a full immune reaction towards the pathogen, 5 x 10^5 CFU from a cryoconserved vial stock of the *Lm-Ova ΔActA* strain were suspended to 200 µl PBS and injected i.p. into either *wild type* or *Nfatc1*$^{fl/fl}$ *Cd4cre* mice. For injections, 1 ml tuberculin syringes were used. Mice were monitored and body weight was noted daily during the experiment. Due to animal healthcare restrictions, mice were sacrificed at day 5 post-infection.

1.6.7.2 Determination of bacterial titers from the liver

As the liver is the primary target organ for *Listeria monocytogenes* infections, whole livers were prepared from sacrificed mice and put separately into plastic waste bags. Addition of 4 ml PBS containing 0,1% TritonX-100 led to the destruction of cellular membranes from the tissue to release intracellular *Listeria* particles. The organs were gently meshed by soft application of pressure to gain a homogeneous suspension from which 1 ml was put into an Eppendorf tube. Serial 1:10 dilutions in PBS were made from those suspensions. 100 µl from each dilution was plated out on *Listeria*-selective agar plates, sealed in a plastic wrap to prevent plates from dehydration and incubated for two d at 37°C. White spots on the agar plates represent single bacteria colonies, which were counted and calculated with the corresponding dilution factor to gain the original bacteria burden per liver.

1.6.7.3 Tetramer staining for single antigen-reactive CD8$^+$ T cell populations

The usage of a transgenic *Lm-Ova ΔActA* strain continuously expressing the chicken-egg derived ovalbumin protein leads to an activation followed by proliferation of Ova-peptide specific CD8$^+$ T cells. The main immunogenic peptide sequence which is recognized by a distinct set of CD8$^+$ T cell populations is the $Ova_{257-264}$ sequence SIINFEKL that serves also as a model antigen. MHC class I tetramer molecules loaded with SIINFEKL peptides and labelled with APC molecules were used to determine SIINFEKL-specific CD8$^+$ T cell populations during the immune response.
For labelling of splenic SIINFEKL-specific CD8$^+$ T cells, single cell suspensions from the spleen were prepared and re-suspended in FACS buffer containing 1:200 diluted F_c-blocking antibody for 15 min at room temperature. Suspensions were washed once with FACS buffer and stained for tetramers at an antibody dilution of 1:200 according to the "Staining of cell surface antigens" section in 1.6.4 followed by fixation with FACS buffer containing 0,2 % formaldehyde before analysis in the flow cytometer.

1.6.8 Western blot analysis

Classical Western blot analysis visualizes proteins from cell extracts separated by size upon antibody-staining. Therefore, five steps have to be performed:

1. Protein preparation from cells
2. Electrophoretic separation on an polyacrylamide gel (SDS-PAGE)
3. Blotting on a nitrocellulose membrane
4. Labelling with primary antibodies
5. Detection of proteins of interest by secondary antibodies and ECL system

Protein preparation

At least 2 x 10^6 cell culture cells were transferred into a 1.5ml Eppendorf tube and washed with PBS. After centrifugation, the cell pellets were re-suspended in 40 µl of RIPA Buffer. The lid of the Eppendorf tube was then closed and the samples were snap-frozen in a box containing liquid N_2 for 10 seconds followed by thawing. After repetition of the procedure, samples were incubated on ice for additional 30 min. To ensure efficient cell lysis, sonification was performed in a further

step. In a cold room, the sonificator was used with the following setup: 30'' pulse and an amplitude of 50%. Cell lysates were then centrifuged at 4°C for 10 min at 10 000 RPM, the supernatants were transferred into a fresh tube and pellets containing cell debris were discarded.

RIPA buffer:	EDTA, pH 8 (1 mM)
	1% NaCl
	1% Na-deoxycholate
	1% Protease Inhibitor
	0.1% SDS
	Tris HCl, pH 7.5 (50 mM)
	1% Triton-X 100

To determine protein amount for equalization of samples, a protein determination assay was performed. This assay is based on characteristic changes in light absorption (from 465 nm of pure solution to 595 nm of protein-containing solution) of the "Protein Assay Dye Reagent" by interacting with acidic residues of proteins. The "Protein Assay Dye Reagent Concentrate" (BioRad) was diluted 1:5 with distilled H_2O and 1 ml of the dilution was added to 1 µl of supernatant in a plastic cuvette and shortly vortexed. Absorption was measured at 595 nm. A blank sample only with 1 µl RIPA buffer was used as negative control.

Electrophoretic separation

To saturate charged amino acid residues in proteins and to denaturate secondary protein structures, the samples were prepared with SDS-containing Laemmli-buffer[103] in a 4:1 ratio and incubated for 10 min at 95°C. Samples were stored at -20°C or immediately loaded on an SDS-PAGE gel.

The polyacrylamide gel consisted of two phases, the stacking gel (5% acrylamide, pH 6.8) – in which protein samples are concentrated – and the separation gel (10% acrylamide, pH 8.8) – in which protein movement is influenced by the gel structure resulting in significantly slower movement of large proteins compared to smaller ones. This movement was mediated by a power supply providing 25 mA in 1x running buffer.

For all samples, 60 µg of protein per sample were used as input and 5 µl of prestained protein ladder (Fermentas) were used as marker. Electrophoresis was stopped when the blue running front was leaking from the gel.

Stacking gel (5%)	Separation gel (10%)	Reagents
2.1 ml	5.9 ml	H_2O
0.5 ml	5.0 ml	30% polyacrylamide mix
0.38 ml 1M pH 6.8	3.8 ml 1M pH 8.8	Tris-HCl
0.03 ml	0.15 ml	10% SDS
0.03 ml	0.15 ml	10% APS
0.00 3ml	0.015 ml	Temed

Running Buffer:	Glycine (192 mM)
	0.1% SDS (w/v)
	Tris-HCl, pH 8.5 (25 mM)

Blotting

After separation, the gel was carefully removed from the running chamber and put on a nitrocellulose membrane. Each side was completely covered with three layers of Whatman paper before insertion into a tank blot chamber filled with 1x transfer buffer. The nitrocellulose blotting was performed at 4°C for 2 h at 300 mA constant current. Successful transfer was verified by Ponceau S staining of the membrane.

Transfer Buffer:	Glycine (40mM)
	20% Methanol
	SDS (14mM)
	Tris HCl, pH 8.5 (48mM)

Protein detection and visualization

Unspecific protein binding sites were blocked by incubation of membrane in 4% non-fat dry milk dissolved in 1x TBS/0.05% Tween (TBST) for 1 h at room temperature. Membranes were incubated at 4°C with primary antibody in 4% non-fat dry milk in TBST overnight with gentle shaking. On the next day, membranes were washed three times with TBST for 5 min each.

For detection, specific horse-radish-peroxidase coupled donkey antibodies were used to induce a light-emitting reaction. Antibodies were diluted in 4% non-fat dry milk in TBST and poured onto the membranes. After 1 h of incubation with gentle shaking, the membranes were washed again three times in TBST for 5 min each. After drying the membranes on Whatman paper, ECL substrate (SuperSignal, West Pico) was prepared by mixing 1 ml of solution A with 1 ml of solution B.

Membranes were covered with the mixture and sealed with plastic film to prevent drying. Light emission was detected with a Fusion SL device (Vilber).

Antibody	Origin	Dilution
β-actin	mouse	1:1000
NFATc1 7A6	mouse	1:330
NFATc1 (α)	rabbit	1:500
NFATc2	rabbit	1:500
NFATc3	rabbit	1:500
murine Ig	donkey	1:5000
rabbit Ig	donkey	1:5000

1x TBS/ 0.05% Tween:	Glycine (150mM)
	Tris-HCl, pH 7.5 (25mM)
	0.05% Tween-20

1.6.9 Molecular biological methods

1.6.9.1 DNA isolation from tissue biopsies

For isolation of genomic DNA from cell tissues or mouse tail tips, samples were incubated in 20 µl of genomic lysis buffer (gLB) and proteinase K (0.6 mg/ml) overnight at 56°C. On the next morning, 480 µl water were added to the digest and samples were incubated at 95°C for 10 min for proteinase K inactivation.

Genomic lysis buffer:	EDTA (25 mM)
	NaCl (300 mM)
	0.2% SDS
	Tris, pH 8 (50 mM)

1.6.9.2 RNA isolation from cell suspensions

To prepare RNA, cells were first washed once with PBS. Then, 350 µl RLT buffer were added to the cell pellet and cells were re-suspended 4 times using a 20GA needle with a 1 ml syringe. Further steps of RNA isolation were performed following the protocol of the "RNeasy Mini Kit" (Quiagen).

RNA was eluted in 30 µl water. For determination of RNA quantity and quality, a photometer (Pharmacia) was used. RNA was diluted 1:50 in nuclease-free water and transferred into a Quartz glass cuvette. The optical density (OD) was measured by absorption at 260 nm. The quality was indicated by a ratio of OD_{260nm}/OD_{280nm} typically around 1.8.
For short-term storage, samples were stored at -20°C, for long-term storage (up to 6 months), RNA was stored at -70°C.

1.6.9.3 Gel electrophoresis

To detect and separate amplified DNA fragments by their size, agarose gel electrophoresis was used. Negative charges on the phosphate residues of the DNA result in the movement to the positive pole in an electric field. A gel electrophoresis chamber was filled with 1 x TAE buffer, and the agarose gel was added. DNA samples were diluted with 6 x loading dye (Thermo Scientific) and loaded in the gel slots. A power supply was switched on (120 V, GPS 200/400). Size analysis was performed by loading of 1 kb DNA ladder (Thermo Scientific) along the samples. DNA bands were detected by UV light excitation of the DNA intercalating dye Midori Green at 270 nm. Emission at 530 nm using a GelDoc™ XR+ (BioRad) system was detected and visualized by the Image Lab 3.0 software (Bio Rad).

Agarose gel (2.5%):	2.5 g Agarose
	5 µl Midori Green
	100 ml 1 x TAE Buffer

1.6.9.4 Generation of cDNA from RNA samples

For each experiment, equal amounts of RNA (generated in 1.6.9.2) were used to perform cDNA synthesis from samples. At least 50 ng of RNA was used as starting material for random hexamer binding. Further steps were performed using manufacturer's instructions from the "First strand synthesis Kit" (Fermentas). After 1:1 dilution, samples were directly used for RT-PCR (1.6.9.6) or stored at -20°C.

1.6.9.5 Polymerase chain reaction (PCR)

PCR is a method to amplify DNA by the use of heat-insensitive enzymes, nucleotide triphosphates, target specific DNA amplification primers and the cognate DNA template in a thermocycler. For a successful amplification, 3 main steps are required:

1. Denaturation of the double stranded target DNA
2. Annealing of primers to the DNA
3. Elongation of DNA

Under optimal conditions, this results in an exponential increase of DNA fragments of the target sequence. For standard PCRs, a ready-to-use PCR master mix (2x) was used. Cycling conditions were the following:

1. Denaturation: 20'' 95°C
2. Annealing: 20'' xx°C (xx: melting temperature of used primers)
3. Elongation: yy'' 72°C (yy: depending on fragment size; ~1 kb/min)

Informations about primer melting temperatures were taken from the Fermentas website (www.fermentas.com).

Elongation times for primers genotyping DNA from *Cd4cre*, *Nfatc1*$^{fl/fl}$ and *Nfatc2*$^{-/-}$ mice were 30''. Analysis of PCR products were performed by agarose gel electrophoresis (1.6.9.3).

PCR reaction mix:

1 µl DNA
0.25 µl Primer 1 (100pmol)
0.25 µl Primer 2 (100pmol)
10 µl PCR Master Mix (2x)
8.5 µl H_2O

1.6.9.6 Real-Time PCR

To quantify cDNA amounts within a probe, Real-Time PCR (RT-PCR) is a standard method to precisely measure initial RNA copy numbers. This method is based on fluorescence intensity detection of substances, such as SYBR-Green, which intercalates into double stranded (ds) DNA. The more dsDNA appears, the more the fluorescence intensity increases until a saturation of amplified DNA copy level is reached. The fluorescence-intensity curve follows a logistic growth function. The beginning of the exponential growth curve – where fluorescence intensity increases significantly compared to background signals – marks the threshold cycle (Ct) value. Cycling

conditions for Real-Time PCR were 2’ 50°C, 10’ 95°C, 40 cycles: (15’’ 95°C, 1’ 60°C), 15’’ 95°C, 20’’ 60°C, 15’’ 95°C.

For calculation of induced gene expression values compared to different treatment conditions, the ΔΔCt method was used[104]. A reference housekeeping gene (here: *Actb*), whose induction is not affected by the treatment, was used for normalization.

1.6.10 Graphical visualization and statistics

Graphical visualization of experimental results was performed with Prism5 (GraphPad) and ImageJ for visualization of time-lapse images. FACS data were processed with FlowJo7 software (TreeStar). For data management, Excel 2013 software (Microsoft) was used. Statistical analysis was made by two-tailed Student’s t-Test, two-way ANOVA and non-parametric Mann-Whitney test.

Results

1.7 Expression of NFAT family members in CD8$^+$ T cells

To gain a better overview of NFAT induction during CD8$^+$ T cell activation, we first investigated the expression of NFAT family members c1 and c2 in CD8$^+$ cytotoxic T cells, compared to their already well known expression patterns in CD4$^+$ T helper cells.

1.7.1 Differential regulation of *Nfatc1* and *Nfatc2* in CD4$^+$ and CD8$^+$ T cells during activation

NFAT transcription factors are directly linked to the TCR signaling cascade and become activated upon TCR stimulation. In a first experiment, naïve CD4$^+$ and CD8$^+$ T cells were purified separately from wild-type mice. In order to get all purified T cells activated *in vitro*, wells of culture dish plates were coated with antibodies against CD3ε and CD28. RNA and protein extraction from the cultured cells was performed at the indicated time points.

Another approach for investigating the transcriptional induction of *Nfatc1* upon T cell activation provides the use of a transgenic mouse model generated in our facility. Those mice bear artificial bacterial chromosomes (BAC) in their nucleated cells. In those artificial chromosomes, which were introduced into the germ line, an *Nfatc1* promoter region was cloned upstream (5') from a GFP-gene[105]. Whenever *Nfatc1* transcription is induced in those cells, a GFP-mRNA (and latter protein) is transcribed as well. This GFP expression can be monitored by FACS analysis or in western blot. In the following experiments, GFP occurrence was measured on the FACS Canto II.

Expression of NFAT family members c1, c2 and c3 upon activation was measured on cDNA (transcribed from mRNA) and protein level. All RNA data were calculated relatively to corresponding unstimulated T cell populations.

The cDNA expression, as a readout for RNA transcript levels, of the inducible P1 promoter of *Nfatc1* in CD4 and CD8 positive T cell populations is elevated after 3 d of αCD3/CD28 stimulation. A 3-4 fold increase of *Nfatc1* mRNA is typical for stimulated lymphoid cells. On the other hand, the P2 promoter activity in both T cell populations is markedly decreased upon activation. Overall *Nfatc1* expression is upregulated in CD8$^+$ T cell populations, whereas *Nfatc2/c3* mRNA expression is not significantly affected upon stimulation.

To verify the findings from qRT-PCR assays, experiments with the BAC-transgenic mouse model were performed in addition to visualize *Nfatc1* promoter activity as a readout of GFP protein intensity within the cell. Mean fluorescence intensity (MFI) values of BAC-transgenic T cell populations are increasing at 24 h of stimulation with αCD3/CD28. They reach a maximum fluorescence level after 3 d. In unstimulated T cell populations, $CD8^+$ T cells show a somewhat higher signal strength indicating an elevated basal *Nfatc1* promoter activity in those cells compared to the $CD4^+$ T cell compartment. Upon stimulation, $CD4^+$ T cells show a higher expression of GFP since at the endpoint of the experiment on day 3, $CD4^+$ T cells show a higher MFI compared to $CD8^+$ T cells.

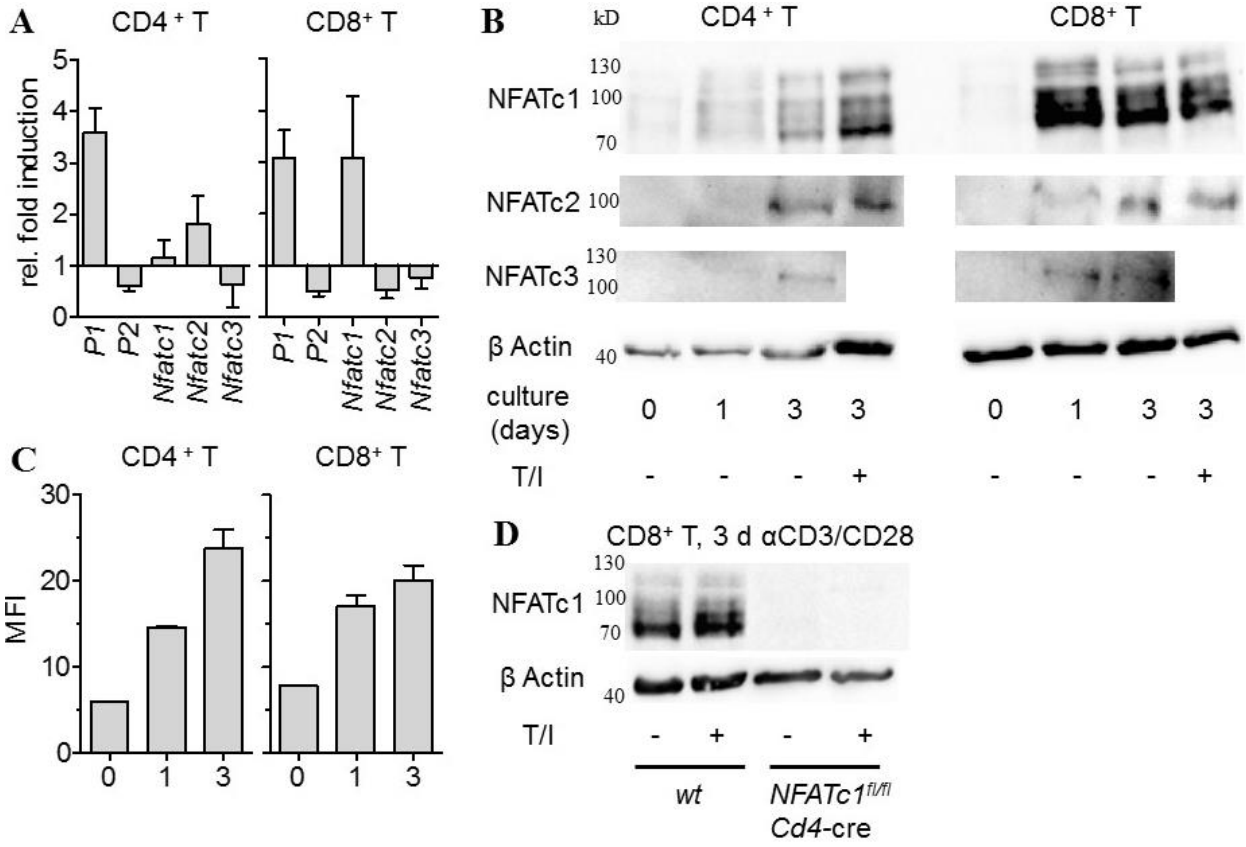

Figure 1: NFAT expression is upregulated upon T cell stimulation. NFAT mRNA (A) and protein (B) expression was measured after 3 d of stimulation with plate-bound αCD3/CD28 antibodies in $CD4^+$ and $CD8^+$ T cells. For western blot analysis (B), cells were additionally re-stimulated for 6 h with TPA/ionomycin. Measurement of transcriptional *Nfatc1* promoter activity (C) was performed using a BAC-transgenic mouse model. Labelling indicates the days of αCD3/CD28 stimulation. *Wild type* and *Nfatc1*$^{-/-}$ $CD8^+$ T cells were stimulated for 3 d, re-stimulated with TPA/ionomycin and equal protein amounts were blotted on a nitrocellulose membrane in (D). Values are shown with mean standard error bars.

On protein level, the overall NFATc1 concentration is drastically elevated after one and 3 d of αCD3/CD28 treatment. Re-stimulation with TPA/ionomycin does not lead to a further increase of total NFATc1 protein amounts neither in $CD4^+$ nor $CD8^+$ T cells compared to β-actin (The strong signal from NFATc1 in re-stimulated $CD4^+$ T cells results from a higher general protein amount loaded onto the gel). The NFATc2 protein amount is slightly elevated upon activation in $CD4^+$ T helper cells and in cytotoxic $CD8^+$ T cells as well. NFATc3 levels are increased only after prolonged stimulation (for 3 d) in both T cell populations.

To investigate if the *Cd4 cre* transgene is also expressed in $CD8^+$ T cells and acts on the cognate loxP sites in the *Nfatc1* gene, western blots of purified $CD8^+$ T cells - either from *wild type* or *Nfatc1*$^{fl/fl}$ *Cd4-cre* mice - after 3 d of αCD3/CD28 stimulation were performed (Figure 1 D). Successful disruption of the *Nfatc1* gene followed by loss of NFATc1 protein expression is shown by a clear luminescence signal for NFATc1 in *wt* but not in *Nfatc1*$^{fl/fl}$ *Cd4-cre* $CD8^+$ T cells. During T cell maturation in the thymus, cells undergo a *Cd4-Cd8* co-expressing stage. Therefore, the expression of *Nfatc1* is also suppressed in mature $CD8^+$ T cells.

Taken together, the results of transcriptional activity and the final protein amounts indicate that NFATc1 protein is induced in both T cell populations upon stimulation, whereas in $CD8^+$ T cells, expression on mRNA and protein level occurs to be stronger and earlier. Post-transcriptional mechanisms may also play a role in differential regulation of NFATc1 expression in $CD4^+$ and $CD8^+$ T cell subsets.

1.7.2 NFATc1 and c2 proteins are translocated to the nuclei of CD8$^+$ T cells upon stimulation

Nuclear translocation is required for the transcriptional activity of NFAT family members and can be easily monitored by confocal microscopy. CD4$^+$ or CD8$^+$ T cells were stained intracellularly for NFATc1 and c2. Since NFATc3 is not significantly affected during T cell activation (see Figure 1), antibody stainings were only done with the two most important NFAT family members in lymphoid organs - c1 and c2. Acquisition and visualization was done on a confocal microscope (TCS SP5 II, Leica) with the ImagePro Plus software (Leica).

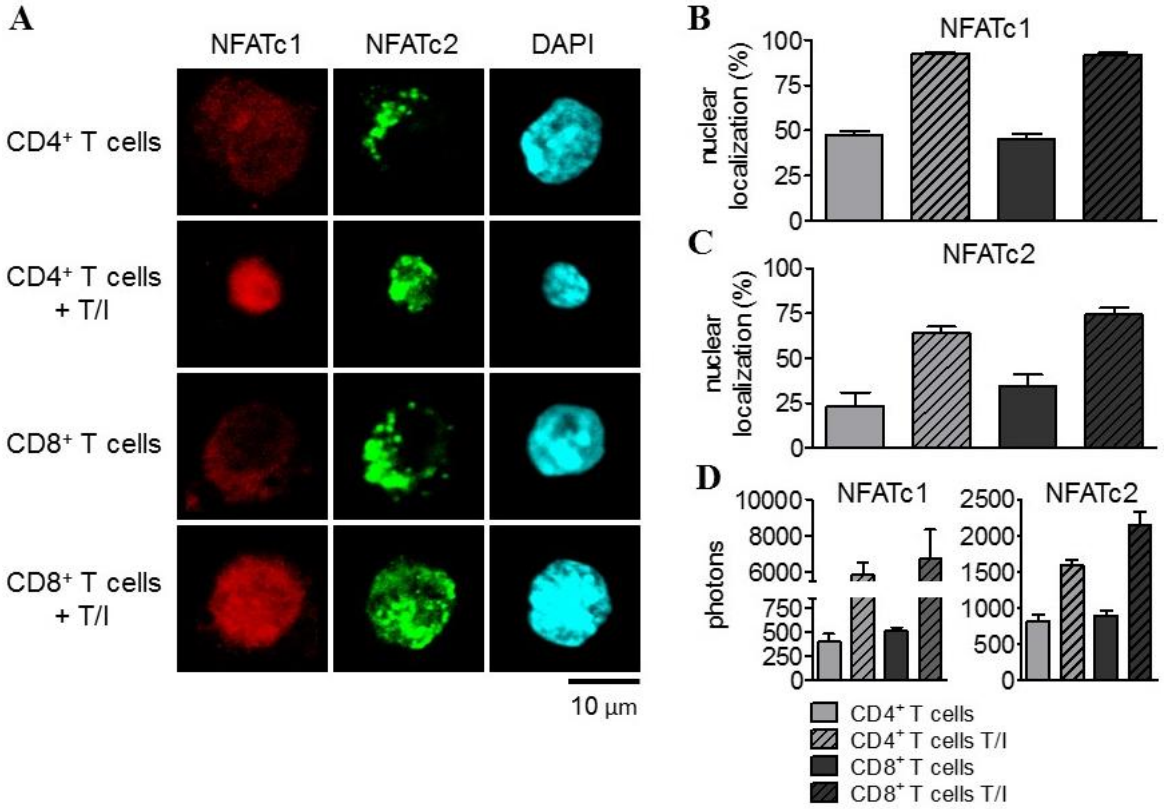

Figure 2: Upon stimulation, NFATc1 and c2 transcription factors are located in the nucleus. CD4$^+$ and CD8$^+$ T cells were purified and stimulated *in* vitro for 3 d with plate-coated CD3/CD28 antibodies. Representative pictures of cytospins from T cell populations were taken which were either re-stimulated with TPA/ionomycin for 6 h (hatched lines) or left in the medium (blank bars). Intracellular stainings for NFATc1, NFATc2 and the T cell nuclei were done (A). The overlapping light emission with the nuclear DAPI staining was correlated with those from bound NFATc1 (B) and NFATc2 (C) antibodies. Total light intensity in CD4$^+$ and CD8$^+$ T cell populations for both treatments is plotted in D. For optimal visualization, the brightness of signals from NFATc1 stainings was increased similarly in all corresponding pictures. Data from two experiments and at least 20 cells per condition are presented. Values are shown with mean standard error bars.

After 3 d of continuous stimulation, NFATc1 proteins were found to be equally distributed between the cytoplasm and nucleus in both cell populations. Ongoing activation leads to an almost complete nuclear import resulting in NFATc1-dependent gene transcription. Complete nuclear translocation – and NFATc1 protein induction itself – can be maintained by the addition of the phorbol ester TPA and the calcium ionophore ionomycin for 6 h. The rising of the signal intensity after re-stimulation is represented by a 10 fold increase in each T cell population. These findings appear to contradict the results from NFATc1 protein expression in T cell populations in Figure 1. Those conflicting results may originate from a different 7A6-NFATc1 antibody-binding affinity to the inactive/phosphorylated and activated/dephosphorylated protein. Since conformational changes upon NFATc1 de-phosphorylation and activation reveal the NLS under physiological conditions, this may be a reason for differential (enhanced) binding of antibodies to nuclear NFATc1. De-naturated proteins (on a nitrocellulose membrane) remain their primary protein structure diminishing different antibody binding affinities towards NFATc1. Different from the massive increase in NFATc1 protein expression, levels of NFATc2 expression were only slightly affected by TPA/ionomycin re-stimulation, as shown in a 2-3 fold increase in fluorescence intensity.

Similar to NFATc1, re-stimulation of T cells triggers translocation of NFATc2 from the cytoplasm to the nucleus. In non-re-stimulated T cells, NFATc2 proteins are mostly located in the cytoplasm but also become translocated to the nucleus upon TPA/ionomycin re-stimulation. Different from the transcriptional activation of NFATc1 where almost all proteins are located in the nucleus, the percentage of signals from cytoplasmatic NFATc2 proteins remains on a level of about 25 % in both T cell populations upon activation.

Taken together, both NFAT family members c1 and c2 are activated and translocated into the nucleus upon T cell stimulation to induce gene transcription. A strong activation-induced increase of NFAT on protein level can be observed for NFATc1. This may be due to modified antibody binding to different activation states because overall NFATc1 protein levels are not affected by TPA/ionomycin re-stimulation (see Figure 1).

1.8 Impaired proliferation capacity of NFATc1/c2-deficient T cells

To characterize the role of NFAT proteins during $CD8^+$ T cell stimulation, we investigated the activation of T cells isolated from NFATc1- and NFATc2-single and NFATc1/c2 double deficient mice. Purified T cells were stimulated with plate-bound CD3/CD28 antibodies for 3 d. Fundamental parameters, as proliferation and apoptosis, were investigated by CFSE staining and annexinV/PI measurements respectively.

The number of late-apoptotic ($annexinV^+$, PI^+) cells after 3 d did not significantly differ between all three knockout models compared to *wild type* cells, although in the *Nfatc1*$^{-/-}$*Nfatc2*$^{-/-}$ $CD8^+$ T cell populations a tendency to an increased apoptosis was observed.

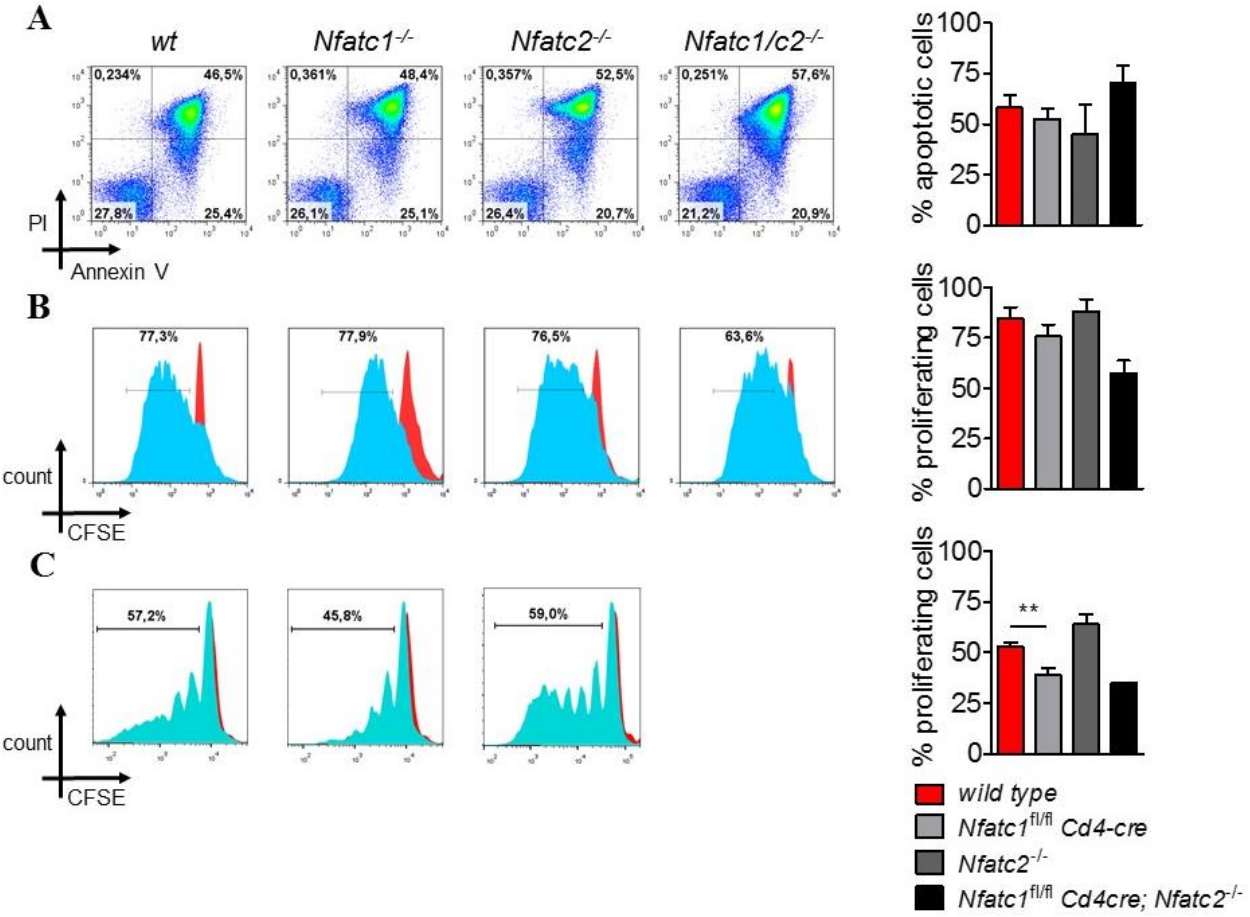

Figure 3: Impaired proliferation capacity of NFAT-deficient $CD8^+$ T cells. Purified $CD8^+$ T cell populations defective in either NFATc1, NFATc2 or in both transcription factors were labelled with CFSE and stimulated for 3 d with αCD3/CD28. The percentage of apoptotic cells was determined by annexinV/PI staining (A). $CD8^+$ T cells were either treated with a strong stimulus of αCD3 (5 µg/ml) (B) or a low dose of 50 ng/ml CD3 antibodies (C) but a constant concentration of αCD28 (2 µg/ml). Statistical analysis was performed by unpaired student's t-tests; ** $P < 0{,}005$. Values are shown with mean standard error bars.

Single deficient T cell populations only showed a moderate decrease in proliferation whereas *Nfatc1/c2* deficiency led to a marked drop in proliferative capacity, as visualized by a reduced rate of $CFSE^-$ cells within the living cell compartment upon strong stimulation (5µg/ml, B). Under those stimulating conditions, defects caused by the absence of either NFATc1 or c2 may be – at least partially - compensated by the other family members whereas a lack of both transcription factors led to a significant drop in the activation and survival rate.

Suboptimal stimulation of T cells (by 50 ng/ml αCD3) revealed a stronger effect of NFATc1/c2 absence on $CD8^+$ T cell proliferation. *Nfatc1*$^{-/-}$ $CD8^+$ T cells showed a significant drop in the proliferating cells from approximately 55% for *wild type* cells to 45% for *Nfatc1*$^{-/-}$ $CD8^+$ T cells whereas *Nfatc2*$^{-/-}$ $CD8^+$ T cells even showed an elevated proliferation level (Figure 3 C). NFATc1/c2-double deficient $CD8^+$ T cells showed a similar phenotype as *Nfatc1*$^{-/-}$ $CD8^+$ T cells in proliferative capacities, emphasizing the importance of NFATc1 during T cell activation and proliferation. NFATc2 has an inhibitory function regarding the proliferation capacity of $CD8^+$ T cells under suboptimal stimulation.

1.8.1 Reduced cytokine expression in NFATc1/c2-deficient T cells

An important physiological function of activated $CD4^+$ and $CD8^+$ T cells is their capacity to secrete and release cytokines with the aim to attract other immune cells, to provide stimulatory functions to components of the immune system (in the case of $CD4^+$ T helper cells) or to act as a direct mediator of cytotoxicity (as for cytotoxic $CD8^+$ T cells). As NFATc1 and c2 are well known transcription factors involved in cytokine gene expression, we observed distinct effects of NFATc1 and NFATc2 ablation of cytokine expression. Two setups were made to investigate the effect of T cell differentiation regarding the cytokine production of $CD4^+$ and $CD8^+$ T cell populations. As a control, naïve $CD3^+$ T cell populations were stimulated for 6 h with TPA/ionomycin and Golgi Plug + Golgi Stop. Other T cells were differentiated towards a T_h1/T_c1 phenotype for 3 d and re-stimulated as described above. To separate $CD4^+$ from $CD8^+$ T cell populations for analysis, fluorochrome labelled antibodies were used for flow cytometry.

In Figure 4, the percentage of cells expressing several cytokines (IFNγ, TNFα and IL-2) already characterized as targets of NFAT-dependent gene expression, are shown. In naïve T cell populations (Figure 4 A and C), only TNFα is rapidly induced after TPA/ionomycin stimulation whereas other cytokines remain low in expression upon TPA/ionomycin stimulation.

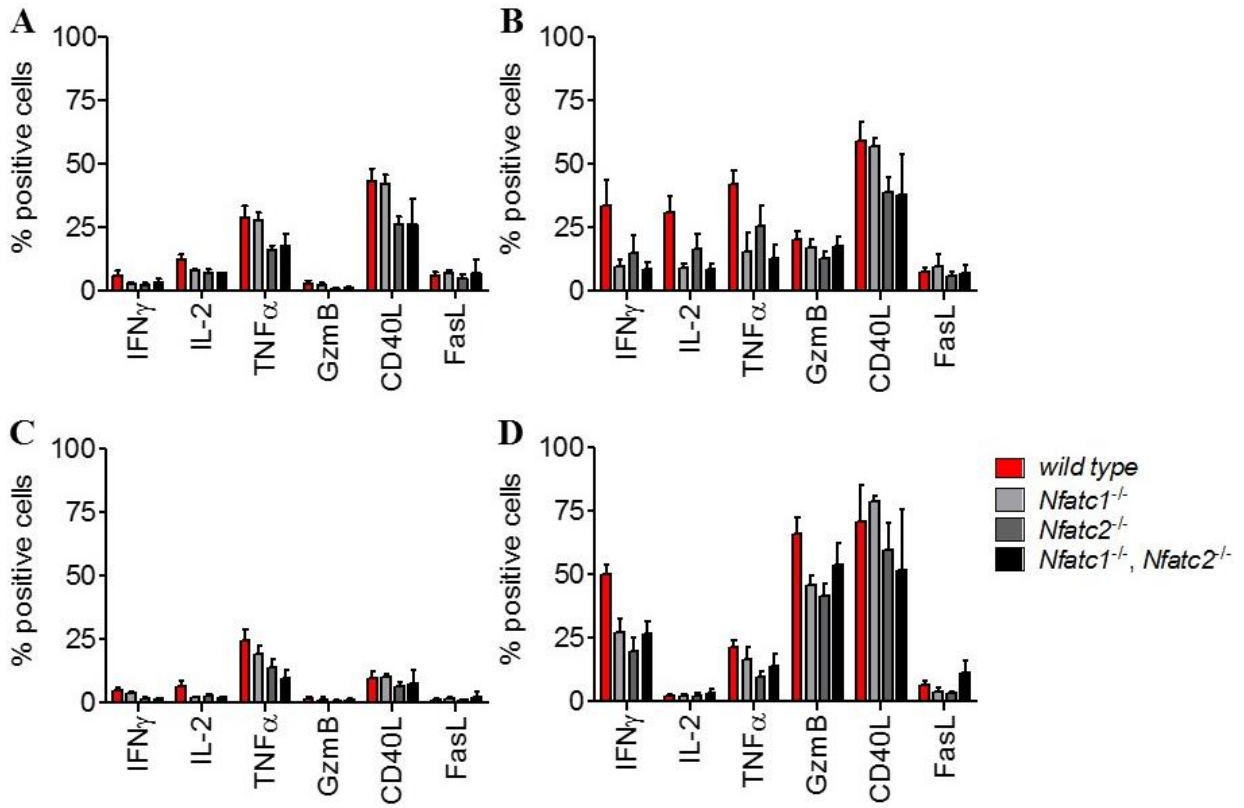

Figure 4: NFAT-deficient T cell populations are defective in cytokine production after T cell differentiation. Whole splenic T cell populations were purified from spleens and lymph nodes. Analysis for cytokine production was done upon addition of TPA/ionomycin (A and C) to freshly prepared naïve T cells or cells were kept for 3 d under T_h1/T_c1 polarizing conditions followed by TPA/ionomycin re-stimulation (B and D). After the incubation, $CD4^+$ (A and B) and $CD8^+$ (C and D) T cell populations were analyzed by flow cytometry for intracellular IFNγ, IL-2, TNFα, granzyme B, CD40L, and FasL expression. Values are shown with mean standard error bars.

The surface molecule CD40 ligand (CD40L) was detected by intracellular staining since it is known that attached antibodies (or CD40 molecules) may already lead to a mild activation followed by internalization of CD40L complexes and the loss of fluorochrome signal. In the naïve state, high numbers of $CD4^+$ T cells express CD40L. After 3 d of T_h1/T_c1 differentiation, the CD40L signal in $CD8^+$ T cells is elevated, even on a higher level compared to stimulated $CD4^+$ T cells. As granzyme B expression is not detectable in naïve T cell populations, after T cell differentiation about 60% of the generated T_c1 cells produce granzyme B whereas only about 20% of the T helper cells generate detectable amounts of granzyme B. However, contrary to naïve $CD8^+$ T cells, cytotoxic T cells are able to produce and secrete Granzyme B and other cytolytic components in high amounts (see also Figure 10).

Another mechanism which is important for the eradication of malformed cells is the Fas-FasL pathway. We did not observe a significant change in FasL expression on the cell surface neither in

$CD4^+$ nor $CD8^+$ T cells. In general, Fas ligand surface expression remained low after T cell differentiation. Because FasL expression is maintained on a very low level, no significant NFAT dependent differences of FasL expression were detectable in all knockout mice although the *Fasl* gene is known to be an NFAT target[106,107].

This model of polyclonal T cell activation seems to depend on cellular-mediated cytotoxicity by Fas-FasL interaction. Also, the impact of NFAT deficiency on cytokine expression upon activation could be monitored well in this context. A general, but moderate inhibition of cytokine production and secretion occurs under all three *Nfatc* knockout conditions, compared to *wild type* cells. Most striking effects were found for IFNγ production of differentiated T cell populations.

With respect to IFNγ and IL-2 expression, NFATc1/c2-double deficient T cells show a phenotype similar to *Nfatc1* single deficient T cells. In naïve T cells, $TNF\alpha^+$ producing *Nfatc1/c2*$^{-/-}$ cells were detected in similar numbers than *Nfatc2*$^{-/-}$ cells suggesting that the *Il2* and *Ifng* genes are NFATc1 targets whereas TNFα production depends more on NFATc2.

Broad variations in the appearance of intracellular CD40 ligand are not correlated with significant differences between activated cells of the four NFAT lines. Only naïve $CD4^+$ T cells showed a dampened CD40L expression upon TPA/ionomycin stimulation when *Nfatc2* is inactivated.

Beside perforin, granzymes – especially granzyme B – are mandatory for the cytotoxic capacities of generated CTLs. Granzyme B protein expression was measured as an evaluation of the availability of cytolotic granules within the cells. No statistical significant differences were found for T_c1 cytotoxic T cells, but a slight reduction in numbers of $GzmB^+$ $CD8^+$ T cells for *Nfatc1*, *Nfatc2* and *Nfatc1c2* knockout mice was found, compared to *wt* T cells. This led to the conclusion that NFAT function is involved in granzyme B expression and cytotoxic granule formation. Still, high granzyme B levels can be maintained in the cells for providing their cytotoxic capacities.

Taken together, the transcription factors NFATc1 and c2 are important for an efficient effector cytokine production in both T_h1 and T_c1 cells whereas other important key factors for CTL physiology, such as granzyme B and CD40L, are less affected by the loss of NFAT factors.

1.8.2 Allogeneic target cell killing is reduced in the absence of NFATc1

Since some effector functions of $CD8^+$ T cells are strongly affected by NFAT-deficiency (as for the production of IFNγ, IL-2 and TNFα) and others less (as granzyme B and FasL expression), the classical function to lyse and kill allogenic or infected target cells appear to be performed in the absence of NFAT. To investigate the killing capacity of polyclonally activated cytotoxic T cells, $CD8^+$ T cell populations from *wt*, *Nfatc1*$^{-/-}$, *Nfatc2*$^{-/-}$ or *Nfatc1/c2* double deficient mice were stimulated with plate-bound antibodies against CD3 (5µg/ml) and CD28 (2µg/ml) for 3 d prior to a killing assay. Living cells were counted and set at different effector:target cell ratios for the time intervals indicated. In addition to the measurement of luciferase signals, intracellular granzyme B expression and Lamp1 (CD107a) appearance on the surface of effector cells were measured by flow cytometry.

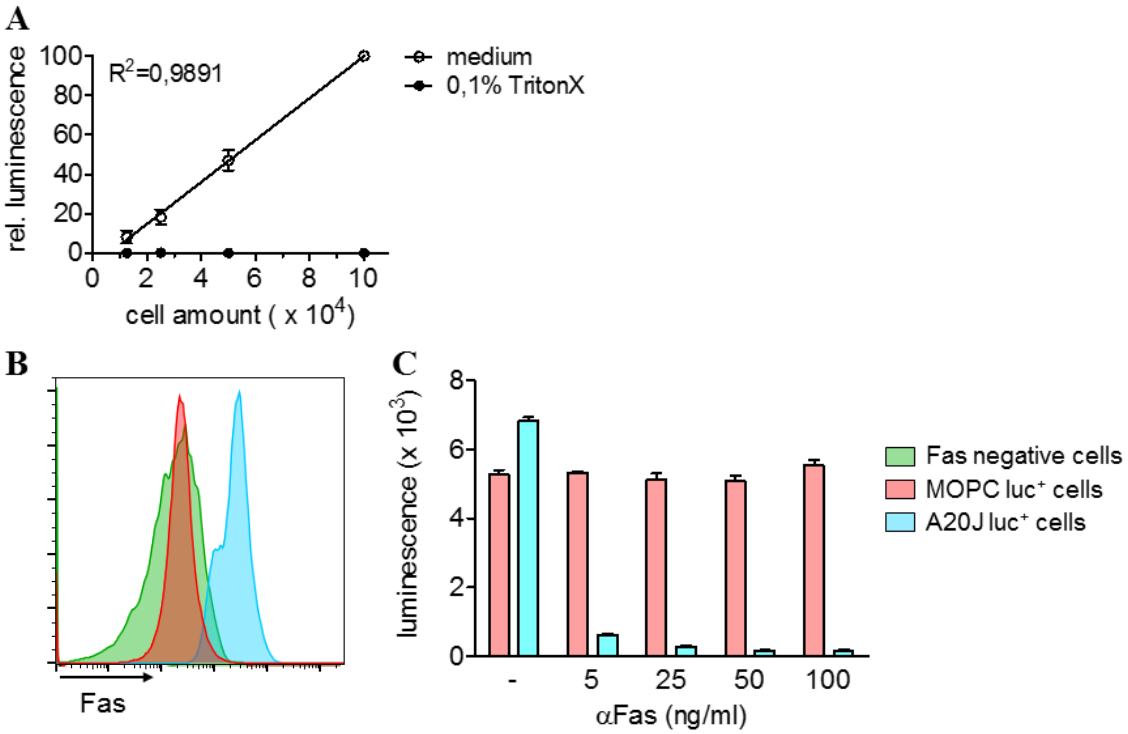

Figure 5: Contrary to Luc$^+$ A20J cells, MOPC cells are resistant to Fas-mediated killing. Luminescence signals from different cell amounts of Luc$^+$ MOPC cells cultured for 30 min were measured in (A). R^2 shows the correlation coefficient from cells cultured in medium. Flow cytometry staining for surface Fas expression was performed for MOPC (red) and control Luc$^+$ A20J cells (blue) in (B). A whole splenic T cell population was taken as negative control (green). The impact of different concentrations of multimeric Fas antibodies on cell luminescence/viability was investigated in (C). Values are shown with mean standard error bars.

To ensure that only granule-mediated killing is determined - and not additional Fas-FasL interaction followed by target cell death - the susceptibility of the MOPC cell line to execute Fas-induced cell death was determined as well.

In Figure 5, the linear dependence of light emission from luciferase positive cells is shown to demonstrate the correlation between the amount of target cells and the corresponding luciferase signal intensity. The more Luc^+ MOPC cell were seeded in a 96-well plate for 30 min prior analysis, the higher the luciferase activity was measured in cell lysates. As a negative control, same amounts of cells were treated with culture medium containing 0,1 % Triton X 100. This chemical acts as a detergent, incorporates into the cell membrane and leads to a disruption of the whole cell complex and induces apoptosis. From these cells, no significant increase of luciferase signal upon elevated cell amounts was detected as values remained at a basal background level.

To ensure that cell death induction can only be delivered by granule release from cytotoxic T cells, MOPC cells were tested for the expression of the Fas-receptor on their cell surface. As a verification for intact Fas-Fas ligand induced apoptosis induction, Fas antibodies were added at different concentrations to cell cultures overnight. To induce cell death, Fas-antibodies were administered as multimers to obtain a clustering of available Fas proteins on the cell surface. On the next day, the luminescence of cellular lysates was measured. As positive control, A20J cells, which were also transfected with a luciferase gene and originate from a murine BALB/c B-cell lymphoma, were used. Contrary to the MOPC cell line, A20J cells express Fas proteins on their cell surface, and, therefore, are susceptible to Fas-mediated killing, even upon administration of very low amounts of Fas antibodies. Moreover, the luminescence from MOPC cells remained unaffected by increasing amounts of Fas antibodies in the supernatant so a decrease of cell luminescence can only originate from reduced cell amounts not being affected by Fasl expression on effector cells.

In a first experiment for the evaluation of a CTL killing capacity, purified $CD8^+$ T cell from wild type mice were either stimulated with plate-bound αCD3 + αCD28 or were left unstimulated for 3 d. Polyclonally activated and unstimulated T cells were counted and seeded in a 96-well plate in various $CD8^+$ T cell and MOPC target cell concentrations and left overnight at 37°C and 5% CO_2 in the incubator.

To track the kinetics of the killing capacity from pre-stimulated *wt* and *Nfatc1*$^{-/-}$ CTLs, CTL-MOPC co-cultures were set in a 2:1 effector/target cell ratio and investigated at different time points from 2 h to 48 h after addition of target cells. The luminescence signals as readout for the amount of surviving target cells were recorded. A significant decrease in the luminescence from target cells was observed after overnight co-culture in both *wt* and *Nfatc1*-deficient cells, compared to target cells cultured without effector CD8$^+$ T cells. The luminescence signals were found to be decreased when co-cultures were kept for longer time periods. Co-cultures containing *Nfatc1*$^{-/-}$ effector cells showed a stronger luminescence readout compared to those from *wt* cells indicating a higher amount of living MOPC target cells (see Figure 5).

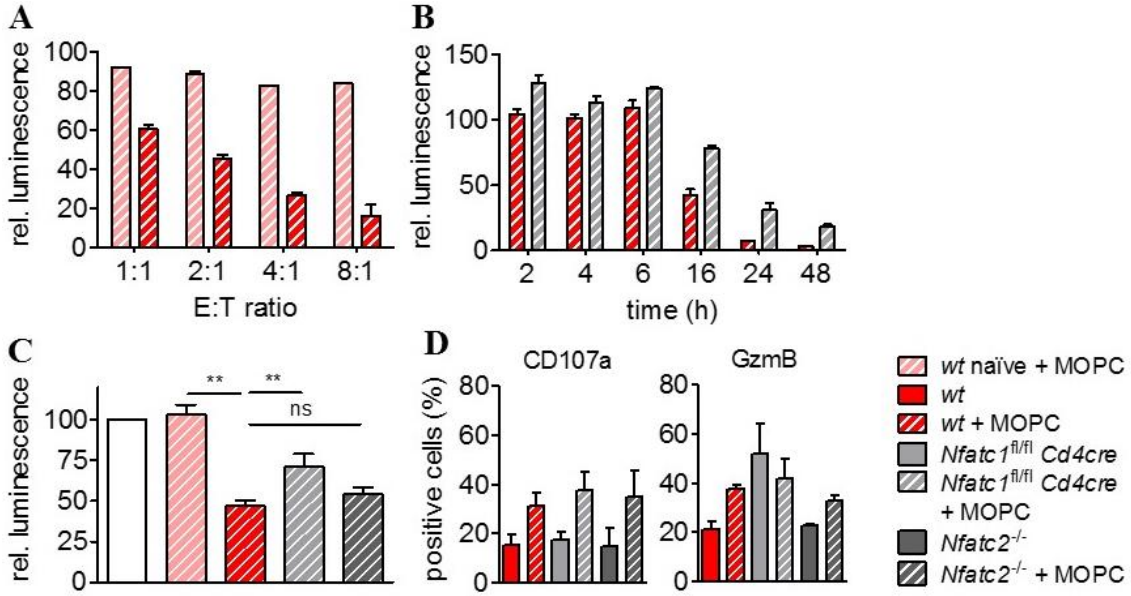

Figure 6: Allogeneic target cell killing depends on NFATc1. Splenic CD8$^+$ T effector cells (E) were either left untreated or stimulated with CD3/CD28 antibodies for 3 d. For the killing assay, effector cells were co-cultured with allogeneic MOPC target cells (T) at indicated ratios overnight followed by a luciferase assay (A). A comparative kinetics experiment between wild type and *Nfatc1*$^{-/-}$ CTLs shows their killing capacities (B). Luciferin signal from living target cells was determined after overnight co-culture with naïve wild type or primary stimulated CTLs from wild type, *Nfatc1* and *Nfatc2* knockout T cell populations (C). Surface Lamp-1 (CD107a) and intracellular granzyme B appearance on activated CD8$^+$ T cells was determined upon addition of target cells in (D); ** P < 0,005. Values are shown with mean standard error bars.

Figure 5 C shows the luminescence from target cells after overnight MOPC cultures with unstimulated *wt* CD8$^+$ T cells as a negative control or with *wt* CTLs or CTLs deficient for NFATc1, c2 or both family members. The effector:target cell ratio was set to 2:1, so that about 50% of the luminescence signal got lost in the killing assay containing wild-type cytotoxic CD8$^+$ T cells. Naïve CD8$^+$ T cells do not show any killing activity to allogeneic MOPC target cells whereas the light

emission from the luciferase is decreased to about 50% (Figure 6 A) upon addition of polyclonally pre-activated CTLs. This goes in line with the kinetics experiment shown before. CTLs lacking NFATc1 show only a mild decrease in target cell luminescence signals to 75% whereas NFATc2 deficient T cells don't show a different phenotype from wild type cytotoxic T cell co-cultures (Figure 6 C).

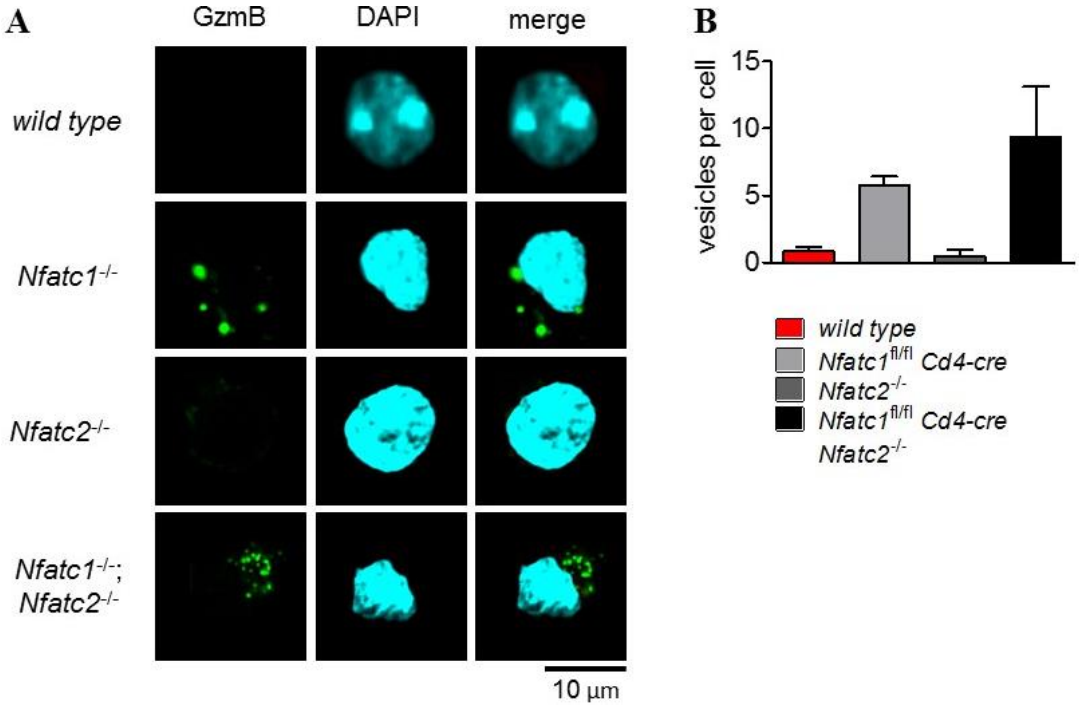

Figure 7: GzmB$^+$ lytic granules appear in stimulated CD8$^+$ T cell populations lacking NFATc1. Purified CD8$^+$ T cells were stimulated with αCD3/CD28 for 3 d. Cells from stimulated CD8$^+$ T cell populations were labelled with DAPI and antibodies against granzyme B (A)and analyzed by confocal microscopy. Green spots close to single cells were enumerated and are shown in (B).The figures show representative single cells from two experiments. Values are shown with mean standard error bars.

To investigate the decreased killing capacity of *Nfatc1*$^{-/-}$ cytotoxic T cells in more detail, flow cytometry stainings for surface expression of CD107a and intracellular granzyme B accumulation as indicators for lytic granule appearance were performed. Degranulated (CD107a$^+$) CTLs and granzyme B protein expression upon target cell-induced activation were traced after a time period of 6 h.

No significant differences were found for the activation-induced CD107a expression in both NFAT-deficient cells compared to wild type cells. A general increase in the percentage of CD107a$^+$ cells indicates successful MOPC-induced activation of several effector cells followed by fusion and degranulation of cytotoxic granules with the cell membrane for target cell killing.

Measurement of granzyme B-expressing compartment of cytotoxic cells showed an interesting phenotype: The expression of granzyme B was markedly upregulated from initially 20 to about 40% when target cells were added during the time of incubation in *wt* and *Nfatc2*-inactivated CTL populations. In *Nfatc1*$^{-/-}$cells, the percentage of GzmB^{+} CTLs was at a level of 50% of the whole CTL population after polyclonal stimulation for 3 d, and got not further increased in a co-culture with MOPC target cells (see Figure 6 C).

In accordance to the elevated numbers of granzyme B^{+} cells observed in the population of *Nfatc1*-deficient cytotoxic T cells, stainings of lytic vesicles with antibodies against granzyme B of polyclonally activated *wild-type*, *Nfatc1*$^{-/-}$, *Nfatc2*$^{-/-}$ and *Nfatc1/c2*$^{-/-}$ CD8^{+} T cells for confocal microscopy were performed. After 3 d of αCD3/CD28 treatment, 1 x 10^{5} cells were directly taken from the cell culture and used for cytospins. In addition to the detection of granzyme B, DAPI stainings were performed for the localization of nuclei.

Binding of FITC-labelled antibodies against granzyme B shows the presence of lytic granules in cytotoxic T cells. Only in *Nfatc1*$^{-/-}$ T cells (i.e. in single *Nfatc1*-inactivated T cells and *Nfatc1/c2*-deficient T cells), cytotoxic granules appeared in the cytoplasm. In *wild-type* and single *Nfatc2*$^{-/-}$ cells, virtually no granzyme B^{+} spots were found close to nuclei. These findings confirm the tendency of the flow cytometry results indicating that polyclonally activated *Nfatc1*$^{-/-}$ CD8^{+} T cells contain a higher percentage of granzyme B^{+} cells than those from *wild-type* mice (Figure 6). This seems to be the result of an accumulation of lytic vesicles in *Nfatc1*$^{-/-}$ CTLs suggesting an impaired granule release that contributes to the impaired killing capacities of cytotoxic *Nfatc1*$^{-/-}$ T cells.

1.9 The phenotype of allogeneically primed NFATc1-deficient CD8^{+} T cells

To generate a viable CD8^{+} T cell population with high affinity to a defined group of antigens, naïve CD8^{+} T cells were purified from *wild type* and *Nfatc*$^{-/-}$ mice in a first step and incubated in co-cultures with irradiated BALB/c splenocytes. Lethal irradiation of BALB/c splenocytes with 30 gray led to an inhibition of transcription and, thereby to the inactivation of cells. Therefore, BALB/c splenocytes (H-2K^{d}) serve as a primary allogeneic stimulator for naïve B6 CD8^{+} T cells (H-2K^{b}) without affecting the physiology of B6 CD8^{+} T cells. BALB/c splenocytes die soon after cell culture for 2 d. After 6 d of cell culture, the surviving CD8^{+} T cells were analyzed for various parameters.

1.9.1 Increased apoptosis of NFATc1-deficient CTLs

Proliferation and apoptosis are major events which regulate the pool of CTLs during immune responses. Those basal parameters of $CD8^+$ T cell survival were recorded by CFSE labelling and annexinV PI-staining after 6 d of MLR culture, respectively.

Counting of total viable cells by staining with trypan blue solution in a Neubauer chamber showed that only about 50% of the *Nfatc1*-deficient $CD8^+$ T cells survived after 6 d of cell culture compared to *wt* cells which were set to 100% for each experiment. Ablation of *Nfatc2* expression did not significantly influence the number of CTLs after 6 d of MLR culture whereas CTLs double deficient for NFATc1 and NFATc2 showed a cell number similar to *Nfatc1*$^{-/-}$ cytotoxic T cells.

To gain a better insight into the cause for the decreased cell numbers of *Nfatc1*$^{-/-}$ cells, the apoptosis of the cells was measured after 6 d, and kinetics in the BALB/c cell stimulation via CFSE staining of $CD8^+$ T cell were measured.

Stainings for annexinV and propidium iodide showed a significant drop in the percentage of AV^- PI^- events representing the viable cell compartment. The number of surviving cells decreased from about 30% in *wt* $CD8^+$ T cells to 15% in NFATc1-deficient T cells. In contrast, *Nfatc2*$^{-/-}$ $CD8^+$ T cells were not significantly reduced in cell viability, compared to *wild type* CTLs.

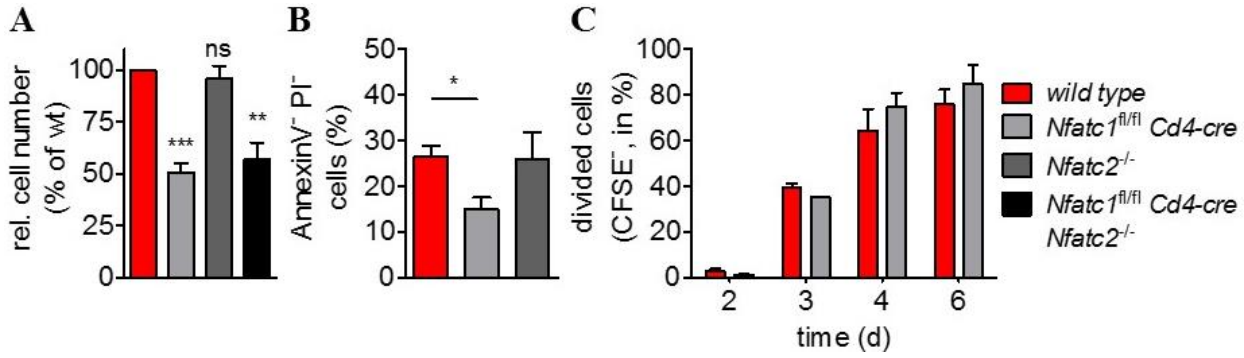

Figure 8: Apoptosis contributes to reduced generation of NFATc1-deficient CTLs during a mixed lymphocyte reaction. After 6 d of co-culture of B6 $CD8^+$ T cells together with irradiated BALB/c splenocytes, the remaining cells were investigated by counting trypan-blue$^-$ cells in a Neubauer chamber (A), moreover, and annexinV/PI staining for FACS analysis (B) was performed. In addition, a CFSE staining showing the percentage of proliferated ($CFSE^-$) CTLs at indicated days of co-culture was done (C). Values are shown with mean standard error bars. Statistical analysis was performed by unpaired student's t-tests; * $P < 0,05$; ** $P < 0,005$; *** $P < 0,0005$.

The other potential mechanism – i.e. decreased cell proliferation – was investigated by CFSE staining. Only a small fraction of $CD8^+$ T cells in both *wild type* and *Nfatc1*$^{-/-}$ populations is reactive to allogeneic MHC complexes in the naïve state. Therefore, a detectable fraction of $CFSE^-$ $CD8^+$ T cells rises from the mixed lymphocyte reaction at 3 d of cell culture. Because unstimulated $CD8^+$

T cells die after several days in cell culture whereas the proliferation of H-2K^{d}-reactive T cells progresses, the percentage of viable CFSE^{-} CTLs compared to the naïve (CFSE^{+}) T cell fraction rises up to about 80% in *wt* and *Nfatc1* inactivated cytotoxic T cells until day 6. Both CTL populations did not show any significant difference in number of proliferating cells at each time point during the whole period of the allogeneic stimulation. On the other hand, a fraction of about 20% CFSE^{+} unstimulated naïve CD8^{+} T cells remained alive in the whole T cell fraction and did not gain any effector function after incubation.

As a primary result, one significant defect of *Nfatc1*$^{-/-}$ CD8^{+} T cells compared to *wild type* and *Nfatc2*$^{-/-}$ CD8^{+} T cells is the increased ratio of activation-induced cell death whereas the general proliferative capacity is maintained in this model of allogeneic reactive CTL generation.

1.9.2 NFATc1-deficiency does not affects the expression of T cell activation markers

Since NFAT transcription factors play an important role in T cell activation, naïve and generated BALB/c reactive CD8^{+} T cell populations were examined for general T cell activation markers.

About 10% of cells from the spleen are CD8^{+} T cells. This ratio does not differ between *wt* and NFATc1-deficient T cell populations. A high percentage of CD62l (L-selectin)$^{+}$ and a low amount of CD44^{+} CD8^{+} T cells represents typical naïve T cell populations which develop towards a CD44^{+} CD62l^{-} effector memory cell population during antigen-induced stimulation. No differences in the expression of these markers were found neither in *wild type* nor in *Nfatc1*$^{-/-}$ cytotoxic T cells before and after allogeneic stimulation of CTLs.

The secretion of IL-2 by activated T cells enhances T cell proliferation in an intrinsic and extrinsic manner through the IL-2 receptor. CD25, which is a part of the IL-2 receptor (notably the α chain), is expressed upon activation to increase the reactivity towards secreted IL-2, and therefore acts as an additional marker for activated T cells. The increase of CD25 expression on unstimulated naïve CD8^{+} T cells from 4% to 20% in effector CTLs visualizes the activation process during the MLR culture. Interestingly, both CTL populations didn't show any differences in CD25 expression after initial activation.

The early T cell activation marker CD69 is expressed on a low level in unstimulated CD8^{+} T cells. After extensive MLR co-culture, CD69 levels are slightly increased but not significantly different between *wt* and *Nfatc1*$^{-/-}$ CTLs.

Interestingly, the expression of Fas-ligand in naïve NFATc1-deficient $CD8^+$ T cells is markedly increased to 5% compared to 2% $Fasl^+$ cells in *wild type* $CD8^+$ T cells. After 6 d of co-culture with BALB/c target cells, the difference disappears, and about 10% of each T cell population show a $Fasl^+$ phenotype.

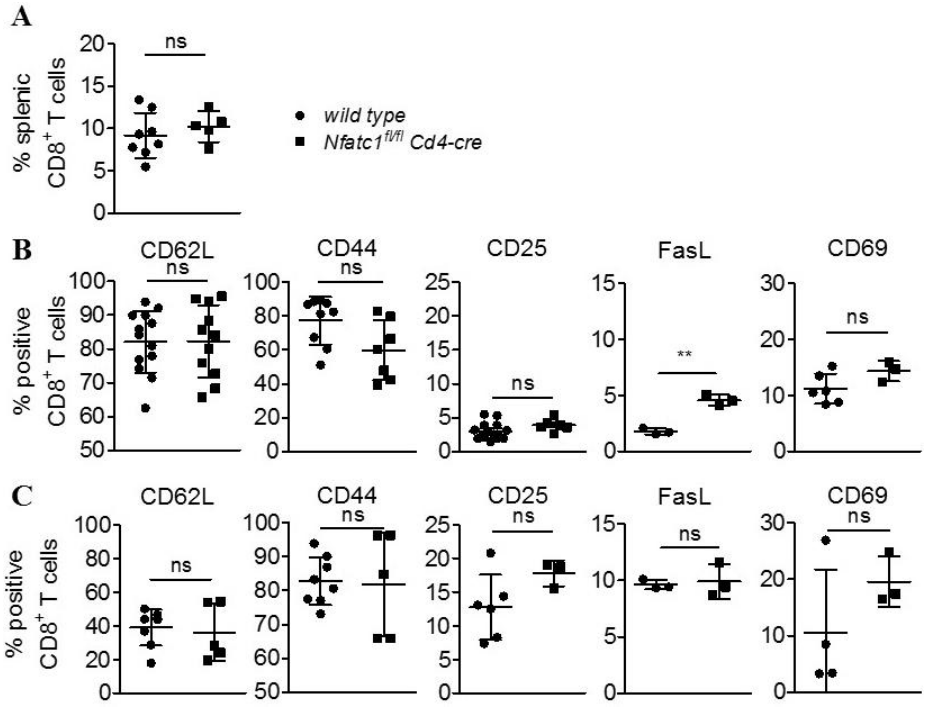

Figure 9: T cell activation markers are not altered in *Nfatc1*$^{-/-}$ $CD8^+$ T cells after allogeneic stimulation. Freshly prepared splenocytes from *wild type* and *Nfatc1*$^{-/-}$ mice were investigated for $CD8^+$ T cell populations (A) and several activation markers (B). After 6 d of $CD8^+$ T cell stimulation with irradiated BALB/c splenocytes, surface marker expression was determined again (C). Values are shown with mean standard error bars. Statistical analysis was performed by unpaired student's t-tests; ** $P < 0{,}005$.

Taken together, the expression of activation markers in *Nfatc1*$^{-/-}$ $CD8^+$ T cells was not significantly different to those in *wt* $CD8^+$ T cells. After 6 d of allogeneic priming of $CD8^+$ T cell population, typical activation- and memory markers were upregulated (CD25, CD44), whereas markers for naïve T cell were down-modulated (CD62l) in both CTL populations. Therefore, the *wild type* and *Nfatc1*$^{-/-}$ $CD8^+$ T cells showed virtually no difference in T cell activation.

1.9.3 Cytokine expression of MLR-generated *Nfatc1*$^{-/-}$ CTLs is impaired

NFAT transcription factors bind to several promoter regions of key cytokines upon T cell activation. Beside NFATc1, NFATc2 is also able to bind to promoter elements to induce gene transcription for various cytokines. In the following experiment, the expression of classical T_h1/T_c1 cytokines as IFNγ, IL-2 and TNFα as well as IL-17 expression was determined by intracellular flow cytometry of the generated CTLs after 6 d of the mixed lymphocyte reaction. After 6 h of TPA/ionomycin re-stimulation, and the addition of brefeldin A and monensin to trap proteins in the Golgi complex, cells were treated according to the IC staining protocol and recorded on a flow cytometer (BD FACS Canto II). However, intracellular granzyme B and perforin expression was only measured in freshly prepared CTL populations after the MLR culture without any re-stimulation. To get a better understanding of target-cell-induced CTL degranulation, granzyme B protein levels in the supernatants were determined by ELISA assays after the incubation of *wild type* and *Nfatc1*$^{-/-}$ CD8$^+$ T cells for 6 d with BALB/c target cells.

The percentage of IFNγ, IL-2 and TNFα expressing cytotoxic T cells was found to be reduced in all *Nfatc1/c2* single and double knockout CTL populations compared to the *wild-type* cytotoxic T cells. The lack of NFATc2 led to a somewhat milder reduction of cytokine-producing T cells, especially for TNFα and IL-2. The strongest decrease occurred in NFATc1/c2-double deficient T cells for IFNγ and TNFα, emphasizing the importance of both NFAT proteins for cytokine gene transcription in cytotoxic T cells. This underlines the overlapping function of NFATc1 and c2 in promoter activation of distinct target genes.

Measurement of perforin and granzyme B expression in CTLs showed slightly different results. NFATc1-deficient CTLs exhibited a higher percentage of cells containing perforin and granzyme B proteins compared to *wild type* and *Nfatc2*$^{-/-}$ CTLs. To investigate the question whether the lytic granule release from the primed CD8$^+$ T cells remains functional, cell culture supernatants from the MLR assays were taken and investigated for granzyme B amounts in ELISA assays.

In several parallel experiments, a significant difference was detected in granzyme B levels between *wild type* and *Nfatc1*$^{-/-}$ CD8$^+$ T cells showing a marked drop in granzyme B levels in the supernatants of *Nfatc1*$^{-/-}$ CTLs.

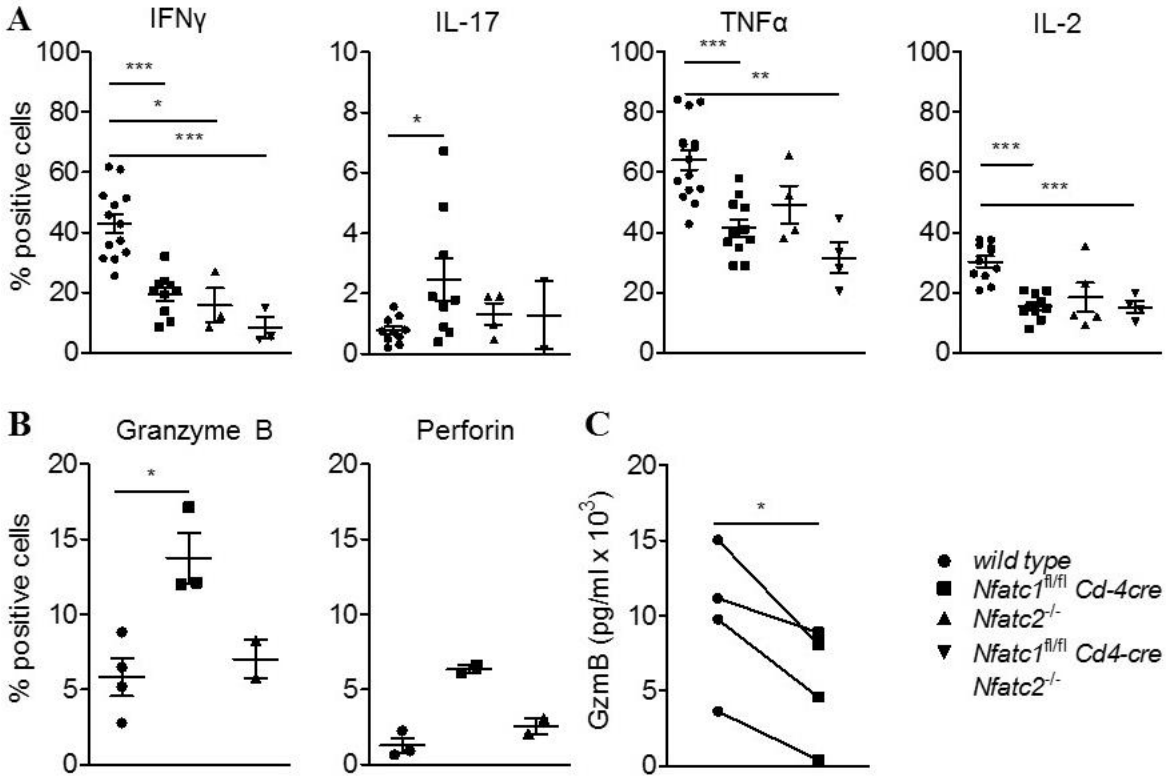

Figure 10: Cytokine expression of CD8⁺ T cells lacking NFATc1 and c2 is altered. Allo-reactive cytotoxic T cells were stained for IFNγ, IL-17, TNFα and IL-2 (A). The appearance of lytic granules was determined by intracellular measurement of granzyme B and perforin (B). Granzyme B protein amounts in the culture supernatant were determined in (C). Values are shown with mean standard error bars. In general, analysis was done by unpaired student's t-test but in (C) a paired t-test was used; * P < 0,05; ** P < 0,005; *** P < 0,0005.

NFATc1 and c2 are mandatory for efficient cytokine production in CD8⁺ T cell populations to sustain effector functions as well as to deliver cytotoxicity to infected or allogeneic target cells. Therefore, a lack of NFATc1 and/or NFATc2 led to a strong decrease in expression of several important cytokines, such as IFNγ, TNFα and IL-2.

1.9.4 Due to the lack of NFATc1, allogeneic target cell killing is reduced

In addition to natural killer (NK) cells, cytotoxic CD8⁺ T cells deliver direct cell-mediated cytotoxic signals to any non-self cell. As one of the two major mechanisms for mediating cytotoxic activity, lytic granule release from the effector CTL towards a target cell at the immunological synapse is an important step to mediate target cell apoptosis. Prominent components of cytolytic granules are Lamp-1 (CD107a, to prevent cytotoxicity towards the effector cell itself), perforin and

granzyme B. Perforin facilitates the uptake of granzyme B and other cytolytic proteins through the target cell membrane to induce target cell apoptosis.

A first set of experiments was set up to observe the effects of calcineurin-mediated NFAT inhibition in MLR-generated cytotoxic T cells upon addition of cyclosporin A (CsA).

The IFNγ promoter is a well-investigated target for NFAT upon T cell activation. Therefore, *wild type* allogeneic CTLs were investigated regarding their effector functions upon target cell and CsA addition. Unstimulated cytotoxic T cells show hardly any IFNγ producing cells. Addition of allogeneic A20J target cells for 4 h led to a marked increase of IFNγ-producing cells since the $CD8^+$ effector cells were initially stimulated with allogenic BALB/c target cells for 6 d. They share the same genetic H-$2K^d$ background. Following the protocol for detection of intracellular proteins, cells were treated with monensin and brefeldin A during the assay.

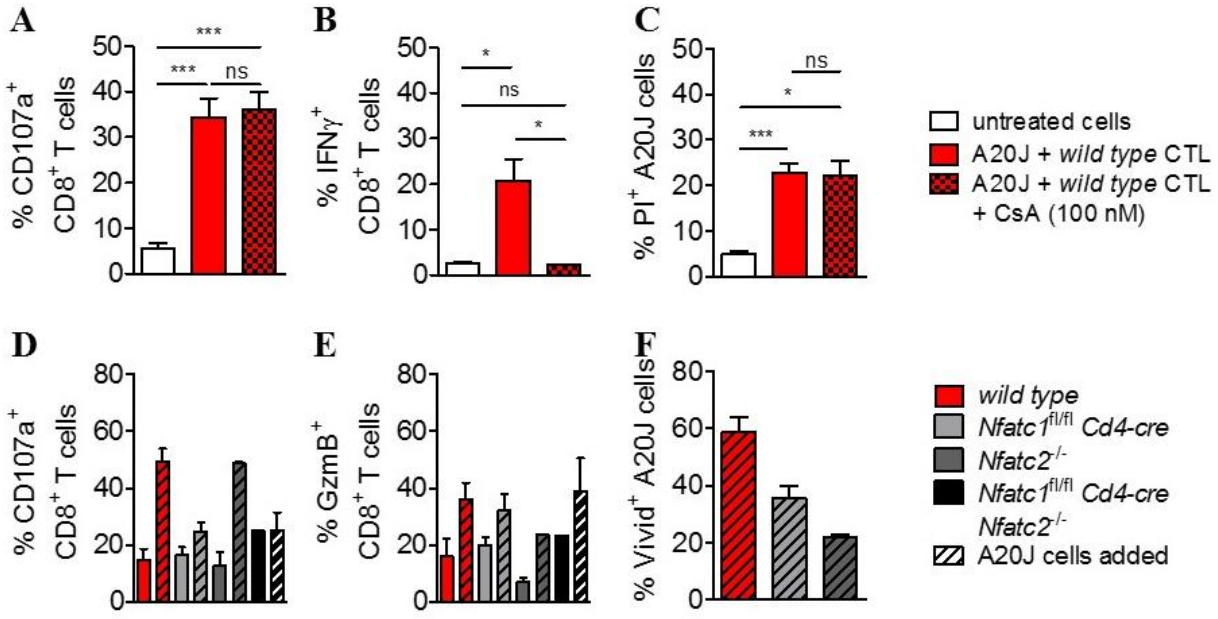

Figure 11: Although cytotoxic functions of *Nfatc1*$^{-/-}$ CTLs are inhibited, defective killing capacity of *Nfatc1*$^{-/-}$ CTLs is not directly linked to Nfat transcriptional function. BALB/c primed CTLs from *wild type* mice were re-stimulated with A20J cells for 4 h and effector cell capacity for degranulation (A), IFNγ production (B) and target cell killing (C) are shown in the presence (dotted bars) or absence (blank bars) of 100 nM CsA. Degranulation (D) and Granzyme B expression (E) upon target cell contact of cytotoxic T cells from *Nfatc1* and *Nfatc2* knockout mice and corresponding induction of cell death in A20J target cells (F) were determined. The effector:target cell ratio was set to 1:1. Values are shown with mean standard error bars. Statistical analysis was performed by unpaired student's t-tests; * $P < 0,05$; *** $P < 0,0005$.

Blockage of the calcineurin-NFAT pathway by addition of 100 nM CsA during the incubation time did not lead to any detectable IFNγ production in the effector $CD8^+$ cells during the allogeneic re-stimulation. This shows that IFNγ production is clearly NFAT-dependent.

However, other effector functions were shown to be calcineurin-NFAT independent. In the same setup as mentioned above – but without monensin and brefeldin A in the supernatant – the addition of CsA to a final concentration of 100 nM did neither influence the degranulation (Figure 11 A) nor the A20J target cell killing (Figure 11 C) of $CD8^+$ cytotoxic T cells.

These results reveal that some CTL effector functions directly depend on NFAT transcriptional activity (as IFNγ production) whereas others do not (such as CTL degranulation and short-term target cell killing).

The characterization of $CD8^+$ cytotoxic T cells generated by MLR co-culture showed an increase in intracellular granzyme B in *wild type* CTLs after re-stimulation with A20J target cells compared to non-re-stimulated T cells (see Figure 11 E). In all NFAT-deficient $CD8^+$ T cell populations, a stimulation-induced increase of granzyme B-producing CTLs was observed.

CD107a (Lamp-1) expression on the effector cell surface was also measured after A20J target cell stimulation. By fusion of lytic granules with the CTL membrane to release cytolytic components, CD107a proteins are distributed on the effector cell surface so that $CD107a^+$ cells can be followed as successfully de-granulated cells. *Wild type* $CD8^+$ T cells showed a strong increase of $CD107a^+$ cells from about 15 to 45 % after contact with A20J target cells for 4 h. NFATc1-deficient CTLs did hardly upregulate CD107a proteins upon cultivation with A20J target cells. NFATc2-deficiency led to a phenotype which did not differ from *wild-type* CTLs whereas lack of both NFATc1 and c2 resulted in no further CD107a up-regulation similar to the *Nfatc1*$^{-/-}$ $CD8^+$ T cells. Thus, the induction of apoptosis in A20J target cells by *Nfatc1*$^{-/-}$ CTLs was not as efficient as apoptosis induction delivered by *wild type* cytotoxic T cells where about 65% of the A20J cells are apoptotic after CTL co-culture for 4 h compared to only 35% non-viable cells with *Nfatc1*$^{-/-}$ $CD8^+$ T cells. Incubation of *Nfatc2*$^{-/-}$ cytotoxic T effector cells together with A20J targets only induced apoptosis in 20% of the target cell population.

In summary, *Nfatc1*$^{-/-}$ cytotoxic T cells showed a decreased cytotoxic capacity towards allogeneic target cells. This is not a direct effect of NFATc1 deficiency and its role of TCR-induced activation and cytokine gene expression, as shown by the CsA-inhibition experiments (see Figure 11 A and C).

1.9.5 Cell-intrinsic Ca^{2+} signaling is mandatory for lytic granule release but unaffected by the absence of NFATc1

$CD8^+$ T cells from *wild type* and *Nfatc1*$^{fl/fl}$ *Cd4-cre* mice were stimulated for 3 d with plate-bound αCD/CD28 and used to determine the calcium flux of activated T cells. Removal of extracellular calcium and addition of thapsigargin in the flow chamber was performed by exchanging the Ringer's solution containing 1 mM free Ca^{2+} with calcium free medium and other reagents.

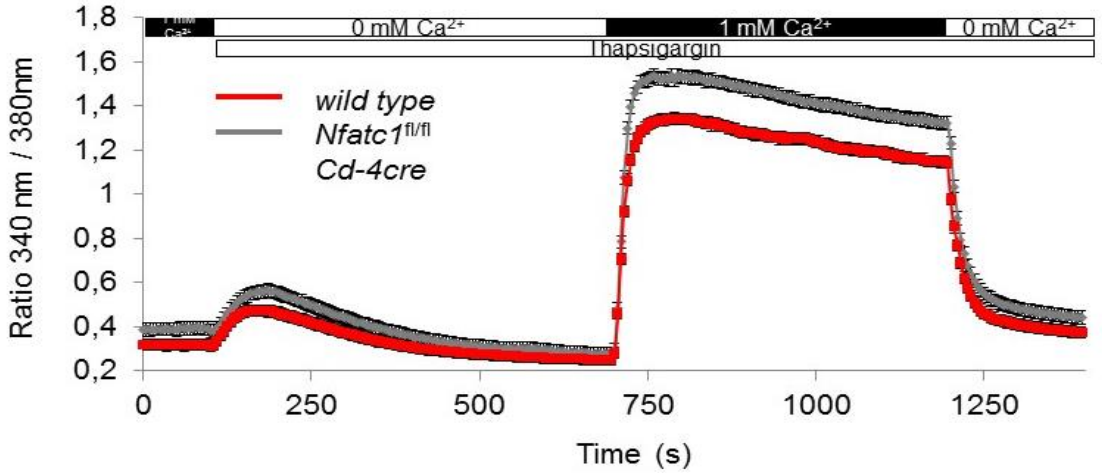

Figure 12: Calcium flux in CTLs lacking NFATc1. αCD3/CD28 stimulated CTLs from either *wild type* or *Nfatc1*$^{fl/fl}$ x *Cd4-cre* mice were stained with the Ca^{2+} sensor dye Fura-2/AM and treated as described at the top of the graph. Values from one experiment are shown with standard mean error bars. 60 cells per condition were evaluated. Values are shown with mean standard error bars.

Cells were kept under resting conditions in medium containing 1 mM calcium. Upon addition of Ca^{2+} free medium together with thapsigargin, a relatively small peak – resulting from elevated calcium levels in the cytosol – occurs and is reduced within minutes. After addition of medium containing 1mM Ca^{2+}, a fast and massive calcium influx into the cells – shown by an increase in the 340/380 nm ratio - occurs and a mild decrease of calcium was observed over time in both T cell populations. When Ca^{2+} is no longer available in the medium, the ratio indicating intracellular calcium rapidly drops. This shows the loss of the Ca^{2+} ions in the cell. By measurement of at least 60 cells per assay – *wild type* or *Nfatc1*$^{-/-}$ CTLs - a statistical significant difference between both populations was found. By showing a higher 340/380 nm ratio in general, NFATc1-deficient $CD8^+$ T cells exhibit a higher capacity for intracellular calcium uptake and an elevated basal calcium level in resting cells after 3 d of αCD3/CD28 stimulation.

Calcium stores and calcium flux are basic components for efficient TCR signaling and CTL granule release. The lack of NFATc1 does not negatively affects the intracellular calcium flux of CTLs.

1.9.6 Cellular reorganization upon T cell re-stimulation is disturbed in *Nfatc1*$^{-/-}$ cytotoxic T cells

Cytotoxic granule release marks the final step of CTL activation upon contact with malformed target cells. To prevent unwanted reactions towards nearby healthy cells, a stable formation of an immunological synapse with the cell has to be maintained. Between those two hallmarks, various processes in intracellular signaling and cellular reorganization are taking place to induce directed lytic granule release at the IS. As the transport processes as well as the lytic granule fusion with the cell membrane requires ATP, mitochondria are also directed towards the effector-target cell contact zone. Mitochondria are also able to modulate Ca^{2+} levels at the IS for calcium-dependent granule release.

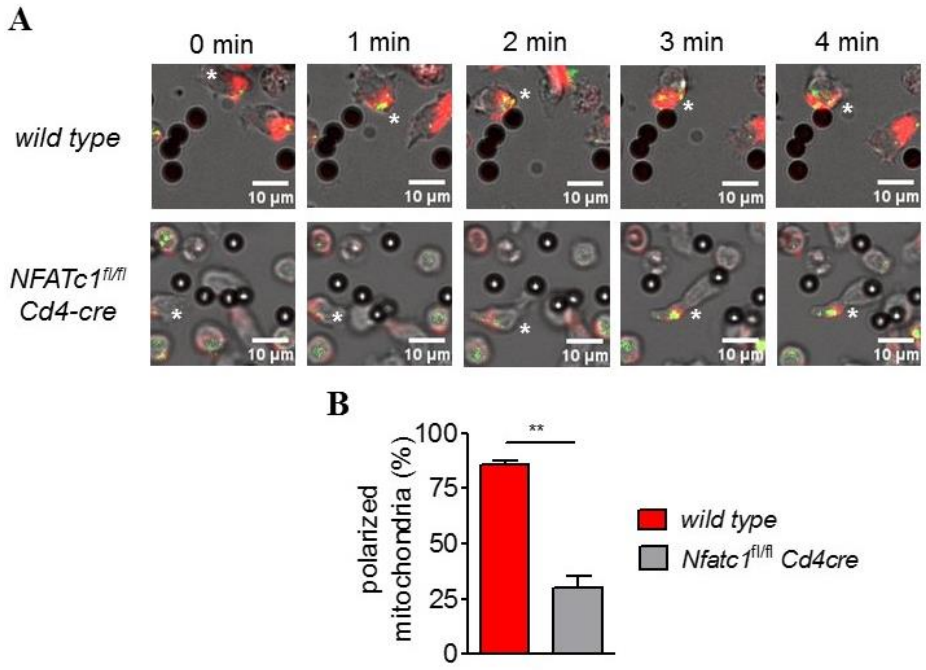

Figure 13: NFATc1-deficient CTLs do not recruit mitochondria and lytic granules towards the immunological synapse. Overlays of bright field and fluorescence pictures from *wild type* and *Nfatc1*$^{-/-}$ cytotoxic T cells show a kinetics of CTL binding to a spheric bead (dark spots) coated with αCD3/CD28 (A). Mitochondria were labelled with mitotracker-red and lytic granules with lysotracker-green. Asterisks mark the cell of interest for each genotype. (B) Percentage of cells showing a continuous localization of mitochondria towards the IS upon bead contact in *wild type* (red) and *Nfatc1*$^{-/-}$ (gray) CTLs. Values are shown with mean standard error bars. Data of at least 15 cells from three *wild type* and *Nfatc1*$^{fl/fl}$ x *Cd4-cre* mice were compiled; ** $P < 0{,}005$.

Wild type and *Nfatc1*$^{-/-}$ allo-reactive cytotoxic $CD8^+$ T cells were generated in a mixed lymphocyte reaction as described before. Cells were labelled with cell-permeable dyes – Mitotracker red and Lysotracker green – to track mitochondrial and lysosomal polarization within single viable cells.

To induce a strong artificial immunological synapse, αCD3/CD28-coated microbeads (Invitrogen) were added to the cell suspension, and the attachment of living cytotoxic T cells to those structures was followed over a total time of 2 h. The microbeads are smaller than viable activated cells and appear as dark round spheres absorbing light in the bright field microscope.

Viable cells containing fluorescence labelled organelles – mitochondria (red) and lytic granules (green) - show an active movement over the plate surface. In Figure 13, two representative cytotoxic T cells of either *wt* or NFATc1-deficient CTLs are shown in the center during different time points of *de-novo* formation of an immunological synapse. The *wild type* CTL recognized and attached to the bead at 2 min, and even the distal area of the cell approached to the contact zone. After 2 min, the mitochondria and acidic granules got into dense contact with the magnetic sphere residing at the contact zone for several min. NFATc1-deficient CTLs showed a significantly different phenotype. The effector cell also recognizes the coated target sphere but is unable to form a stable synapse towards the target cells. In line with this, mitochondria as well as lytic granules hardly get in dense contact with the target structure. In numerous cells which were investigated, their mitochondria still resided at the distal pole upon target sphere binding of the cytotoxic T cell (Figure 13, B).

Obviously, in $CD8^+$ T cells, NFATc1 enhances the polarization of mitochondria and lytic granules towards the immunological synapse.

1.10 *Nfatc1*$^{-/-}$ mice cannot properly clear *Listeria monocytogenes* infections *in vivo*

Pathogens are known to induce distinct cellular subsets of the immune system. *Listeria monocytogenes* is an intracellular bacterium which infiltrates the liver and attacks hepatocytes and - to a lesser extent - the spleen. The attenuated *ΔActA* Lm-Ova strain used for the experiments here shows the same phenotype as *wild type Listeria* but exhibits a reduced pathogenicity[102]. As $CD8^+$ T cells are recognizing peptides derived from intracellular pathogens to mediate lysis of infected cells, *Listeria* infections are a versatile model to study CTL generation and effector function in an *in-vivo* model.

Several parameters from splenic $CD8^+$ T cells of mice infected with the pathogen were measured 5 d after i.p. injection of 5×10^5 CFU of the *ΔActA* Lm-Ova strain.

In several liver lysates from *Nfatc1*$^{fl/fl}$ x *Cd4-cre* (8 of 15), *Listeria monocytogenes* bacteria were detected by plating out lysates in serial dilutions on agar plates selective for *Listeria* bacteria. In liver lysates from *wild type* mice, only in fluids from two individuals a low amount of bacteria was

detected, so most of the *wt* mice successfully eradicated the pathogen until day 5. In general, a slight decrease in mouse weights to about 97% was observed in the following days after *Lm* injection in mice of both groups. During this short period of time until day 5, individuals from both groups did not gain any additional mass.

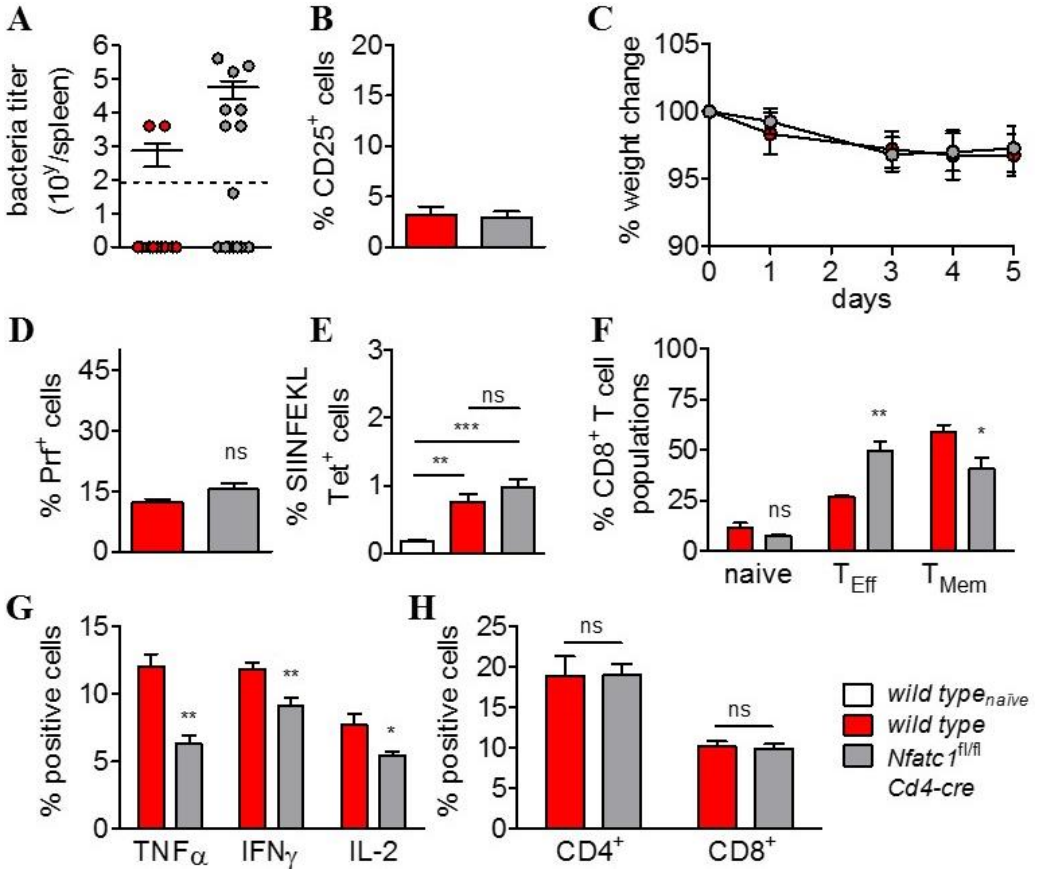

Figure 14: The clearance of intracellular *Listeria* bacteria is disturbed in *Nfatc1*$^{fl/fl}$ x *Cd4-cre* mice. Mice were infected with *Lm-Ova ΔActA*. After 5 d, they were sacrificed to determine the bacterial titers in the liver (A). The hatched line shows the detection level of liver-derived bacteria. Until the end of the experiment, daily weight changes were monitored (C). By flow cytometric analysis, splenic $CD8^+$ T cell populations were analyzed for CD25 (B), perforin (D), $Ova_{257-264}$ specific T cells (E), CD62l and CD44 - for determination of T cell subpopulations (F, naïve: $CD62l^+CD44^-$; T_{Eff}: $CD62l^+CD44^+$; T_{Mem}: $CD62l^-CD44^+$), several key cytokines (G) and the relative $CD4^+$ and $CD8^+$ T cell numbers (H). For (A), combined results from two experiments are shown. Values are shown with standard mean error bars, and the analysis was done by two-tailed student's t-test; * $P < 0,05$; ** $P < 0,005$.

To verify the generation of similar $CD8^+$ T cell amounts which are reactive towards *Listeria* peptides, surface CD25 (IL-2 receptor α chain) expression and the binding capacity towards SIINFEKL-MHC tetramer complexes were measured. CD25 serves as a typical activation marker of stimulated T cells providing reactivity towards extracellular IL-2. However, no difference in activated $CD25^+$ $CD8^+$ T cell populations between *wt* and *Nfatc1*$^{fl/fl}$ x *Cd4-cre* mice was detected.

Due to the fact that the *Lm*-Ova transgenic mouse strain expresses the Ovalbumin protein, the strong T-cell stimulating $OVA_{257-264}$ SIINFEKL peptide is also expressed and presented on MHC class I molecules of infected cells. $OVA_{257-264}$ reactive $CD8^+$ T cells are activated, proliferate and rise in number. The overall number of splenic $CD4^+$ and $CD8^+$ T cells did not significantly differ between *wt* and *Nfat*$^{fl/fl}$ *Cd4 cre* mice 5 d after the i.p. injection of *Lm*-Ova (H). Related to that, an investigation of *wild type* and *Nfatc1*$^{-/-}$ $CD8^+$ T cells from infected mice did not show any difference between both genetic backgrounds in the percentage of SIINFEKL-tetramer$^+$ reactive $CD8^+$ T cells. This indicates a similar generation of an immune response and reactivity towards the intracellular pathogenic infection. Thus, absolute $CD8^+$ T cell numbers do not play a major role for the clearance of the infection.

On the other side, perforin expression in *Nfatc1*$^{-/-}$ $CD8^+$ T cell populations was slightly, but not significantly increased compared to *wild type* $CD8^+$ T cells.

To differentiate between major $CD8^+$ T cell activation stages, fluorescence labelled antibodies against CD62l and CD44 were used for the determination of naïve ($CD62l^+$, $CD44^-$), effector ($CD62l^+$, $CD44^+$) and memory ($CD62l^-$, $CD44^+$) cells[108]. The percentage of effector $CD8^+$ T cells was drastically increased whereas the memory cell compartment is reduced in *Nfatc1*$^{-/-}$ $CD8^+$ T cells, in comparison with *wild type* populations suggesting a different $CD8^+$ T cell composition. This leads to the conclusion that T cell maturation is negatively affected in the absence of NFATc1.

Another important point is the decreased capacity of *Nfatc1*$^{-/-}$ $CD8^+$ T cells to produce cytokines that are important for direct apoptosis-induction (TNFα), T_h1 differentiation and proliferation (IFNγ and IL-2). Significantly less $CD8^+$ cells were able to produce those cytokines in the *Nfat*$^{fl/fl}$ *Cd4 cre* mice after 5 d of *Lm* infection, compared to *wt* mice.

Taken together, the eradication of *Listeria* infections is decreased in mice bearing *Nfatc1*$^{-/-}$ T cells. Although similar amounts of antigen-reactive $CD8^+$ T cells arise during infection, defective cytokine production (of IFNγ, IL-2 and TNFα) and disturbed $CD8^+$ T cell maturation may lead to diminished T cell reactivity. Contrary to these findings, perforin-expressing $CD8^+$ T cells are not affected, but even slightly elevated in number.

Discussion

1.11 NFATc1 regulates CD8$^+$ T cell proliferation and cytokine production

The T cell receptor signaling cascade is the main step for NFAT activation that controls CD4$^+$ and CD8$^+$ T cell activation, proliferation and differentiation[68] as well as T cell tolerance[109]. The role of NFAT itself – as a transcription factor – relies on the nuclear import of the activated dephosphorylated version followed by promoter binding to specific target genes together with distinct interaction partners, either as NFAT monomers, homodimers[110] or as cooperative complexes with partner proteins as e.g. AP-1[111,112]. The cooperative binding of NFAT-AP-1 complexes to promoter elements is needed for a strong induction of a T cell effector program[113]. These various possibilities of transcriptional activities of NFATs lead to a context-dependent induction of a broad transcriptional program[114]. For example, a genetically modified version of NFATc2 not being able to interact with AP-1 emphasizes the need of functional NFAT proteins to prevent a clinical phenotype, called T cell exhaustion that leads to an impaired CD8$^+$ T cell function *in vivo*[115].

Physiological activation of naïve CD4$^+$ and CD8$^+$ T cells is performed by a strong TCR interaction with the cognate MHC-peptide complex[116] on antigen-presenting cells in the context of CD28 co-stimulation. Otherwise, T cells enter a state called T cell unresponsiveness or anergy[117]. *In* vitro, TCR signaling can be mimicked by a strong antibody mediated CD3 + CD28 activation. As shown in Figure 1, activation of T cells for 3 d induces an upregulation of *Nfatc1-P1* promoter transcripts and down-modulation of *P2* transcripts as well as a strong increase in overall NFATc1 protein amounts. For CD4$^+$ T cells, Hock et al. showed similar findings in 2013[105]. The switch from the transient *P2* promoter towards the highly inducible *P1* promoter is a typical finding for activated lymphoid cells[118]. Interestingly, overall comparison of *P1* transcript induction and *P2* suppression did not show a massive activation-induced *Nfatc1* RNA upregulation (as well as the overall *Nfatc1* expression in CD4$^+$ T cells), although protein levels were drastically increased after 3 d in both populations indicating important post-transcriptional mechanisms in NFAT protein expression. Contrary to CD4$^+$ T cells, *Nfatc1* expression in CD8$^+$ T cells is about 3-fold upregulated leading to the conclusion of a differential regulation of *Nfatc1* expression in those T cell populations, although the GFP-expression as an indicator for *Nfatc1*- promoter activity is not severely changed. Only a slightly higher activity level was observed in unstimulated CD8$^+$. In line with these findings,

Leung-Teung-long et al. found that the activation-induced transcriptional activity of *Nfat* family differs between $CD4^+$ and $CD8^+$ T cells[80]. This confirms the results from the Nfatc1-BAC-transgenic T cell experiments shown in Figure 1 C and that a differential transcriptional activity on *Nfat* in CD8 may base on a defective phosphorylation site. This group also found that NFATc1 is not completely localized in the nuclei of $CD4^+$ and $CD8^+$ T cells upon αCD3/CD28 stimulation. Instead, the nuclear localization was enhanced upon addition of the calcium ionophore ionomycin for 4 h prior to confocal microscopy (see also Figure 2).

On mRNA level, *Nfatc2* is not severely affected during T cell stimulation, but a peak expression of NFATc2 proteins was observed after 3 d of stimulation with αCD3/CD28 in $CD4^+$ T cells. NFAT proteins are able to regulate and bind to several cytokine promoter regions – namely to the *IL-2, IL-3, IL-4, TNFα, CD40l* and *IFNγ* promoter[32,119], being important for T cell activation and $CD4^+$ T helper cell differentiation. Exemplarily, the opposing functions of NFATc1 and NFATc2 in gene expression can be demonstrated for the *IL-4* gene. Whereas mice lacking NFATc1 proteins in the lymphoid compartment showed a mildly decreased proliferation and a reduced IL-4 expression in the T cell compartment[53,54], T cells from *NFATc2*$^{-/-}$ mice showed a different phenotype. *Nfatc2*$^{-/-}$ cells were hyperproliferative, and the levels of T_h2 cytokines, such as IL-4, were markedly elevated. Finally, the susceptibility towards T_h1 mediated infections with *Leishmania major* was increased[57,65,120] as well. These contradictory functions of NFAT family members show their potential action not only as an activator but also as a repressor during T cell activation.

Depletion of NFATc1 and c2 leads to a massive drop in protein expression for IL-2, IL-4 and IFNγ emphasizing the need of both family members to gain optimal T cell effector functions[121]. In a group of patients suffering from bronchial adenocarcinoma, Maxeiner et al. found a reduced *NFATC2* expression. This finding was verified in an *Nfatc2*$^{-/-}$ carcinoma mouse model developing more and larger lung carcinomas through an altered induction of $CD4^+$ $CD25^+$ $Foxp\text{-}3^+$ T cells by elevated IL-2 levels and a defective TNFα production in general[78].

NFATc1 is thought to have an activating and anti-apoptotic function whereas NFATc2 shows apoptosis-inducing activity. Whereas NFATc1 and c2 are mandatory for the activation and differentiation of mature T cells[122], NFATc3 does not directly affect cytokine expression of mature single positive $CD4^+$ or $CD8^+$ T cell populations but is rather important for their generation during maturation in the thymus.

In line with these findings made by several groups before, we observed that *NFATc1*$^{-/-}$ $CD8^+$ T cells show a stimulus-dependent reduced activation-induced proliferation (Figure 3) and an

increased rate of apoptosis (Figure 8). One reason for the defective proliferation displays the cytokine expression profiles of Tc_1 differentiated $CD8^+$ T cell populations lacking NFATc1 and c2 (Figure 4). IL-2 is the major proliferation-associated cytokine for $CD4^+$ and $CD8^+$ effector cell generation[123] and $CD8^+$ memory cell expansion[73] but it also promotes activation-induced cell death of T cells[124]. Regarding the generation of T_{h1} cells, IL-2 also provides their generation and maintenance[75]. As we observed a decreased percentage of IL-2 and IFNγ expressing $CD4^+$ and $CD8^+$ T cells, the T cell differentiation towards a T_h1/ T_c1 phenotype was inhibited in the absence of NFATc1 and/or NFATc2. NFATc2 (together with NFATc3) was reported earlier to enhance a T_h1 phenotype[125] so that those NFATc2$^{-/-}$ $CD8^+$ T cells are inhibited in the generation of a T_1 immune response. In MLRs, the generated NFAT-deficient cytotoxic $CD8^+$ T cells also showed a decreased cytokine expression (see Figure 10) indicating a defective T_c1 function. Although surface activation markers remained unaffected by the absence of NFATc1 (see Figure 9), the reduced cytokine expression to maintain an antigen-reactive CTL population may be one explanation for a defective allogeneic target cell killing. The reduced number of surviving cytotoxic T cells on the *Nfatc1*$^{-/-}$ background (see Figure 8) results from a suboptimal activation, as seen for less $CD8^+$ T cells being able to produce IL-2.

Regarding surface receptor expression, the *Fasl* promoter is known to be activated by IL-2[126] and is an indirect, through Egr3-expression and cooperation[127], NFATc2-dependent target gene[128]. We did not observe an induction of surface Fasl expression after T cell differentiation neither in NFATc1 nor NFATc2-deficient T cells. In this context, the expression of Fasl remained at a very low level. After 6 d of CTL generation in MLR cultures, an increase in Fasl expression on both *wt* and Nfatc1$^{-/-}$ CTLs was observed. In naïve $CD8^+$ T cells from *Nfatc1*$^{fl/fl}$ *x Cd4-cre* mice, an elevated basal number of $CD8^+$ T cells which express Fasl was found (Figure 9 B). This finding is contrary to the *Fasl* dependence on NFAT[32] but as the final percentage of $Fasl^+$ $CD8^+$ T cells does not differ between both genotypes after CTL generation (Figure 9 C), the *Fasl* induction in general is decreased in Nfatc1$^{-/-}$ $CD8^+$ T cells.

Other classical activation markers for T cell differentiation in *wild type* and *Nfatc1*$^{fl/fl}$ *x Cd4-cre* mice were investigated as well (Figure 9), but significant differences resulting from initial T cell activation were not detected. Effect mediated by altered cytokine expression patterns (as described above) may contribute to a defective T cell maturation and surface receptor expression as seen in the *in vivo* model for *Listeria monocytogenes* (Figure 14 F and G).

1.12 NFATc1 is a critical factor for CTL function *in vitro*

Several $CD8^+$ T cell specific hallmarks are affected by the lack of NFATc1 and c2. Mature naïve $CD8^+$ T cells are activated, differentiate towards cytotoxic effector T cells and eradicate target cells infected with bacteria and viruses. Moreover, they are able to detect an MHC-mismatch on cellular surfaces. This is a very important step since some viruses are able to modulate peptide presentation on MHC-I proteins of infected cells. For this reason, regulating the $CD8^+$ T cell response after transplantation of MHC-mismatched organs or hematopoietic stem cells is mandatory to prevent allograft-rejection in a graft-versus-host disease (GvHD). $CD8^+$ T cells mainly mediate a strong cytotoxic response and release cytokines in the acute phase of GvHD[90,129]. In clinics, this disease is mostly treated by administering CsA/FK506 to the patients[130]. CsA and FK506 are calcineurin-inhibitors. After application, a down-modulation of any NFAT-dependent immune reaction[131] occurs, not only in T cells but also in other immune cells (like B cells, NK cells and dendritic cells). Therefore, patients treated with those agents after transplantation are potentially prone to other severe microbial infections, such as *Clostridium difficile*[132]. The discovery by Putz et al. in 2012 that the PI3Kδ is essential for a successful allogeneic tumor cell clearance *in vivo* showed that NFAT-signaling in $CD8^+$ T cells mediates the clearance of malformed cells for this kind of antigen-challenge[133]. In the context of TCR activation, PI3Kδ is a catalytic protein enhancing the phosphorylation of phosphatidylinositol which is an important step of TCR signaling upstream of the calcineurin-NFAT pathway[134]. So, depletion of this enzyme led to similar findings in $CD8^+$ T cell cytokine expression compared to our *in vitro* data.

The discovery of FK506 and cyclosporine A led to the finding that NFAT activity could be blocked by those reagents trough inactivation of the Ca^{2+} sensitive phosphatase calcineurin[135]. Although some reports showed a clear CsA-mediated dependence of CTL degranulation and target cell killing from calcineurin activity[95], we did not observe a cyclosporine A-dependent inhibition of these effector functions after generating cytotoxic $CD8^+$ T cells by MLR cultures (see Figure 11). As the first experiments were made with cell lines and not mature naïve $CD8^+$ T cells, the physiological basis and activation status was drastically different regarding freshly prepared murine $CD8^+$ T cells and stimulating them in an MLR for 6 d or for 3 d with αCD3/CD28.

After activation by viral or bacterial antigens *in vivo*, T cell populations undergo different stages of expansion, contraction and memory. Those populations are all defined by distinct functions and can be followed up by a distinct pattern of surface markers[136,137]. After 6 d of an allogeneic co-

culture with irradiated target cells (here: BALB/c splenocytes), most of the cytotoxic T cells are in the effector phase of CTL maturation. They efficiently eradicate infected or allogeneic target cells[138]. As seen for the high expression of CD44 and the down-modulation of CD62l (see Figure 9), naïve $CD8^+$ T cells developed towards full effector and memory CTLs[139] in *wild type* and *Nfatc1*$^{-/-}$ populations.

The *in vitro* MLR-model for the generation of allo-reactive CTL populations to generate a large amount of reactive cytotoxic T cells was established long ago with BALB/c derived dendritic cells (DC's)[140]. Inaba et al. showed that irradiated BALB/c DC's serve as "stimulating agent" for naïve C57BL/6 $CD8^+$ T cells even without the help of $CD4^+$ T helper cells to provide $CD8^+$ T cell proliferation and cytokine secretion. In our findings, a direct TCR-signaling-cascade-dependent block of CTL degranulation and allogenic target cell killing was excluded for the MLR-generated allo-reactive cytotoxic T cells by the CsA experiments (Figure 11 A and C). Since a drop in CTL killing function was detectable in both killing assays (CTLs and MOPC cells in Figure 6, allo-reactive CTLs and A20J cells in Figure 11) in cytotoxic T cells lacking NFATc1, another pathway must be involved which is affected by NFATc1. Earlier findings by Smyth and Ortaldo in 1993 already suggested some alternative – NFAT independent and therefore CsA insensitive - roles of the calcineurin activation cascade directly involving $CD8^+$ T cell cytotoxic functions[94] depending on the stimulus delivered to the cytotoxic T cell. Interestingly, in both cases of CTL-generation *in vitro* done here, the percentage of $GzmB^+$ $CD8^+$ T cells from *Nfatc1*$^{-/-}$ mice was markedly higher to those of *wild type* $CD8^+$ T cells, whereas after *in vitro* MLR culture, the supernatant contained lower levels of granzyme B (Figure 11). This indicates that the lytic granules were somehow stuck in the cytosol and unable to fuse with the CTL membrane upon target cell recognition.

As a possible explanation for the defective granule release, we observed a significantly reduced polarization of mitochondria and lysosomes towards the immunological synapse in a life-cell-imager (see Figure 13) in *NFATc1*$^{-/-}$ $CD8^+$ T cells compared to *wt* cells. This may explain the diminished degranulation and target cell killing. Several steps are needed to maintain cytotoxic T cell effector function, starting with centrosome reorganization and microtubule formation[141] to provide a polarized secretion of cytotoxic granules towards the IS[142]. During the formation of an IS, in addition to other cell organelles, mitochondria are usually polarized towards the contact zone to deliver reactive oxygen species (ROS) and to maintain a continuous Ca^{2+} influx across the plasma cell membrane by its Ca^{2+} buffer capacities[143]. This ensures successful fusion of lytic granule to the synaptic cleft[81]. Due to a defective mitochondrial function (e.g. in the generation of

ROS), NFAT activation, for example, is also reported to be impaired[144]. One explanation may be a malfunction in degranulation of NFATc1-deleted CTLs which is based on a defective mitochondria movement towards the IS. In turn, this may not provide the cognate "environment" for granule-mediated killing. A general defect in the transportation mechanism to generate a functional IS which cannot be induced in *Nfatc1*$^{-/-}$ CTLs may serve as another explanation. As a result, this leads to an accumulation of lytic granules in *Nfatc1*$^{-/-}$ CTLs during their generation (see Figure 6 D, Figure 7 and Figure 10 B). Those granules are not able to get secreted towards the synaptic cleft upon stimulation (see Figure 10 C) followed by an impaired degranulation upon re-stimulation (see Figure 11 D). Finally, a reduced target cell killing was observed in different experimental setups for CTL-generation (see Figure 6 D and Figure 11 F).

An NFATc1-related defect which affects the Ca^{2+} release from internal and external stores was excluded by our findings (see Figure 12). Calcium is an important molecule involved in various intracellular signal transduction events. While calcium release from internal stores like the ER and the influx from the extracellular environment is not only mandatory for neuronal signal transmission and maintaining synaptic activity[145], Ca^{2+} flux is necessary for lytic granule release from cytotoxic T cells and NK cells to kill malformed cells[29]. Therefore we investigated the capacity of internal ER stores and cell-membrane-bound CRAC channels to provide a Ca^{2+} flux in *wild type* and *Nfatc1*$^{fl/fl}$ *x Cd4-cre* $CD8^+$ T cells. Therefore, no differences in the Ca^{2+} release and flux through the ER- and plasma cell membrane were found. A more physiological stimulus would clarify the role of misleading mitochondrial polarization and its' impact regarding the activation-induced store-operated calcium entry (SOCE).

Another explanation for the decreased killing potential of *Nfatc1*$^{-/-}$ cytotoxic T cells is the reduced expression of the tumor-necrosis factor α (TNF α). Earlier findings showed that TNFα secretion by $CD8^+$ T cells induces clearance of virus-infected cells[146,147] by binding to TNF receptors on target cells. This induces cell death by activation of the caspase cascade in a caspase-8-dependent manner[148,149]. Regarding the cytokine-expression data after 6 d MLR (see Figure 10 A), TNFα-production is markedly impaired in CTLs lacking NFATc1 as well as we found a tendency for *Nfatc2*$^{-/-}$ CTLs to produce less TNFα. This is in line with published data showing *Tnfa* as a target of NFATc2[150].

But still, the role of TNFα-induced apoptosis in cytotoxic T cells seems to be smaller compared to the main Fas-Fasl and granule-exocytosis pathways which are the main players for the eradication of malformed cells[13,14].

These findings shed light on a novel mechanism by which NFATc1 regulated CTL function beside the already well known feature of its' influence on the cytokine expression profile in T cells, and other important target genes for cell proliferation. This may be one reason for a decreased functionality and a reduced cytotoxicity. NFATc1 has an impact on the generation of functional CTLs not only for the cytokine production, but is probably also involved in a more complex physiological context, i.e. in intracellular transport processes.

Another hint for an important role of NFATc1 to be involved in cellular physiology, beside classical B-/T- cell signaling, was given by Semsarian et al. and Musaro et al.[151,152]. These groups found that NFATc1 is continuously activated in cases of skeletal and cardiac hypertrophy in a CsA-dependent manner. Studies on calcineurin-, connexin 45- and NFATc1-deficient mice also suggested a gap-junction related malformation of cardiac valves which influences the cellular morphology by the generation of intracellular NFAT-gradients[153]. NFATc1 was also found to mediate the migration and proliferation of vascular smooth muscle cells by binding to and activating *Cyclin A* and *Cyclin D* elements[154,155]. For keratinocytes, Brun et al. showed in 2014 a direct NFATc1-dependence of the actin-cytoskeleton mediated by the actin-bundling protein T-plastin whose synthesis is under the control of the calcineurin-NFAT pathway[156].

Although it is still unknown, which NFATc1-dependent genes are involved in the defective formation of a cytotoxic synapse are, some NFATc1-dependent target genes may play an important role in the formation of the cytotoxic synapse. As the defective target-cell-killing capacity is not a short-term malfunction (see CsA experiments above), a dysregulation of target genes must have occurred already during CTL generation.

To emphasize the necessity of NFATc1 in CTL function *in vivo*, we investigated the well-established intracellular *Listeria monocytogenes* infection model[157].

1.13 Proper clearance of intracellular *Listeria* infection requires NFATc1

One of the main function of $CD8^+$ cells is the recognition and the eradication of intracellular pathogens which reside and replicate in host cells. Listeriosis mediated by *Listeria monocytogenes* is a food-borne disease[158] being able to cause gastroenteritis, meningitis and abortion in pregnant women[157]. *Listeria* bacteria are taken up from contaminated food, enter the intestine - where they are taken up by macrophages in the phagosome[159]. Finally, *Listeria monocytogenes* is able to enter draining lymph nodes for intracellular replication and spread by cell-to-cell transmission. The two major target organs which are infected by *Lm* are the spleen and the liver[160].

For the efficient eradication of intracellular *Listeria* particles, $CD8^+$ T cells are mandatory but a productive generation of long-lived $CD8^+$ effector memory cells demands also for $CD4^+$ T cell help[161]. Exclusively, an optimal protection against a re-infection can be provided by perforin-expressing $CD8^+$ T cells whereas inactivation of *Pfn* in $CD8^+$ T cells does not lead to an increased outcome of disease during primary *Listeria* infections[162]. The role of perforin expression in $CD8^+$ T cells during *Listeria* infections is not completely understood since in some reports perforin was reported not to be required for pathogen clearance[163,164].

During an immune response towards a secondary infection with *Listeria*, it was shown that IFNγ secretion by memory $CD8^+$ T cells provided rapid protection[165]. This emphasizes the need of a rapid chemokine availability for a productive $CD8^+$ T cell-mediated immune response to also involve the innate immune system[166,167], e.g. by activation of microbicidal macrophages[168]. Therefore, $CD8^+$ T cells – as well as $CD4^+$ T cells - are required to maintain a successful potent immune response[169]. Parts of the innate immune system also play an important role for the clearance of *Listeria* infections[170].

Finding of several CFU *Listeria* in liver lysates from *Nfatc1$^{fl/fl}$ Cd4-cre* mice (see Figure 14 A) and hardly any in lysates from *wildtype* mice infected 5 d before shows a diminished clearance of this pathogen when NFATc1 was knocked out in the T cell compartment. This suggests that *Listeria*-derived peptide presentation on MHC I molecules did not induce strong $CD8^+$ T cell activation to secrete cytolytic components[169].

The mutant *dActA Listeria* strain shows a reduced pathogenicity by the inactivation of the cell-to-cell transmission[102] compared to the *wt* strain. As the natural transmission pathway is blocked, the bacteria are trapped in those cells because the *dActA* strain is highly susceptible to autophagy[171]. As a result, the virulence is drastically reduced[157]. Only few *Listeria* particles enter the blood stream to reach their primary target cells for replication – hepatocytes in the liver – where they are eradicated by $CD8^+$ T cells[172]. The replication in infected target cells is not affected by the mutant strain so that a productive antigenic presentation of infected cells can still be maintained. Due to the reduced pathogenicity, we could only extract and cultivate *Listeria* cultures from 10 of overall 26 livers in two combined experiments. In those assays, 8 of 10 infected livers were derived from *Nfatc1$^{fl/fl}$ Cd4-cre* mice.

Because we showed a reduced proliferation and cytokine expression of *Nfatc1$^{-/-}$* $CD8^+$ T cells *in vitro* (see Figure 3 and Figure 4), we were interested to see if similar amounts of *Lm*-reactive $CD8^+$ T cells were generated within the whole T cell pool of the spleen for the eradication of the infection.

Neither the relative $CD4^+$ T cell numbers nor those from $CD8^+$ T cells differed between *wt* and *Nfatc1*$^{-/-}$ *Cd4* cre mice. For $CD8^+$ T cells, these findings go in line with the cell numbers in untreated individuals (see Figure 9 A). Only a small fraction in both groups – about 15% (from the values of Pfn expressing cells among all splenic $CD8^+$ T cells, Figure 14 D) of the overall T cell pool is reactive towards a defined pathogen, like *Listeria monocytogenes*. The similar values from *wt* and *Nfatc1*$^{fl/fl}$ *Cd4-cre* mice do not to show a general impaired ability to generate Pfn^+ cytotoxic $CD8^+$ T cells.

For the verification of a similar $CD8^+$ T cell activation, the expression of the T cell activation marker CD25[173] – the IL-2 receptor α chain - was measured. But a significantly different expression was not detected between both groups. By the usage of the $OVA_{257-264}$-expressing *Listeria* strain, the $CD8^+$ T cell-reactivity towards a specific (model-) antigen was measured by fluorochrome-labelled SIINFEKL-tetramers and evaluation by flow cytometry. This model antigen was used, since a higher percentage of naïve $CD8^+$ T cells is able to react and expand towards challenging with the $OVA_{257-264}$ peptide compared to *Listeria*-related epitopes like $LLO_{91–99}$, $p60_{217–225}$, $p60_{49–457}$ and $mpl_{84–92}$[163,174]. Similar to the Pfn and CD25 expression, tetramer stainings of SIINFEKL-epitopes did not show a significant difference in the generation of antigen-reactive CTL populations (Figure 14).

As there were lots of other *Listeria*-derived antigens around and the generation of a robust antigen-specific $CD8^+$ T cell population occurs few days later at day 8 in infected organs[163], the percentage of SIINFEKL-tetramer$^+$ $CD8^+$ T cells remained relatively low but significantly higher than in non-infected *wt* mice. Observations from Pope et al. in 2001 from mice which received a primary *Listeria* infection by gavage revealed a peak level of SIINFEKL-reactive $CD8^+$ T-cells after 8-9 days p.i. whereas after 5 days, only a small fraction of splenic $CD8^+$ T cells expressed the cognate SIINFEKL-MHC I reactive T cell receptor. However, the percentage of tetramer-reactive $CD8^+$ T cells did not differ between *Listeria*-experienced *wt* and *Nfatc1*$^{-/-}$ mice on d 5 p.i. (Figure 14 E).

Intracellular stainings of freshly prepared splenocytes for perforin expression from 5 d infected mice also did not show a significant difference in the percentage of lytic-granule-containing $CD8^+$ T cells. As a general remark, a slightly higher – though not significant – percentage of $CD8^+$ T cells from *Nfatc1*$^{fl/fl}$ *Cd4-cre* mice showed a perforin$^+$ phenotype. This may contribute to the defective capacity of *Nfatc1*$^{-/-}$ CTLs to secrete lytic granules as already described from the *in vitro* studies before. Comparing the expression of cytokines like IFNγ, IL-2 and TNFα in the *in vivo* *Listeria* model, the results from our findings *in vitro* - T_h1/ T_c1 differentiation (see Figure 4) and

allogeneic challenge (see Figure 10 A) - were confirmed in all experimental setups. After $CD8^+$ T cell activation/differentiation *in vivo*, NFATc1 is also mandatory for an efficient cytokine expression to clear intracellular pathogens.

Although a similar generation of *Listeria*-restricted $CD8^+$ T cell populations was shown for both *wt* and *Nfatc1*$^{-/-}$ genotypes, the transition from $CD8^+CD62l^+CD44^+$ effector T cells to $CD8^+CD62l^-CD44^+$ memory T cells was defective in *Nfatc1*$^{fl/fl}$ *Cd4-cre* mice (see Figure 14 F). This may be due to the fact that IL-2 (and IL-15) mediate the conversion towards $CD8^+$ memory T cells[175] to generate an optimal immune response upon re-infection[73]. Central memory and effector memory $CD8^+$ T cells (T_{CM} and T_{EM}) show specific functions: T_{CM} reside in lymphoid organs, do not show cytotoxic activity and are $CD62l^+$ $CCR7^+$ whereas T_{EM} are mostly found in non-lymphoid tissue, show a rapid effector function and are $CD62l^-$ $CCR7^-$ [8,108]. However, the same antigen specificity was found in both populations[176]. Interestingly, a higher percentage of splenic $CD8^+$ T cells from *Nfatc1*$^{fl/fl}$ *Cd4-cre* mice show an effector T cell phenotype compared to *wild type* mice (see Figure 14). Those mice show distinct defects in the clearance of *Listeria* particles - although elevated in number - indicating reduced effector functions in the T cell compartment.

Together with the findings for a decreased cytokine expression and impaired lytic-granule-exocytosis *in vitro* (see Figure 4 and Figure 10), the reduced clearance of *Listeria monocytogenes* infections in *Nfatc1*$^{fl/fl}$ *Cd4-cre* mice contributes to defects in the cytokine production of the $CD8^+$ T cell compartment when challenged with bacteria. The lack of NFATc1 in $CD4^+$ T cells also impairs their cytokine-secretion similarly to $CD8^+$ T cells, as already shown for a GvHD mouse model *in vitro* (see Figure 4 A and B) and *in vivo*[90]. $CD4^+$ T cells are also necessary for the clearance of intracellular bacteria, especially for the $CD8^+$ memory cell generation to protect from re-infection[161] since $CD8^+$ memory T cells are a key factor for the rapid protection from an anew re-infection[177]. To clarify the question which T cell compartment contributes more to the outcome of the reduced bacterial clearance, either an adoptive transfer model with mixed T cell populations has to be established, or a cre-recombinase strain has to be used that expresses cre exclusively in $CD8^+$ T cells[178]. But as seen from the *in vitro* experiments with allogeneic target cells, the reduced granule polarization of CTLs followed by a reduced lytic granule release may also be important for the defective clearance of intracellular pathogens. Beside the possibility of other structural defects in *Nfatc1*$^{fl/fl}$ *Cd4* cre mice, the disability of mitochondria to get in contact with the IS upon target structure binding and IS formation may lead to a reduced T cell activation. Normally, T cell

activation is enhanced by polarized mitochondria enabling a continuous calcium flux in an ORAI-dependent manner[179].

In general, an efficient delivery of cytolytic compounds like granzymes and perforin contributes to an effective immune response after vaccination against pathogens like *Listeria monocytogenes*[180]. In our experiments, we showed an altered function for *Nfatc1*$^{-/-}$ CD8^{+} T cells to execute lytic granule release upon stimulation either by allogeneic cells or upon αCD3/CD28 activation. Due to this phenotype (together with other defects, like a reduced cytokine expression), *Nfatc1*$^{fl/fl}$ *Cd4* cre mice showed a defective clearance of intracellular *Listeria monocytogenes* infections.

To the best of our knowledge, these novel findings haven't been made before and shed another light on the role of NFATc1 beside its' well-investigated function as transcription factor.

Literature

1 Fleming, A. On a Remarkable Bacteriolytic Element Found in Tissues and Secretions. *Proceedings of the Royal Society of London. Series B, Containing Papers of a Biological Character* **93**, 306-317, doi:10.1098/rspb.1922.0023 (1922).

2 Rus, H., Cudrici, C. & Niculescu, F. The role of the complement system in innate immunity. *Immunologic research* **33**, 103-112, doi:10.1385/ir:33:2:103 (2005).

3 Medzhitov, R. & Janeway, C. A., Jr. Innate immunity: the virtues of a nonclonal system of recognition. *Cell* **91**, 295-298 (1997).

4 Aderem, A. & Ulevitch, R. J. Toll-like receptors in the induction of the innate immune response. *Nature* **406**, 782-787 (2000).

5 Dustin, M. L. A dynamic view of the immunological synapse. *Seminars in immunology* **17**, 400-410, doi:10.1016/j.smim.2005.09.002 (2005).

6 Abbas, A., Lichtman, A. & Pillai, S. Vol. 6 Ch. 9, 194 (Saunders Elsevir, 2010).

7 Masopust, D., Vezys, V., Marzo, A. L. & Lefrancois, L. Preferential localization of effector memory cells in nonlymphoid tissue. *Science (New York, N.Y.)* **291**, 2413-2417, doi:10.1126/science.1058867 (2001).

8 Sallusto, F., Lenig, D., Forster, R., Lipp, M. & Lanzavecchia, A. Two subsets of memory T lymphocytes with distinct homing potentials and effector functions. *Nature* **401**, 708-712, doi:10.1038/44385 (1999).

9 Janeway, C. A., Jr. Thymic selection: two pathways to life and two to death. *Immunity* **1**, 3-6 (1994).

10 Germain, R. N. T-cell development and the CD4-CD8 lineage decision. *Nature reviews. Immunology* **2**, 309-322, doi:10.1038/nri798 (2002).

11 Lenz, L. L., Butz, E. A. & Bevan, M. J. Requirements for bone marrow-derived antigen-presenting cells in priming cytotoxic T cell responses to intracellular pathogens. *The Journal of experimental medicine* **192**, 1135-1142 (2000).

12 den Haan, J. M., Lehar, S. M. & Bevan, M. J. CD8(+) but not CD8(-) dendritic cells cross-prime cytotoxic T cells in vivo. *The Journal of experimental medicine* **192**, 1685-1696 (2000).

13 Lowin, B., Hahne, M., Mattmann, C. & Tschopp, J. Cytolytic T-cell cytotoxicity is mediated through perforin and Fas lytic pathways. *Nature* **370**, 650-652, doi:10.1038/370650a0 (1994).

14 Kagi, D. *et al.* Fas and perforin pathways as major mechanisms of T cell-mediated cytotoxicity. *Science* **265**, 528-530 (1994).

15 Lopez, J. A., Brennan, A. J., Whisstock, J. C., Voskoboinik, I. & Trapani, J. A. Protecting a serial killer: pathways for perforin trafficking and self-defence ensure sequential target cell death. *Trends in immunology* **33**, 406-412, doi:10.1016/j.it.2012.04.001 (2012).

16 Stinchcombe, J. C., Bossi, G., Booth, S. & Griffiths, G. M. The immunological synapse of CTL contains a secretory domain and membrane bridges. *Immunity* **15**, 751-761 (2001).

17 Dustin, M. L. & Long, E. O. Cytotoxic immunological synapses. *Immunological reviews* **235**, 24-34, doi:10.1111/j.0105-2896.2010.00904.x (2010).

18 Peters, P. J. *et al.* Cytotoxic T lymphocyte granules are secretory lysosomes, containing both perforin and granzymes. *The Journal of experimental medicine* **173**, 1099-1109 (1991).

19 Praper, T. *et al.* Human perforin permeabilizing activity, but not binding to lipid membranes, is affected by pH. *Molecular immunology* **47**, 2492-2504, doi:10.1016/j.molimm.2010.06.001 (2010).

20 Lettau, M., Schmidt, H., Kabelitz, D. & Janssen, O. Secretory lysosomes and their cargo in T and NK cells. *Immunology letters* **108**, 10-19, doi:10.1016/j.imlet.2006.10.001 (2007).

21 Hirst, C. E. *et al.* The intracellular granzyme B inhibitor, proteinase inhibitor 9, is up-regulated during accessory cell maturation and effector cell degranulation, and its overexpression enhances CTL potency. *Journal of immunology (Baltimore, Md. : 1950)* **170**, 805-815 (2003).

22 Cohnen, A. *et al.* Surface CD107a/LAMP-1 protects natural killer cells from degranulation-associated damage. *Blood* **122**, 1411-1418, doi:10.1182/blood-2012-07-441832 (2013).

23 Betts, M. R. *et al.* Sensitive and viable identification of antigen-specific CD8+ T cells by a flow cytometric assay for degranulation. *J Immunol Methods* **281**, 65-78 (2003).

24 Yang, X. *et al.* Granzyme B Mimics Apical Caspases: DESCRIPTION OF A UNIFIED PATHWAY FOR TRANS-ACTIVATION OF EXECUTIONER CASPASE-3 AND -7. *Journal of Biological Chemistry* **273**, 34278-34283, doi:10.1074/jbc.273.51.34278 (1998).

25 Jiang, X. & Wang, X. Cytochrome c promotes caspase-9 activation by inducing nucleotide binding to Apaf-1. *The Journal of biological chemistry* **275**, 31199-31203, doi:10.1074/jbc.C000405200 (2000).

26 Brunner, T. *et al.* Cell-autonomous Fas (CD95)/Fas-ligand interaction mediates activation-induced apoptosis in T-cell hybridomas. *Nature* **373**, 441-444, doi:10.1038/373441a0 (1995).

27 Griffith, T. S., Brunner, T., Fletcher, S. M., Green, D. R. & Ferguson, T. A. Fas ligand-induced apoptosis as a mechanism of immune privilege. *Science (New York, N.Y.)* **270**, 1189-1192 (1995).

28 Abbas, A., Lichtman, A. & Pillai, S. Vol. 6 Ch. 6, 123 ff (Saunders Elsevir, 2010).

29 Schwarz, E. C., Qu, B. & Hoth, M. Calcium, cancer and killing: the role of calcium in killing cancer cells by cytotoxic T lymphocytes and natural killer cells. *Biochimica et biophysica acta* **1833**, 1603-1611, doi:10.1016/j.bbamcr.2012.11.016 (2013).

30 Luo, C. *et al.* Interaction of calcineurin with a domain of the transcription factor NFAT1 that controls nuclear import. *Proceedings of the National Academy of Sciences of the United States of America* **93**, 8907-8912 (1996).

31 Jain, J. *et al.* The T-cell transcription factor NFATp is a substrate for calcineurin and interacts with Fos and Jun. *Nature* **365**, 352-355, doi:10.1038/365352a0 (1993).

32 Rao, A., Luo, C. & Hogan, P. G. Transcription factors of the NFAT family: regulation and function. *Annual review of immunology* **15**, 707-747, doi:10.1146/annurev.immunol.15.1.707 (1997).

33 Condotta, S. A., Richer, M. J., Badovinac, V. P. & Harty, J. T. Probing CD8 T cell responses with Listeria monocytogenes infection. *Adv Immunol* **113**, 51-80, doi:10.1016/b978-0-12-394590-7.00005-1 (2012).

34 Nolz, J. C. Molecular mechanisms of CD8(+) T cell trafficking and localization. *Cell Mol Life Sci* **72**, 2461-2473, doi:10.1007/s00018-015-1835-0 (2015).

35 Dabiri, G. A., Sanger, J. M., Portnoy, D. A. & Southwick, F. S. Listeria monocytogenes moves rapidly through the host-cell cytoplasm by inducing directional actin assembly. *Proc Natl Acad Sci U S A* **87**, 6068-6072 (1990).
36 Cossart, P. & Lecuit, M. Interactions of Listeria monocytogenes with mammalian cells during entry and actin-based movement: bacterial factors, cellular ligands and signaling. *Embo j* **17**, 3797-3806, doi:10.1093/emboj/17.14.3797 (1998).
37 Hof, H. Listeriosis: therapeutic options. *FEMS Immunol Med Microbiol* **35**, 203-205 (2003).
38 Portnoy, D. A. & Jones, S. The cell biology of Listeria monocytogenes infection (escape from a vacuole). *Ann N Y Acad Sci* **730**, 15-25 (1994).
39 Allerberger, F. & Wagner, M. Listeriosis: a resurgent foodborne infection. *Clin Microbiol Infect* **16**, 16-23, doi:10.1111/j.1469-0691.2009.03109.x (2010).
40 Bachmann, M. F., Wolint, P., Schwarz, K. & Oxenius, A. Recall proliferation potential of memory CD8+ T cells and antiviral protection. *J Immunol* **175**, 4677-4685 (2005).
41 Mielke, M. E., Niedobitek, G., Stein, H. & Hahn, H. Acquired resistance to Listeria monocytogenes is mediated by Lyt-2+ T cells independently of the influx of monocytes into granulomatous lesions. *J Exp Med* **170**, 589-594 (1989).
42 Harty, J. T., Lenz, L. L. & Bevan, M. J. Primary and secondary immune responses to Listeria monocytogenes. *Curr Opin Immunol* **8**, 526-530 (1996).
43 Shaw, J. P. *et al.* Identification of a putative regulator of early T cell activation genes. *Science (New York, N.Y.)* **241**, 202-205 (1988).
44 Ranger, A. M. *et al.* The transcription factor NF-ATc is essential for cardiac valve formation. *Nature* **392**, 186-190, doi:10.1038/32426 (1998).
45 Miyakawa, H., Woo, S. K., Dahl, S. C., Handler, J. S. & Kwon, H. M. Tonicity-responsive enhancer binding protein, a rel-like protein that stimulates transcription in response to hypertonicity. *Proceedings of the National Academy of Sciences of the United States of America* **96**, 2538-2542 (1999).
46 Daniel, C., Gerlach, K., Vath, M., Neurath, M. F. & Weigmann, B. Nuclear factor of activated T cells - a transcription factor family as critical regulator in lung and colon cancer. *International journal of cancer. Journal international du cancer* **134**, 1767-1775, doi:10.1002/ijc.28329 (2014).
47 Serfling, E. *et al.* Ubiquitous and lymphocyte-specific factors are involved in the induction of the mouse interleukin 2 gene in T lymphocytes. *Embo j* **8**, 465-473 (1989).
48 Emmel, E. A. *et al.* Cyclosporin A specifically inhibits function of nuclear proteins involved in T cell activation. *Science* **246**, 1617-1620 (1989).
49 Rush, D. The impact of calcineurin inhibitors on graft survival. *Transplant Rev (Orlando)* **27**, 93-95, doi:10.1016/j.trre.2013.04.003 (2013).
50 Randak, C., Brabletz, T., Hergenrother, M., Sobotta, I. & Serfling, E. Cyclosporin A suppresses the expression of the interleukin 2 gene by inhibiting the binding of lymphocyte-specific factors to the IL-2 enhancer. *The EMBO journal* **9**, 2529-2536 (1990).
51 McCaffrey, P. G. *et al.* Isolation of the cyclosporin-sensitive T cell transcription factor NFATp. *Science* **262**, 750-754 (1993).
52 Jain, J., Burgeon, E., Badalian, T. M., Hogan, P. G. & Rao, A. A similar DNA-binding motif in NFAT family proteins and the Rel homology region. *The Journal of biological chemistry* **270**, 4138-4145 (1995).

53 Yoshida, H. *et al.* The transcription factor NF-ATc1 regulates lymphocyte proliferation and Th2 cytokine production. *Immunity* **8**, 115-124 (1998).

54 Ranger, A. M. *et al.* Delayed lymphoid repopulation with defects in IL-4-driven responses produced by inactivation of NF-ATc. *Immunity* **8**, 125-134 (1998).

55 Xanthoudakis, S. *et al.* An enhanced immune response in mice lacking the transcription factor NFAT1. *Science (New York, N.Y.)* **272**, 892-895 (1996).

56 Kiani, A. *et al.* Regulation of interferon-gamma gene expression by nuclear factor of activated T cells. *Blood* **98**, 1480-1488 (2001).

57 Kiani, A., Viola, J. P., Lichtman, A. H. & Rao, A. Down-regulation of IL-4 gene transcription and control of Th2 cell differentiation by a mechanism involving NFAT1. *Immunity* **7**, 849-860 (1997).

58 Diehl, S. *et al.* Induction of NFATc2 expression by interleukin 6 promotes T helper type 2 differentiation. *J Exp Med* **196**, 39-49 (2002).

59 Northrop, J. P. *et al.* NF-AT components define a family of transcription factors targeted in T-cell activation. *Nature* **369**, 497-502, doi:10.1038/369497a0 (1994).

60 Chuvpilo, S. *et al.* Alternative polyadenylation events contribute to the induction of NF-ATc in effector T cells. *Immunity* **10**, 261-269 (1999).

61 Zhou, B. *et al.* Regulation of the murine Nfatc1 gene by NFATc2. *The Journal of biological chemistry* **277**, 10704-10711, doi:10.1074/jbc.M107068200 (2002).

62 Waters, J. P., Pober, J. S. & Bradley, J. R. Tumour necrosis factor in infectious disease. *The Journal of pathology* **230**, 132-147, doi:10.1002/path.4187 (2013).

63 Waters, J. P., Pober, J. S. & Bradley, J. R. Tumour necrosis factor and cancer. *The Journal of pathology* **230**, 241-248, doi:10.1002/path.4188 (2013).

64 Kaminuma, O. *et al.* Differential contribution of NFATc2 and NFATc1 to TNF-alpha gene expression in T cells. *Journal of immunology (Baltimore, Md. : 1950)* **180**, 319-326 (2008).

65 Hodge, M. R. *et al.* Hyperproliferation and dysregulation of IL-4 expression in NF-ATp-deficient mice. *Immunity* **4**, 397-405 (1996).

66 Rooney, J. W., Sun, Y. L., Glimcher, L. H. & Hoey, T. Novel NFAT sites that mediate activation of the interleukin-2 promoter in response to T-cell receptor stimulation. *Mol Cell Biol* **15**, 6299-6310 (1995).

67 Fathman, C. G. & Lineberry, N. B. Molecular mechanisms of CD4+ T-cell anergy. *Nature reviews. Immunology* **7**, 599-609, doi:10.1038/nri2131 (2007).

68 Macian, F. NFAT proteins: key regulators of T-cell development and function. *Nature reviews. Immunology* **5**, 472-484, doi:10.1038/nri1632 (2005).

69 Agarwal, S., Avni, O. & Rao, A. Cell-type-restricted binding of the transcription factor NFAT to a distal IL-4 enhancer in vivo. *Immunity* **12**, 643-652 (2000).

70 Rothenberg, E. V. & Ward, S. B. A dynamic assembly of diverse transcription factors integrates activation and cell-type information for interleukin 2 gene regulation. *Proceedings of the National Academy of Sciences of the United States of America* **93**, 9358-9365 (1996).

71 Cho, J. H. *et al.* Unique features of naive CD8+ T cell activation by IL-2. *Journal of immunology (Baltimore, Md. : 1950)* **191**, 5559-5573, doi:10.4049/jimmunol.1302293 (2013).

72 Kundig, T. M. *et al.* Immune responses in interleukin-2-deficient mice. *Science (New York, N.Y.)* **262**, 1059-1061 (1993).

73 Williams, M. A., Tyznik, A. J. & Bevan, M. J. Interleukin-2 signals during priming are required for secondary expansion of CD8+ memory T cells. *Nature* **441**, 890-893, doi:10.1038/nature04790 (2006).

74 Pepper, M., Pagan, A. J., Igyarto, B. Z., Taylor, J. J. & Jenkins, M. K. Opposing signals from the Bcl6 transcription factor and the interleukin-2 receptor generate T helper 1 central and effector memory cells. *Immunity* **35**, 583-595, doi:10.1016/j.immuni.2011.09.009 (2011).

75 Liao, W., Lin, J. X., Wang, L., Li, P. & Leonard, W. J. Modulation of cytokine receptors by IL-2 broadly regulates differentiation into helper T cell lineages. *Nat Immunol* **12**, 551-559, doi:10.1038/ni.2030 (2011).

76 Bueno, O. F., Brandt, E. B., Rothenberg, M. E. & Molkentin, J. D. Defective T cell development and function in calcineurin A beta -deficient mice. *Proceedings of the National Academy of Sciences of the United States of America* **99**, 9398-9403, doi:10.1073/pnas.152665399 (2002).

77 Vaeth, M. *et al.* Dependence on nuclear factor of activated T-cells (NFAT) levels discriminates conventional T cells from Foxp3+ regulatory T cells. *Proceedings of the National Academy of Sciences of the United States of America* **109**, 16258-16263, doi:10.1073/pnas.1203870109 (2012).

78 Maxeiner, J. H. *et al.* A key regulatory role of the transcription factor NFATc2 in bronchial adenocarcinoma via CD8+ T lymphocytes. *Cancer Res* **69**, 3069-3076, doi:10.1158/0008-5472.can-08-1678 (2009).

79 Shimizu, J., Yamazaki, S., Takahashi, T., Ishida, Y. & Sakaguchi, S. Stimulation of CD25(+)CD4(+) regulatory T cells through GITR breaks immunological self-tolerance. *Nature immunology* **3**, 135-142, doi:10.1038/ni759 (2002).

80 Leung-Theung-Long, S. *et al.* Impaired NFAT transcriptional activity in antigen-stimulated CD8 T cells linked to defective phosphorylation of NFAT transactivation domain. *J Immunol* **182**, 6807-6814, doi:10.4049/jimmunol.0803539 (2009).

81 Quintana, A. *et al.* T cell activation requires mitochondrial translocation to the immunological synapse. *Proc Natl Acad Sci U S A* **104**, 14418-14423, doi:10.1073/pnas.0703126104 (2007).

82 Pores-Fernando, A. T. & Zweifach, A. Calcium influx and signaling in cytotoxic T-lymphocyte lytic granule exocytosis. *Immunological reviews* **231**, 160-173, doi:10.1111/j.1600-065X.2009.00809.x (2009).

83 Rouvier, E., Luciani, M. F. & Golstein, P. Fas involvement in Ca(2+)-independent T cell-mediated cytotoxicity. *The Journal of experimental medicine* **177**, 195-200 (1993).

84 Aramburu, J. *et al.* Affinity-driven peptide selection of an NFAT inhibitor more selective than cyclosporin A. *Science (New York, N.Y.)* **285**, 2129-2133 (1999).

85 Choi, J. M., Sohn, J. H., Park, T. Y., Park, J. W. & Lee, S. K. Cell permeable NFAT inhibitory peptide Sim-2-VIVIT inhibits T-cell activation and alleviates allergic airway inflammation and hyper-responsiveness. *Immunology letters* **143**, 170-176, doi:10.1016/j.imlet.2012.01.016 (2012).

86 Moskophidis, D., Lechner, F., Pircher, H. & Zinkernagel, R. M. VIRUS PERSISTENCE IN ACUTELY INFECTED IMMUNOCOMPETENT MICE BY EXHAUSTION OF ANTIVIRAL CYTOTOXIC EFFECTOR T-CELLS. *Nature* **362**, 758-761, doi:10.1038/362758a0 (1993).

87 Ou, R., Zhou, S., Huang, L. & Moskophidis, D. Critical role for alpha/beta and gamma interferons in persistence of lymphocytic choriomeningitis virus by clonal exhaustion of cytotoxic T cells. *Journal of virology* **75**, 8407-8423 (2001).
88 Wherry, E. J., Blattman, J. N., Murali-Krishna, K., van der Most, R. & Ahmed, R. Viral persistence alters CD8 T-cell immunodominance and tissue distribution and results in distinct stages of functional impairment. *Journal of virology* **77**, 4911-4927 (2003).
89 Agnellini, P. *et al.* Impaired NFAT nuclear translocation results in split exhaustion of virus-specific CD8+ T cell functions during chronic viral infection. *Proceedings of the National Academy of Sciences* **104**, 4565-4570, doi:10.1073/pnas.0610335104 (2007).
90 Vaeth, M. *et al.* Selective NFAT targeting in T cells ameliorates GvHD while maintaining antitumor activity. *Proc Natl Acad Sci U S A* **112**, 1125-1130, doi:10.1073/pnas.1409290112 (2015).
91 Flanagan, W. M., Corthesy, B., Bram, R. J. & Crabtree, G. R. Nuclear association of a T-cell transcription factor blocked by FK-506 and cyclosporin A. *Nature* **352**, 803-807, doi:10.1038/352803a0 (1991).
92 Borel, J. F., Feurer, C., Gubler, H. U. & Stahelin, H. Biological effects of cyclosporin A: a new antilymphocytic agent. *Agents Actions* **6**, 468-475 (1976).
93 Suhrbier, A., Fernan, A., Burrows, S. R., Saul, A. & Moss, D. J. BLT esterase activity as an alternative to chromium release in cytotoxic T cell assays. *J Immunol Methods* **145**, 43-53 (1991).
94 Smyth, M. J. & Ortaldo, J. R. Mechanisms of cytotoxicity used by human peripheral blood CD4+ and CD8+ T cell subsets. The role of granule exocytosis. *J Immunol* **151**, 740-747 (1993).
95 Dutz, J. P., Fruman, D. A., Burakoff, S. J. & Bierer, B. E. A role for calcineurin in degranulation of murine cytotoxic T lymphocytes. *J Immunol* **150**, 2591-2598 (1993).
96 Blumberg, P. M. In vitro studies on the mode of action of the phorbol esters, potent tumor promoters: part 1. *Critical reviews in toxicology* **8**, 153-197, doi:10.3109/10408448009037493 (1980).
97 Han, Z. T. *et al.* 12-O-Tetradecanoylphorbol-13-acetate (TPA)-induced increase in depressed white blood cell counts in patients treated with cytotoxic cancer chemotherapeutic drugs. *Proceedings of the National Academy of Sciences of the United States of America* **95**, 5362-5365 (1998).
98 Cavarra, M. S., Assef, Y. A. & Kotsias, B. A. Effects of ionomycin and thapsigargin on ion currents in oocytes of Bufo arenarum. *Journal of experimental zoology. Part A, Comparative experimental biology* **297**, 130-137 (2003).
99 Lytton, J., Westlin, M. & Hanley, M. R. Thapsigargin inhibits the sarcoplasmic or endoplasmic reticulum Ca-ATPase family of calcium pumps. *Journal of Biological Chemistry* **266**, 17067-17071 (1991).
100 Chen-Woan, M., Sajewski, D. H. & McGregor, D. D. T-cell co-operation in the mediation of acquired resistance to Listeria monocytogenes. *Immunology* **56**, 33-42 (1985).
101 Bishop, D. K. & Hinrichs, D. J. Adoptive transfer of immunity to Listeria monocytogenes. The influence of in vitro stimulation on lymphocyte subset requirements. *J Immunol* **139**, 2005-2009 (1987).
102 Goossens, P. L. & Milon, G. Induction of protective CD8+ T lymphocytes by an attenuated Listeria monocytogenes actA mutant. *Int Immunol* **4**, 1413-1418 (1992).
103 Laemmli, U. K. Cleavage of structural proteins during the assembly of the head of bacteriophage T4. *Nature* **227**, 680-685 (1970).

104 Livak, K. J. & Schmittgen, T. D. Analysis of Relative Gene Expression Data Using Real-Time Quantitative PCR and the 2−ΔΔCT Method. *Methods* **25**, 402-408, doi:http://dx.doi.org/10.1006/meth.2001.1262 (2001).

105 Hock, M. *et al.* NFATc1 Induction in Peripheral T and B Lymphocytes. *Journal of Immunology* **190**, 2345-2353, doi:10.4049/jimmunol.1201591 (2013).

106 Latinis, K. M., Norian, L. A., Eliason, S. L. & Koretzky, G. A. Two NFAT transcription factor binding sites participate in the regulation of CD95 (Fas) ligand expression in activated human T cells. *J Biol Chem* **272**, 31427-31434 (1997).

107 Jayanthi, S. *et al.* Calcineurin/NFAT-induced up-regulation of the Fas ligand/Fas death pathway is involved in methamphetamine-induced neuronal apoptosis. *Proc Natl Acad Sci U S A* **102**, 868-873, doi:10.1073/pnas.0404990102 (2005).

108 Williams, M. A. & Bevan, M. J. Effector and memory CTL differentiation. *Annu Rev Immunol* **25**, 171-192, doi:10.1146/annurev.immunol.25.022106.141548 (2007).

109 Sundrud, M. S. & Rao, A. New twists of T cell fate: control of T cell activation and tolerance by TGF-beta and NFAT. *Curr Opin Immunol* **19**, 287-293, doi:10.1016/j.coi.2007.04.014 (2007).

110 Giffin, M. J. *et al.* Structure of NFAT1 bound as a dimer to the HIV-1 LTR kappa B element. *Nat Struct Biol* **10**, 800-806, doi:10.1038/nsb981 (2003).

111 Macian, F., Lopez-Rodriguez, C. & Rao, A. Partners in transcription: NFAT and AP-1. *Oncogene* **20**, 2476-2489, doi:10.1038/sj.onc.1204386 (2001).

112 Chen, L., Glover, J. N., Hogan, P. G., Rao, A. & Harrison, S. C. Structure of the DNA-binding domains from NFAT, Fos and Jun bound specifically to DNA. *Nature* **392**, 42-48, doi:10.1038/32100 (1998).

113 Macian, F., Garcia-Rodriguez, C. & Rao, A. Gene expression elicited by NFAT in the presence or absence of cooperative recruitment of Fos and Jun. *Embo j* **19**, 4783-4795, doi:10.1093/emboj/19.17.4783 (2000).

114 Hogan, P. G., Chen, L., Nardone, J. & Rao, A. Transcriptional regulation by calcium, calcineurin, and NFAT. *Genes Dev* **17**, 2205-2232, doi:10.1101/gad.1102703 (2003).

115 Martinez, G. J. *et al.* The transcription factor NFAT promotes exhaustion of activated CD8(+) T cells. *Immunity* **42**, 265-278, doi:10.1016/j.immuni.2015.01.006 (2015).

116 Saito, T. & Germain, R. N. Predictable acquisition of a new MHC recognition specificity following expression of a transfected T-cell receptor beta-chain gene. *Nature* **329**, 256-259, doi:10.1038/329256a0 (1987).

117 Macian, F., Im, S. H., Garcia-Cozar, F. J. & Rao, A. T-cell anergy. *Curr Opin Immunol* **16**, 209-216, doi:10.1016/j.coi.2004.01.013 (2004).

118 Serfling, E. *et al.* NFATc1/alphaA: The other Face of NFAT Factors in Lymphocytes. *Cell Commun Signal* **10**, 16, doi:10.1186/1478-811x-10-16 (2012).

119 Feske, S., Giltnane, J., Dolmetsch, R., Staudt, L. M. & Rao, A. Gene regulation mediated by calcium signals in T lymphocytes. *Nat Immunol* **2**, 316-324, doi:10.1038/86318 (2001).

120 Viola, J. P., Kiani, A., Bozza, P. T. & Rao, A. Regulation of allergic inflammation and eosinophil recruitment in mice lacking the transcription factor NFAT1: role of interleukin-4 (IL-4) and IL-5. *Blood* **91**, 2223-2230 (1998).

121 Peng, S. L., Gerth, A. J., Ranger, A. M. & Glimcher, L. H. NFATc1 and NFATc2 together control both T and B cell activation and differentiation. *Immunity* **14**, 13-20 (2001).

122 Oukka, M. *et al.* The transcription factor NFAT4 is involved in the generation and survival of T cells. *Immunity* **9**, 295-304 (1998).
123 Liao, W., Lin, J. X. & Leonard, W. J. Interleukin-2 at the crossroads of effector responses, tolerance, and immunotherapy. *Immunity* **38**, 13-25, doi:10.1016/j.immuni.2013.01.004 (2013).
124 Lenardo, M. J. Interleukin-2 programs mouse alpha beta T lymphocytes for apoptosis. *Nature* **353**, 858-861, doi:10.1038/353858a0 (1991).
125 Rengarajan, J., Tang, B. & Glimcher, L. H. NFATc2 and NFATc3 regulate T(H)2 differentiation and modulate TCR-responsiveness of naive T(H)cells. *Nat Immunol* **3**, 48-54, doi:10.1038/ni744 (2002).
126 Xiao, S. *et al.* FasL promoter activation by IL-2 through SP1 and NFAT but not Egr-2 and Egr-3. *European Journal of Immunology* **29**, 3456-3465, doi:10.1002/(sici)1521-4141(199911)29:11<3456::aid-immu3456>3.3.co;2-2 (1999).
127 Li-Weber, M., Laur, O. & Krammer, P. H. Novel Egr/NF-AT composite sites mediate activation of the CD95 (APO-1/Fas) ligand promoter in response to T cell stimulation. *Eur J Immunol* **29**, 3017-3027, doi:10.1002/(sici)1521-4141(199909)29:09<3017::aid-immu3017>3.0.co;2-r (1999).
128 Rengarajan, J. *et al.* Sequential involvement of NFAT and Egr transcription factors in FasL regulation. *Immunity* **12**, 293-300 (2000).
129 Truitt, R. L. & Atasoylu, A. A. Contribution of CD4+ and CD8+ T cells to graft-versus-host disease and graft-versus-leukemia reactivity after transplantation of MHC-compatible bone marrow. *Bone Marrow Transplant* **8**, 51-58 (1991).
130 Choi, S. W. & Reddy, P. Current and emerging strategies for the prevention of graft-versus-host disease. *Nat Rev Clin Oncol* **11**, 536-547, doi:10.1038/nrclinonc.2014.102 (2014).
131 Liu, J. *et al.* Calcineurin is a common target of cyclophilin-cyclosporin A and FKBP-FK506 complexes. *Cell* **66**, 807-815 (1991).
132 Lee, J. T. *et al.* Calcineurin inhibitors and Clostridium difficile infection in adult lung transplant recipients: the effect of cyclosporine versus tacrolimus. *J Surg Res* **184**, 599-604, doi:10.1016/j.jss.2013.03.041 (2013).
133 Putz, E. M. *et al.* PI3Kdelta is essential for tumor clearance mediated by cytotoxic T lymphocytes. *PLoS One* **7**, e40852, doi:10.1371/journal.pone.0040852 (2012).
134 Okkenhaug, K. *et al.* Impaired B and T cell antigen receptor signaling in p110delta PI 3-kinase mutant mice. *Science* **297**, 1031-1034, doi:10.1126/science.1073560 (2002).
135 Schreiber, S. L. & Crabtree, G. R. The mechanism of action of cyclosporin A and FK506. *Immunol Today* **13**, 136-142, doi:10.1016/0167-5699(92)90111-j (1992).
136 Gessner, A., Moskophidis, D. & Lehmann-Grube, F. Enumeration of single IFN-gamma-producing cells in mice during viral and bacterial infection. *J Immunol* **142**, 1293-1298 (1989).
137 Ahmed, R. & Gray, D. Immunological memory and protective immunity: understanding their relation. *Science* **272**, 54-60 (1996).
138 Bevan, M. J. Helping the CD8(+) T-cell response. *Nat Rev Immunol* **4**, 595-602, doi:10.1038/nri1413 (2004).
139 Kaech, S. M. & Ahmed, R. Memory CD8+ T cell differentiation: initial antigen encounter triggers a developmental program in naive cells. *Nat Immunol* **2**, 415-422, doi:10.1038/87720 (2001).

140 Inaba, K., Young, J. W. & Steinman, R. M. Direct activation of CD8+ cytotoxic T lymphocytes by dendritic cells. *J Exp Med* **166**, 182-194 (1987).
141 Martin-Cofreces, N. B. *et al.* End-binding protein 1 controls signal propagation from the T cell receptor. *Embo j* **31**, 4140-4152, doi:10.1038/emboj.2012.242 (2012).
142 Angus, K. L. & Griffiths, G. M. Cell polarisation and the immunological synapse. *Curr Opin Cell Biol* **25**, 85-91, doi:10.1016/j.ceb.2012.08.013 (2013).
143 Parekh, A. B. & Putney, J. W., Jr. Store-operated calcium channels. *Physiol Rev* **85**, 757-810, doi:10.1152/physrev.00057.2003 (2005).
144 Sena, L. A. *et al.* Mitochondria are required for antigen-specific T cell activation through reactive oxygen species signaling. *Immunity* **38**, 225-236, doi:10.1016/j.immuni.2012.10.020 (2013).
145 Brini, M., Cali, T., Ottolini, D. & Carafoli, E. Neuronal calcium signaling: function and dysfunction. *Cell Mol Life Sci* **71**, 2787-2814, doi:10.1007/s00018-013-1550-7 (2014).
146 Abougergi, M. S., Gidner, S. J., Spady, D. K., Miller, B. C. & Thiele, D. L. Fas and TNFR1, but not cytolytic granule-dependent mechanisms, mediate clearance of murine liver adenoviral infection. *Hepatology* **41**, 97-105, doi:10.1002/hep.20504 (2005).
147 Kafrouni, M. I., Brown, G. R. & Thiele, D. L. The role of TNF-TNFR2 interactions in generation of CTL responses and clearance of hepatic adenovirus infection. *J Leukoc Biol* **74**, 564-571, doi:10.1189/jlb.0103035 (2003).
148 Chen, G. & Goeddel, D. V. TNF-R1 signaling: a beautiful pathway. *Science* **296**, 1634-1635, doi:10.1126/science.1071924 (2002).
149 Alikhani, M., Alikhani, Z., Raptis, M. & Graves, D. T. TNF-alpha in vivo stimulates apoptosis in fibroblasts through caspase-8 activation and modulates the expression of pro-apoptotic genes. *J Cell Physiol* **201**, 341-348, doi:10.1002/jcp.20067 (2004).
150 McCaffrey, P. G., Goldfeld, A. E. & Rao, A. The role of NFATp in cyclosporin A-sensitive tumor necrosis factor-alpha gene transcription. *J Biol Chem* **269**, 30445-30450 (1994).
151 Semsarian, C. *et al.* Skeletal muscle hypertrophy is mediated by a Ca2+-dependent calcineurin signalling pathway. *Nature* **400**, 576-581, doi:10.1038/23054 (1999).
152 Musaro, A., McCullagh, K. J., Naya, F. J., Olson, E. N. & Rosenthal, N. IGF-1 induces skeletal myocyte hypertrophy through calcineurin in association with GATA-2 and NF-ATc1. *Nature* **400**, 581-585, doi:10.1038/23060 (1999).
153 Crabtree, G. R. & Olson, E. N. NFAT signaling: choreographing the social lives of cells. *Cell* **109 Suppl**, S67-79 (2002).
154 Karpurapu, M., Wang, D., Singh, N. K., Li, Q. & Rao, G. N. NFATc1 targets cyclin A in the regulation of vascular smooth muscle cell multiplication during restenosis. *J Biol Chem* **283**, 26577-26590, doi:10.1074/jbc.M800423200 (2008).
155 Karpurapu, M. *et al.* Cyclin D1 is a bona fide target gene of NFATc1 and is sufficient in the mediation of injury-induced vascular wall remodeling. *J Biol Chem* **285**, 3510-3523, doi:10.1074/jbc.M109.063727 (2010).
156 Brun, C. *et al.* T-plastin expression downstream to the calcineurin/NFAT pathway is involved in keratinocyte migration. *PLoS One* **9**, e104700, doi:10.1371/journal.pone.0104700 (2014).
157 Cossart, P. Illuminating the landscape of host-pathogen interactions with the bacterium Listeria monocytogenes. *Proc Natl Acad Sci U S A* **108**, 19484-19491, doi:10.1073/pnas.1112371108 (2011).

158 Schlech, W. F., 3rd *et al.* Epidemic listeriosis--evidence for transmission by food. *N Engl J Med* **308**, 203-206, doi:10.1056/nejm198301273080407 (1983).
159 Tilney, L. G. & Portnoy, D. A. Actin filaments and the growth, movement, and spread of the intracellular bacterial parasite, Listeria monocytogenes. *J Cell Biol* **109**, 1597-1608 (1989).
160 Conlan, J. W. Early pathogenesis of Listeria monocytogenes infection in the mouse spleen. *J Med Microbiol* **44**, 295-302 (1996).
161 Pamer, E. G. Immune responses to Listeria monocytogenes. *Nat Rev Immunol* **4**, 812-823, doi:10.1038/nri1461 (2004).
162 Kagi, D., Ledermann, B., Burki, K., Hengartner, H. & Zinkernagel, R. M. CD8+ T cell-mediated protection against an intracellular bacterium by perforin-dependent cytotoxicity. *Eur J Immunol* **24**, 3068-3072, doi:10.1002/eji.1830241223 (1994).
163 Pope, C. *et al.* Organ-specific regulation of the CD8 T cell response to Listeria monocytogenes infection. *J Immunol* **166**, 3402-3409 (2001).
164 Kerksiek, K. M. & Pamer, E. G. T cell responses to bacterial infection. *Curr Opin Immunol* **11**, 400-405, doi:10.1016/s0952-7915(99)80067-3 (1999).
165 Bajenoff, M., Narni-Mancinelli, E., Brau, F. & Lauvau, G. Visualizing early splenic memory CD8+ T cells reactivation against intracellular bacteria in the mouse. *PLoS One* **5**, e11524, doi:10.1371/journal.pone.0011524 (2010).
166 Soudja, S. M. *et al.* Memory-T-cell-derived interferon-gamma instructs potent innate cell activation for protective immunity. *Immunity* **40**, 974-988, doi:10.1016/j.immuni.2014.05.005 (2014).
167 Lara-Tejero, M. & Pamer, E. G. T cell responses to Listeria monocytogenes. *Curr Opin Microbiol* **7**, 45-50, doi:10.1016/j.mib.2003.12.002 (2004).
168 Bancroft, G. J., Schreiber, R. D., Bosma, G. C., Bosma, M. J. & Unanue, E. R. A T cell-independent mechanism of macrophage activation by interferon-gamma. *J Immunol* **139**, 1104-1107 (1987).
169 Brunt, L. M., Portnoy, D. A. & Unanue, E. R. Presentation of Listeria monocytogenes to CD8+ T cells requires secretion of hemolysin and intracellular bacterial growth. *J Immunol* **145**, 3540-3546 (1990).
170 Edelson, B. T. & Unanue, E. R. Immunity to Listeria infection. *Curr Opin Immunol* **12**, 425-431 (2000).
171 Yoshikawa, Y. *et al.* Listeria monocytogenes ActA-mediated escape from autophagic recognition. *Nat Cell Biol* **11**, 1233-1240, doi:10.1038/ncb1967 (2009).
172 Gregory, S. H. & Liu, C. C. CD8+ T-cell-mediated response to Listeria monocytogenes taken up in the liver and replicating within hepatocytes. *Immunol Rev* **174**, 112-122 (2000).
173 Zola, H. Markers of cell lineage, differentiation and activation. *J Biol Regul Homeost Agents* **14**, 218-219 (2000).
174 Busch, D. H., Pilip, I. M., Vijh, S. & Pamer, E. G. Coordinate regulation of complex T cell populations responding to bacterial infection. *Immunity* **8**, 353-362 (1998).
175 Mitchell, D. M., Ravkov, E. V. & Williams, M. A. Distinct roles for IL-2 and IL-15 in the differentiation and survival of CD8+ effector and memory T cells. *J Immunol* **184**, 6719-6730, doi:10.4049/jimmunol.0904089 (2010).
176 Sallusto, F., Geginat, J. & Lanzavecchia, A. Central memory and effector memory T cell subsets: function, generation, and maintenance. *Annu Rev Immunol* **22**, 745-763, doi:10.1146/annurev.immunol.22.012703.104702 (2004).

177 Khan, S. & Badovinac, V. Listeria monocytogenes: a model pathogen to study antigen-specific memory CD8 T cell responses. *Seminars in Immunopathology* **37**, 301-310, doi:10.1007/s00281-015-0477-5 (2015).
178 Maekawa, Y. *et al.* Notch2 integrates signaling by the transcription factors RBP-J and CREB1 to promote T cell cytotoxicity. *Nat Immunol* **9**, 1140-1147, doi:10.1038/ni.1649 (2008).
179 Quintana, A. *et al.* Calcium microdomains at the immunological synapse: how ORAI channels, mitochondria and calcium pumps generate local calcium signals for efficient T-cell activation. *Embo j* **30**, 3895-3912, doi:10.1038/emboj.2011.289 (2011).
180 Harty, J. T., Tvinnereim, A. R. & White, D. W. CD8+ T cell effector mechanisms in resistance to infection. *Annu Rev Immunol* **18**, 275-308, doi:10.1146/annurev.immunol.18.1.275 (2000).

Abbreviations

5′	5 prime
3′	3 prime
A	adenine
ABB	AnnexinV binding buffer
ActA	Actin assembly-inducing protein
Ag	antigen
AP-1	activator protein 1
APC	antigen presenting cell
APC-Cy7	allophycocyanin-Cy7
APS	ammonium persulfate
ATP	adenosine triphosphate
b	bases
BAC	bacterial artificial chromosome
BALB/c	laboratory white inbred mouse strain
BLT	benzyloxycarbonyl-L-lysine thiobenzyl ester
BSA	bovine serum albumin
BSS	balanced salt solution
C	cytosine
C57/B6	laboratory black inbred mouse strain
Ca^{2+}	calcium ion
Can	calcineurin
CCR-7	chemokine receptor 7
CD	cluster of differentiation
cDNA	complementary DNA
CFSE	carboxyfluorescein diacetate succinimidyl ester
CFU	colony forming unit
CO_2	carbon dioxide
CRAC	Calcium-release-activated Ca^{2+} channel
cre	cre-recombinase
CsA	cyclosporine A

CTL	cytotoxic T cell
D	diversity (locus)
DAG	diacylglycerol
DAPI	4′, 6-Diamidin-2-phenylindol
DC	dendritic cell
dH_2O	distilled water
DISC	death-inducing signaling complex
DMEM	Dulbecco's Modified Eagle Medium
DMSO	dimethyl sulfoxide
DNA	deoxyribonucleic acid
DTT	dithiothreitol
e.g.	*exempli gratia*
ECL	enhanced chemiluminescence
EDTA	ethylene diamine tetraacetic acid
eGFP	enhanced GFP
EGTA	ethylene glycol tetra-acetic acid
ELISA	enzyme-linked immunosorbent assay
ER	endoplasmatic reticulum
et al.	*et aliter*
EtBr	ethidium bromide
EtOH	ethanol
ex3	exon 3
FA	formaldehyde
FACS	fluorescence activated cell sorting
FADD	Fas-associated protein with death domain
Fc	fragment-cristalline
FCS	fetal cow serum
Fig.	figure
FITC	fluorescein-isothiocyanate
FK506	tacrolimus
fl	loxP site (floxed)
G	guanine

GA	gauge
GC	germinal centre
GFP	green fluorescing protein
GITR	glucocorticoid induced regulatory T cells
gLB	genomic lysis buffer
GvHD	graft-versus-host disease
HEK	human embryonic kidney
hIL	human interleukine
HIV	human immunodeficiency virus
HRP	horseradish peroxidase
I	ionomycin
i.e.	*id est*
IFN	interferon
Ig	immunoglobulin
IL	interleukin
IMDM	Iscove's Modified Dulbecco's Medium
i.p.	intraperitoneal
IP_3	inositol 1,4,5-triphosphate
IS	immunological synapse
ITAM	immunoreceptor tyrosine based activation motif
iTreg	induced regulatory T cells
J	joining (locus)
KO	knock-out
Lamp	lysosomal-associated membrane protein
LAT	linker of activated T cells
LB	lysogeny broth
Lck	lymphocyte-specific protein tyrosine kinase
Lm	*Listeria monocytogenes*
Lm-Ova	*Listeria monocytogenes*, expressing the OVA proteine
LPS	lipopolysaccharide
MACS	magnetic cell sorting
MES	2-(N-morpholino) ethanesulfonic acid

MFI	mean fluorescence intensity
MHC	major histocompatibility complex
mIL	murine interleukin
MLR	mixed lymphocyte reaction
MOPC	mineral oil induced plasmacytoma cell
mRNA	messenger RNA
N_2	nitrogen
NEAA	non-essential amino acid
NES	nuclear-export signal
NFAT	nuclear factor of activated T cells
NF-κB	nuclear factor kappa-light-chain-enhancer of activated B cells
NHD	NFAT-homology domain
NK	natural killer
NLS	nuclear-localization signal
NO	nitric oxide
nTreg	natural regulatory T cells
OD	optical density
ORAI	calcium-release activated calcium channel
OVA	ovalbumin
$Ova_{257-264}$	peptide sequence derived from OVA: SIINFEKL
p.i.	post-infection
P1	promoter 1
P2	promoter 2
PAMP	pattern-associated molecular pattern
PBS	phosphate buffered saline
PCR	polymerase chain reaction
PE	phycoerythrin
PI	propidium iodide
PIP_2	phosphatidyl-Innositol-biphophate
PLCγ	phospholipase C γ
polyA	polyadenylation
PRR	pattern-recognition receptor

qRT-PCR	quantitative RT-PCR
Rag-1	Recombination activating Gene-1
RBL	red blood cell lysis
RHD	Rel-homology domain
RNA	ribonucleic acid
ROS	reactive oxygen species
RPMI	culture medium (developed at the Roswell Park Memorial Institute)
RPM	rounds per min
RSD	Rel-similarity domain
RT-PCR	reverse transcriptase-PCR
SDS	sodium dodecyl sulfate
SERCA	sarco- and endoplasmic reticulum ATPase
SRR	serine-rich regions
STIM	stromal interaction molecule
T	thymine
T_1	T cells differentiated towards the T_h1 and T_c1 subsets
TAD	transactivation domain
TAE	TRIS-Acetate-EDTA
TBS	TRIS buffered saline
TBST	TBS - Tween
T_c	cytotoxic T cell subset
T_{cm}	central memory T cell
TCR	T cell receptor
T_{em}	effector memory T cell
TEMED	tetramethylethylendiamin
TGF	transforming growth factor
T_h	T helper cell
TLR	Toll-like receptor
T_m	melting temperature
TNF	tumor necrosis factor
TonEBP	Tonicity-Responsive Enhancer Binding Protein
TPA	12-*O*-Tetradecanoylphorbol-13-acetate

wt	wild type
V	variable (locus)
ZAP-70	Zeta-chain-associated protein kinase 70

SI units and prefixes

°C	degree celsius
A	Ampere
c-	centi-
d	day
g	gramm
Gy	Gray
h	hour
k-	kilo-
l	liter
m-	milli-
m	meter
M	Molar
µ-	micro-
min(’)	minute
n-	nano-
p-	pico-
s(’’)	second
V	volt
wk	week

Summary

While numerous experiments on NFAT were already performed with $CD4^+$ T cells showing defective cytokine release and a reduced T helper cell development, no detailed studies existed for $CD8^+$ T cells. From this point, we wanted to examine the impact of NFATc1 and c2 on the physiological functions of $CD8^+$ T cells *in vitro* and *in vivo*. Therefore, we used a murine infection model with the bacteria *Listeria monocytogenes* and mice in which NFATc1 was specifically depleted in the T cell compartment.

Our first *in vitro* studies showed a typical NFATc1 and c2 nuclear translocation and changes on mRNA levels upon T cell activation similarly in $CD4^+$ as well as in $CD8^+$ T cells extracted from *wild type* mice. NFAT nuclear translocation is important for target gene activation and generation of effector functions. Stimulated T cell populations lacking NFATc1 and/or NFATc2 showed a markedly decreased expression of T_h1/T_c1 cytokines, as e.g. IL 2 and IFNγ being important for the clearance of intracellular pathogens. From our *in vitro* model for the generation of allogenically reactive cytotoxic $CD8^+$ T cells, we revealed a decreased killing and lytic granule-release capacity in *Nfatc1* inactivated $CD8^+$ T cells whereas $NFATc2^{-/-}$ cytotoxic T cells did not show an altered cytotoxic response compared to *wild type* cells.

Interestingly, we found lytic granules accumulated and mitochondria not getting translocated to the immunological synapse upon re-stimulation in NFATc1-deficient $CD8^+$ T cells. Together with results showing the CsA insensitivity of the CTL killing/degranulation capacities, we assume that some major cellular processes are affected by NFATc1 which are not directly linked to the TCR-induced signal transduction cascade.

We also showed the importance of NFATc1 in T cells during intracellular infections with the bacteria *Listeria monocytogenes* in an *in vivo* mouse model. After five days, only few bacteria were detected in *wt* mice whereas high amounts of *Listeria* particles were extracted from livers of $Nfatc1^{fl/fl}$ x *Cd4 cre* mice. Although the reactivity towards the pathogen was similar in both groups, a decreased cytokine expression in $NFATc1^{-/-}$ $CD8^+$ T cells was observed together with an altered memory cell generation.

Our results show the importance of NFATc1 in $CD8^+$ T cells and give some clue for a possible connection to other basal cellular functions, as e.g. the formation of an immunological synapse.

Zusammenfassung

Viele Experimente zur Rolle von NFAT wurden bereits anhand von $CD4^+$ T Zellen durchgeführt und zeigten eine veränderte Zellphysiologie. Hingegen wurden $CD8^+$ T Zellen diesbezüglich noch nicht intensiv studiert. Deshalb untersuchten wir den Einfluss von NFATc1 und NFATc2 auf die Funktion von $CD8^+$ T Zellen *in vitro* und *in vivo* anhand des murinen Infektionsmodells mit dem Bakterium *Listeria monocytogenes*. Für die Versuche benutzen wir Mäuse, in denen das Protein NFATc1 spezifisch im T Zellkompartiment entfernt wurde.

Erste Ergebnisse zeigten eine typische Translokation von NFATc1 und NFATc2 in den Zellkern. Eine Veränderung in der mRNA Expression nach Aktivierung, sowohl in $CD4^+$ T Zellen als auch in $CD8^+$ T Zellen, fand ebenfalls statt. NFATc defiziente $CD4^+$ und $CD8^+$ T Zellen wiesen eine verminderte Expression von T_h1/T_c1 Zytokinen wie z.B. Interleukin-2 und Interferon γ auf, welche für die Bekämpfung intrazellulärer Pathogene wichtig sind. In unserem *in vitro* Modell fanden wir eine verminderte Abtötungsfähigkeit und eine Reduktion in der Freisetzung lytischer Granula in $NFATc1^{-/-}$ $CD8^+$ T Zellen wohingegen eine NFATc2 Defizienz keine Auswirkungen auf die Zytotoxizität - verglichen mit wildtypischen Zellen - aufweist.

Interessanterweise fanden wir eine Anhäufung von lytischen Granula und eine verminderte intrazelluläre Migration von Mitochondrien nach Ausbildung einer immunologischen Synapse in $NFATc1^{-/-}$ $CD8^+$ T Zellen. Zusammen mit den Ergebnissen unserer CsA-Inhibierungsversuche nehmen wir an, dass einige allgemeine zelluläre Prozesse von NFATc1 beeinflusst werden, die nicht direkt von der T Zellrezeptor-induzierten Signalkaskade abhängen.

Anhand eines *in vivo* Mausmodells zeigten wir auch die wichtige Rolle von NFATc1 in T Zellen während der Infektion mit *Listeria monocytogenes*. Fünf Tage nach Infektion konnten aus $Nfatc1^{fl/fl}$ x *Cd4 cre* Mäusen mehr Bakterienpartikel extrahiert werden als aus *wt* Mäusen. Wie in den *in vitro* Versuchen konnte auch hier eine geringere Zytokinproduktion der $CD8^+$ T Zellen festgestellt werden allerdings wiesen die Mäuse auch eine geringere Bildung von Gedächniszellen auf.

Unsere Ergebnisse zeigen, dass NFATc1 in $CD8^+$ T Zellen eine wichtige Rolle spielt und auch Auswirkungen auf grundlegendere zelluläre Funktionen, wie die Ausbildung einer immunologischen Synapse, hat.

Eidesstattliche Erklärung

Hiermit erkläre ich an Eides statt, die Dissertation „The transcription factor NFATc1 mediates cytotoxic T cell function *in vitro* and *in vivo*" eigenhändig, das heißt selbstständig und ohne die Hilfe eines kommerziellen Promotionsberaters angefertigt wurde, und keine anderen als die von mir angegebenen Quellen und Hilfsmittel verwendet wurden.
Ich erkläre außerdem, dass die Dissertation weder in gleicher noch in ähnlicher Form bereits in einem anderen Prüfungsverfahren vorgelegt wurde.
Bisher habe ich keinen früheren akademischen Grad erworben oder zu erwerben versucht.

Würzburg, Oktober 2015
Tobias Pusch

Affidavit

I hereby confirm that my thesis entitled „The transcription factor NFATc1 mediates cytotoxic T cell function *in vitro* and *in vivo*" is the result of my own work.
I did not receive any help or support from commercial consultants. All sources and/or materials applied are listed and specified in this thesis.
Furthermore, I confirm that my thesis has not yet been submitted as part or another examination process neither in identical nor in similar form.

Würzburg, October 2015
Tobias Pusch

Veröffentlichungen

Hock M, Vaeth M, Rudolf R, Patra AK, Pham DA, Muhammad K, Pusch T, Bopp T, Schmitt E, Rost R, Berberich-Siebelt F, Tyrsin D, Chuvpilo S, Avots A, Serfling E, Klein-Hessling S. NFATc1 induction in peripheral T and B lymphocytes. *Journal of Immunology*, March 2013.

Vaeth M, Bäuerlein C, Pusch T, Findeis J, Chopra M, Mottok A, Rosenwald A, Beilhack A, Berberich-Siebelt F. Selective NFAT targeting in T cells ameliorates GvHD while maintaining antitumor activity. *Proc Natl Acad Sci U S A*. January 2015.

Lebenslauf

Tobias Pusch

Geburtsdatum/-ort	12.01.1986 Cottbus
Staatsangehörigkeit	deutsch

Ausbildung

Aug. 1992 –Juni 2005	Gymnasium Weikersheim, Abitur
Okt. 2006 – Jan. 2011	Universität Würzburg, Diplomstudium Biologie
seit Feb. 2011	Institut für Pathologie, Abt. für molekulare Pathologie, Universität Würzburg, Promotionsstudium

Berufserfahrung und Nebenbeschäftigungen

Okt. 2005 – Juni 2006	Grundwehrdienst
April 2007 – Dez. 2010	Angestellter
	Funpark-Kinderland Würzburg
Sept. 2009 – Dez. 2010	studentische Hilfskraft
	Lehrstuhl für Biotechnologie, Universität Würzburg
seit Feb. 2011	Wissenschaftlicher Mitarbeiter
	Institut für Pathologie, Abt. für molekulare Pathologie, Universität Würzburg

Würzburg, Oktober 2015